MINISTRY OF INDUSTRY AND TRADE

ELECTRIC POWER UNIVERSITY

DINH VAN THIN

PROPOSED MODELS FOR DESIGNING WIND TURBINE BLADES AND INSTALLED CONFIGURATIONS OF ONSHORE WIND FARMS IN VIETNAM

DOCTOR OF PHILOSOPHY THESIS IN ENERGY ENGINEERING

Ha Noi – 2025

MINISTRY OF INDUSTRY AND TRADE

ELECTRIC POWER UNIVERSITY

DINH VAN THIN

PROPOSED MODELS FOR DESIGNING WIND TURBINE BLADES AND INSTALLED CONFIGURATIONS OF ONSHORE WIND FARMS IN VIETNAM

Major: Energy Engineering

Code: Pilot

DOCTOR OF PHILOSOPHY THESIS IN ENERGY ENGINEERING

SCIENTIFIC SUPERVISORS:

1. Assoc. Prof. Dr. Nguyen Huu Duc
2. Dr. Le Quang Sang

Ha Noi – 2025

DECLARATION

This thesis is my scientific research work under the advice and guidance of two scientific supervisors, Assoc. Prof. Dr. Nguyen Huu Duc and Dr. Le Quang Sang. This thesis was carried out from 2022 to 2025 at the Faculty of New Energy, Electric Power University, Vietnam.

I hereby certify that the theoretical basis used in the thesis is fully cited according to regulations. The models built and the results presented in this thesis are researched and proposed by myself. These results are not duplicated and have not been published before. Most of the results presented in this thesis have been published in prestigious domestic and international scientific journals or conferences by my research group. The data analysis and processing tools used in this thesis ensure the provisions on copyright and intellectual property as prescribed. I hereby guarantee and take full responsibility for the contents presented in this thesis.

Ha Noi, 24th December 2025

Dinh Van Thin

ACKNOWLEDGEMENTS

This thesis was conducted under the scientific guidance of Assoc. Prof. Dr. Nguyen Huu Duc and Dr. Le Quang Sang during the period of 2022 - 2025. During the research process, the two supervisors always encouraged and helped me overcome difficulties and obstacles to find new results. They always gave me confidence and clearly oriented the goals and meanings of the research. I would like to express my deep gratitude to the scientific supervisors.

During the studying process at the Faculty of New Energy, Electric Power University, I was directly taught, helped and created many favorable conditions by the lecturers so that I could complete the courses well. I would like to thank Dr. Nguyen Dang Toan - Dean of the Faculty, Assoc. Prof. Dr. Vu Hoang Giang - Vice Dean of the Faculty, and all the lecturers are working at the Faculty of New Energy.

In addition, I would like to thank the leaders of Electric Power University, the leaders and staffs at the Department of Academic Affairs for creating the most favorable conditions, helping me complete the necessary documents to complete this postgraduate training course during the period of 2022 - 2025.

Especially, I would like to send my most sincere thanks to my beloved extended family. My parents, brothers and sisters are always the motivation for me to strive to reach higher in life. I would like to send my most special thanks to my wife and son. They have been the source of life, the source of inspiration for me to know that I must try harder, to reach higher targets in work and life.

Finally, I would like to thank Vingroup Innovation Foundation - VinIF (VINIF) for providing funding to support my research in 2024. This study was supported by the Master, PhD Scholarship Programme of Vingroup Innovation Foundation (VINIF): “Dinh Van Thin was funded by the Master, PhD Scholarship Programme of Vingroup Innovation Foundation (VINIF), code VINIF.2024.TS.090”.

Contents

NOMENCLATURE

Acronyms	
3D	Three-dimensional
BEM	Blade element momentum
BOM	Betz optimization method
CFD	Computational Fluid Dynamics
FIDM	Full-inverse design method
GIS	Geographic information system
LLFVWM	A lifting line free vortex wake method
MC	Maximum camber
MCP	Maximum camber position
MT	Maximum thickness
MTP	Maximum thickness position
PM	Panel method
RANS	Reynolds-averaged Navier-Stokes
Variables and Operators	
A	Cross-section area, m^2
a	Axial induction factor
AEP	Annual energy production, kWh/year
AoA	Angle of attack, ^{o}
B	Number of turbine blade
CapEx	Capital investment cost, $/kW
C_d	Drag coefficient
C_l	Lift coefficient
C_P	Power coefficient
C_{th}	Thrust coefficient
d	Distance, m
D_{rotor}	Rotor diameter, m
ε	Diffusivity of the turbulent flow

f_b	Gravity, m^2/s
f (U)	Weibull distribution function
h_{tot}	Total enthalpy
i, j	Index of a turbine
K	Eddy viscosity, kg/(m.s)
k	Kinetic energy of the turbulent flow
l	Eddy length, m
m	Number of wind speed intervals
n	Number of turbine rows
η_g	Generator conversion efficiency
η_m	Mechanical conversion efficiency
LCOE	Levelized costs of energy, $/MWh
OpEx	Operating and maitaince cost, $/kW/year
P	Power, W
p	Static pressure, Pa
P_e	Output electrical power, W
Ps	The term that forms due to shear stress
S	Scale parameter
S_E	External sources of energy
R	Blade length, m
r	Distance from the rotor center, m
r_{cw}	Rate of change of wind speed with terrain slope
rd	Discount rate, %
T	Temperature, K
t	Time, s
TI	Turbulence intensity
Th	Thrust force, N
TSR	Tip speed ratio

U	Wind speed, m/s
U_h	Wind speeds at height h, m/s
U_{h0}	Wind speeds at height $h_{0,}$ m/s
VD	Velocity deficit
W	Width parameter
WL	Wake loss
∇	Gradient operator
α	Hellmann coefficient
ρ	fluid density, kg/m^3
ν	Air viscosity, kg/(m.s)
λ	Air conductivity, W/(m.K)
γ	Vortex sheet of strength on the airfoil surface and wake
σ	Source sheet of strength on the airfoil surface and wake
$\sigma_{\bar{U}}$	The standard deviation of average wind speed
$\Psi(x, y)$	Stream function
ω	Rotor rotation speed, rad/s

LIST OF TABLES

LIST OF FIGURES

INTRODUCTION

Statement of problem

Currently, the climate change process is happening at a faster rate and the scope of influence has spread on a global scale. The consequences of climate change are becoming increasingly serious, especially the problem of rising temperatures and air pollution. According to the WMO report [1], the average global air temperature in 2024 has increased $(1.55 \pm 0.13)^{o}C$ compared to the period 1850 - 1900. The main cause of global warming is due to the concentration of gases such as CO_2, CH_4 and N_2O in the air being too high. These gases cause the greenhouse effect, preventing the escaping processes of heat radiations from the Earth's surface. At the end of 2023, the concentration of CO_2 reached (420.0 ± 0.1) ppm, the concentration of CH_4 reached (1.934 ± 0.002) ppm, the concentration of N_2O reached (0.3369 ± 0.0001) ppm. These substances are mainly created from the burning of fossil fuels such as coal, gasoline, and oil for electricity production and human transportation. The more developed a country is, the greater its demand for electricity and transportation fuels. Therefore, it is necessary to have binding regulations and policies on a global scale to ensure a fair and sustainable development of the world. No country is left out in preventing climate change.

At COP 26, Prime Minister Pham Minh Chinh committed that Vietnam will develop and implement strong measures to reduce greenhouse gas emissions to achieve net-zero emissions by 2050. Vietnam has since taken many specific actions to implement this commitment. In particular, the Prime Minister has signed and issued a number of important projects and plans such as: Establishing a National Steering Committee to implement Vietnam's commitments at COP26 under Decision No. 2157/QD-TTg dated December 21, 2021 [2]; Approving the Project to implement the Political Declaration on establishing the Just Energy Transition Partnership (JETP) under Decision No. 1009/QD-TTg dated August

31, 2023 [3]; Approving the revised National Power Development Plan VIII under Decision No. 768/QD-TTg dated April 15, 2025 [4].

Through the declarations and the revised National Power Development Plan VIII, Vietnam will maximize the development of electricity from renewable energy, continuing to increase the proportion of renewable energy in the power structure. In particular, promoting the development of onshore, nearshore and offshore wind power in accordance with the absorption capacity of the grid system, reasonable transmission costs associated with ensuring operational safety and economy, making the most of the existing grid infrastructure. Total onshore and nearshore wind power capacity will reach about 26,066 MW - 38,029 MW in 2030, about 84,696 MW - 91,400 MW in 2050. Total offshore wind power capacity for power generation will reach about 6,000 MW - 17,032 MW in the period 2030 - 2035 and about 113,503 MW - 139,097 MW by 2050. Offshore wind power capacity for new energy production will reach about 15,000 MW in 2035 and about 240,000 MW in 2050 [4]. According to EVN's report on April 30, 2025 [5], no offshore wind power plant has been built, while the onshore wind power capacity receiving COD has only reached 1,214.5 MW. Clearly, the Vietnamese Government needs to take stronger and more practical actions to achieve the commitments and goals in the revised National Power Development Plan VIII.

According to the Government's viewpoint as issued in the revised National Power Development Plan VIII, the planning for the development of power source projects must have a long-term, effective and sustainable vision. Power development must be based on the principle of optimizing the overall factors of power source, transmission, and distribution associated with ensuring energy security and environmental protection. However, wind power projects that have been deployed in practice show many shortcomings, such as the lack of a national-scale master plan; have not mastered the technology of surveying, designing, manufacturing, installing, operating, maintaining, and handling wind turbines;

completely dependent on foreign consulting, investment, and equipment supply companies. As a result, many new factories have had incidents and accidents such as broken turbine blades, generator explosions, operating below design capacity, etc. or some wind power plants have transferred ownership to foreign corporations after signing PPA. This leads to low investment efficiency, causing energy insecurity and reducing people's trust in wind power projects in general.

Based on practical issues, this thesis has been titled "Proposed models for designing wind turbine blades and installed configurations of onshore wind farms in Vietnam". This research topic is a scientific work that can be used as a reliable reference source, helping managers and investors make more accurate decisions in the stages of surveying, planning, selecting project locations, designing, selecting turbines and optimizing the installation configuration of turbines in an onshore wind farm, in accordance with the specific features of terrain, infrastructure and wind resources.

Target, object and scope

Target of this research is to build models for designing turbine blades and wind farm configurations in Vietnam. The models are used to determine the development area, design turbine blades and installation configurations in onshore wind farms. Thereby helping to improve the operational efficiency of the onshore wind farms by maximizing the AEP value and ensuring the LCOE value is consistent with the current electricity purchase price in Vietnam.

The scope of this research is wind power generation technology using small three-bladed horizontal axis turbines. The research objects of this thesis are the blade profiles of under-100kW horizontal axis turbines and the installation configuration of onshore wind farms in Vietnam.

Scientific and practical significance

Researching, analyzing, selecting and designing turbine blades and installation locations in an onshore wind farm area is an issue of concern worldwide. This is a complex issue, involving many practical factors such as

terrain characteristics, wind resources, turbine types, infrastructure and power grids, and specific policies in each country. Therefore, this research topic has great practical significance. The design models proposed in this thesis can be widely applied and bring great benefits not only in terms of economy but also in other aspects such as environment and society. In particular, in the context of the world implementing the energy transition process and Vietnam is one of the leading countries.

The design models proposed in this thesis uses a combination of physical theories, statistical theories and computational models. Physical and statistical theories form the basic and reliable foundation for computational models implemented on computers. GIS and CFD models are the main simulation and computational models in this thesis. GIS with geographic data sources is continuously updated from satellite image data with increasingly high accuracy. Exploiting the powerful features of GIS to select suitable locations for wind farm development has high scientific significance. In addition, CFD is a state-of-the-art computational model with a combination of many advanced mathematical solutions. Establishing effective and highly accurate CFD calculation models in aerodynamic problems for wind turbines according to different terrain and wind resource characteristics is a very difficult task, with very high scientific significance. The perfect combination of GIS and CFD is being carried out by many scientific research groups in the world and increasingly brings about analysis results with almost absolute accuracy. The analysis results based on GIS - CFD in this thesis also show an error of only a few percent compared to the experiment and reality. Obviously, this combined model can contribute and has scientific significance to the global scientific community.

Research methods

To conduct the research contents in the thesis, a number of research methods have been used including:

- Method of searching, collecting, and processing information and data

online: This method is used to solve problems related to data sources such as terrain characteristics, infrastructure, wind resources, design parameters of turbines; theoretical basis of BEM, BOM, AEP, WL and LCOE; theoretical basis and data library of GIS, CFD, PM, LLFVWM models.

- Physical simulation method: Different physical theories are used to describe, analyze, and interpret the processes of movement and interaction of air flows under different specific conditions. Physical conservation equations are the basic foundation for analytical models, numerical simulations such as numerical weather forecasting, GIS and CFD models. The characteristics of terrain, infrastructure, wind resources in the interest areas will be built and displayed on digital maps based on BlenderGIS, QGIS or Ansys CFX, Fluent. Then, creating 2D, 3D models of the objects. Then, these models will be used to simulate the interaction processes of wind under different conditions. From there, the interaction processes, wake effects, energy loss when the wind blows through this area will be determined. These results will be used to calculate the operating parameters of different turbines to evaluate and select the suitable locations to install turbines in the surveyed areas.

- Statistical method: This method is based on large historical data to make forecasts. This method is implemented according to time series analysis to build wind speed frequency distribution functions in areas or wind speed distribution functions according to terrain height at different locations. These functions will provide important input data for design calculations and simulation models.

- Analytical method:

+ BEM, BOM theories combined with PM, LLFVWM, CFD models will be used to study and optimally design wind turbine blade profiles according to terrain characteristics and wind resources in the surveyed areas. From there, the most suitable turbine designs will be determined.

+ BEM, Jensen theories combined with GIS, CFD models will be used to study the optimal turbine installation configurations in the wind farm

development areas to obtain the largest AEP and reasonable LCOE. Finally, the optimal turbine installation configurations for the entire wind farm development areas will be determined.

This thesis combines the above methods to obtain values and results according to the research objects. Then, these results will be analyzed, evaluated, and compared with experimental and practical values in some specific cases.

CHAPTER I. OVERVIEW

I.1. Wind power development trends

Wind power is expected to be an alternative energy source to fossil energy sources to simultaneously solve major problems such as ensuring energy security, reducing greenhouse gas emissions, reducing environmental pollution, and ensuring sustainable development of mankind on Earth.

According to the GWEC 2025 report [6], the total installed wind power capacity worldwide has reached 1,136 GW. Of which, onshore wind power capacity has exceeded 1,000 GW, offshore wind power capacity has reached 83.2 GW. GWEC forecasts that the growth rate of global wind power capacity will be about 8.8% per year in the period 2025 - 2030. Onshore wind power still maintains strong growth momentum, offshore wind power will gradually grow. This shows that onshore wind power projects will still play a leading role in the global energy transition in the coming time.

For Vietnam, the revised National Power Development Plan VIII [4] states that the total onshore and nearshore wind power capacity will reach about 26,066 MW - 38,029 MW (14.2% - 16.1%) in 2030, about 84,696 MW - 91,400 MW (10.9%) in 2050. The total offshore wind power capacity serving power generation needs will reach about 6,000 MW - 17,032 MW in the 2030 - 2035 period and about 113,503 MW - 139,097 MW (14.7% - 16.6%) by 2050. The offshore wind power capacity for new energy production will reach about 15,000 MW in 2035 and about 240,000 MW in 2050. In the field of power transmission, penetration of large wind power is a very difficult problem. Because wind is an intermittent and highly unstable energy source. This will cause incidents in the operation of the national power transmission system. To limit the risks, studies to forecast power generation capacity or power output in the short term, medium term and long term are necessary.

The appendices attached to the revised National Power Development Plan VIII list a number of areas where onshore and offshore wind power projects are

expected to be built. However, the exact locations for these projects have not yet been determined. In addition, most of the onshore areas of Vietnam have wind speeds between 4.5 m/s and 6.5 m/s. This wind speed is significantly lower than the rating wind speed of commercial turbines on the market. Therefore, studies on the models for designing suitable turbine blade profiles and installation configurations also need to be conducted in the specific areas.

I.2. Main phases of wind power farm development

For a wind farm to be operational in practice, it needs to go through many different stages. The main stages may include: Planning; obtaining license and approval; negotiating and signing a Power Purchase Agreement; conducting Engineering, Procurement and Construction Agreement; operating, maintaining, and decommissioning.

- Planning: A wind power project needs to be well planned to shorten the time for licensing and approval. The first task of planning is to choose a strategic location for the wind power plant. To choose the best location, the characteristics of the terrain and wind resources need to be collected and evaluated. These locations need to be considered whether they are located in areas that need conservation (nature, culture), national security, or near residential areas. In addition, whether the location is close to infrastructure such as roads, rivers, power transmission systems and especially has good wind energy potential also needs to be carefully considered. After that, feasibility studies such as transportation, detailed design and grid connection will need to be carried out to evaluate the cost and investment efficiency of the project.

- Licensing and approval: Onshore wind farms need to apply for land lease and construction permits. In addition to documents related to the feasibility study phase, investors also need to have environmental impact assessment research documents attached during the project approval process.

- Negotiating and signing a Power Purchase Agreement: This type of long-term contract stipulates the price of electricity and the amount of electricity to be

supplied. The price terms in a Power Purchase Agreement are important in the development of a wind farm, as the price allows the developer to estimate the total revenue available for the terms of the contract. If the price is too low, the cash flow may not be sufficient to fund the project, leading to the project not being able to proceed with the chosen location. On the other hand, if the energy price is too high, the customers will not agree to buy at an uneconomical price. Obviously, the developers need to demonstrate what price is appropriate for each specific wind power project. Long-term forecasting of electricity production is very important for accurate pricing.

- Execution of Engineering, Procurement and Construction Agreement: The developers will execute a contract for the design, procurement and construction of the wind farm. In this contract, the contractor is responsible for all stages of the work. However, the contract for a wind farm may be different, as the developers will usually be responsible for the procurement of the components of the wind turbine and the contractor will be responsible for the procurement of the remaining materials required for construction. Studies of the terrain characteristics and wind resources play a decisive role in selecting the most suitable turbine design.

In Vietnam, EVN is in charge of implementing Power Purchase Agreement. According to Decision No. 1508/QD-BCT dated May 30, 2025 [7], the purchase price of onshore wind power in the Northern region is 1,959.4 VND/kWh, the Central region is 1,807.4 VND/kWh, the Southern region is 1,840.3 VND/kWh; the purchase price of nearshore wind power is 1,987.4 VND/kWh for all regions. According to Decision No. 1824/QD-BCT dated June 26, 2025 [8], the maximum price for offshore wind power plants in the Northern sea area is 3,975.1 VND/kWh, the South Central sea is 3,078.9 VND/kWh, the Southern sea is 3,868.5 VND/kWh. Obviously, with the current electricity purchase price calculation, investors who want to have high investment efficiency need to conduct research, choose the suitable wind turbine designs and locations for wind

farms. In addition, managers also need to conduct research closely following reality to provide more detailed prices, to ensure that the prices offered are appropriate and attract domestic and foreign investors.

Through the above analysis, the main stages play the important role, deciding the success or failure of a wind power project. In which, the problem of determining the terrain characteristics, infrastructure, and wind energy potential plays a key role in choosing a strategic location. Next, determining the type of turbine and the installation configuration in a selected farm area will play a decisive role in the operating efficiency of the turbines and the investment efficiency of the entire project. This requires detailed studies for each region, province, and locality. Because Vietnam has a long terrain, the mainland is mainly mountainous, which greatly affects the transportation and installation of turbines. A more serious problem is that the interaction of air flow when blowing through mountainous areas will be disturbed, causing energy and force losses to the components of the turbine, especially the blades.

I.3. Related research contents and methods

In general, each country in the world has its own characteristics in terms of terrain, infrastructure, wind resources, regulations and policies. Therefore, each country has its own research groups to conduct the above contents. In recent years, groups in Vietnam have also been participating in research in many fields with the aim of supporting the overall development of the wind energy sector. Related domestic and international studies:

In recent years, domestic wind turbine researches are still limited. In general, domestic research directions are mainly related to the problem of surveying and evaluating the theoretical potential of wind energy. Some notable published contents are in the article "Observation and Simulation of Wind Speed and Wind Power Density over Bac Lieu Region" by the authors at the Institute of Geophysics, Vietnam Academy of Science and Technology [9]. The authors used the WRF weather forecast model to simulate wind speed and wind power density

in Bac Lieu province, with a spatial resolution of 2.0 km. The obtained results are wind speed and wind power density in the height range from 50 m to 200 m. The simulation method based on the WRF weather forecast model is a modern method, providing high reliability and is widely used in the world. However, the basis of this method is based on weather data from NASA satellites, then based on weather data that occurred in a certain period of time in the past, and finally giving forecasts on the average wind characteristics of the area. In addition, this method has a large spatial resolution, usually about kilometers, so the accuracy is also limited. The study "Offshore wind resources in the context of global climate change over a tropical area" by the authors at VNU-Hanoi – University of Engineering and Technology [10] also used the RegCM4 weather model combined with 2 climate change scenarios RCP4.5 and RCP8.5, the spatial resolution used is 25km. The result of this study is the forecast of annual electricity production of offshore wind power in Vietnam reaching about 30.7 GWh to 50.9 GWh in the period 2080 to 2099. The method used in this study also has the same limitations as in the research paper of the authors from the Institute of Geophysics.

Also studying the forecast of wind resource potential, the study " Marine spatial planning for offshore wind power using GIS" by the researchers at Power Engineering Consulting Joint Stock Company 2 [11]. The authors used the GIS method combined with the Fuzzy Logic method to forecast some areas with potential for nearshore and offshore exploitation in Vietnam. The method is based on data based on maps of sea areas, continental shelves and regulations on the development of marine and island resources of Vietnam, then combined with analytical calculation models to determine areas with potential for wind energy exploitation. This method is not highly accurate and reliable, only suitable for the preliminary survey stage of wind resources.

The second research direction is research topics and articles on the field of calculation and design of wind turbines. The study "Study the overview of wind

turbines and the factors that affect the power output of the turbine" by the author at Quang Binh University [12]. The author has conducted an overview of some theories to determine the output capacity of a wind turbine. This publication is only intended to introduce some basic information in the field of wind turbine calculation. In addition, a study on wind turbine design that can be mentioned is "Research and calculation design for counter – rotating wind turbine use with low wind speed range" by the researchers at Hanoi University of Science and Technology [13]. The authors used the BEM method, combined with the Krangten and Glauert model to design a horizontal axis turbine with a double-blade type, the capacity of this type of turbine reaches from 1.5-5.0 kW operating at a wind speed of 6.0 -9.0 m/s. The methods are mainly based on analytical formulas, not comprehensively evaluating the influencing factors. The turbines have blade diameters of 4.2 m and 5.2 m, but generate too low power, ineffective in wind regions with speeds of 6.0 – 9.0 m/s.

Recently, a number of studies on the design of vertical axis wind turbines of the Savonius and Darrieus types have also attracted [14], [15]. These researches use different methods to design and improve the blades of vertical axis turbines. Then, the researchers use CFD methods to simulate, verify the results, and finally manufacture pilot models. These turbine designs are all compact, about a few meters in size, suitable for installation in densely populated areas such as urban areas and large cities. However, the capacity of these types of turbines is quite small, so they cannot achieve high operating efficiency.

From the analysis of domestic research topics and publications related to the field of wind energy as above, the author believes that domestic researches are still lacking in both quantity and quality. This shows that there is a need for more in-depth research, using more modern methods, especially in the field related to design, improving the operational efficiency of wind turbines.

For international researches, research on wind resource assessment for wind farm construction areas is of great interest, such as in the article “Micro-

scale wind resource assessment in complex terrain based on CFD coupled measurement from multiple masts" by German scientists [16]; or the article "Topology optimization of wind farm layouts" by Danish scientists [17]; The article "Wind energy evaluation for a highly complex terrain using CFD" by Mauritian scientists [18], etc. The methods used by these groups are all based on CFD combined with a number of different models to evaluate the wind resources at each specific location, and finally provide an optimal configuration for installing wind turbines.

In addition, there are currently tens of thousands of studies on the design and improvement of aerodynamic performance of wind turbine blades under different operating conditions around the world. For example, the article "CFD-based curved tip shape design for wind turbine blades" [19], using the CFD method to redesign the shape of the turbine blades; The article "NACA2412 airfoil based method for design and aerodynamic analysis of small HAWT using modified BEM approach" [20] using the BEM method to design small turbine blades based on the NACA2412 model; Or the article "Aerodynamic performance enhancement of horizontal axis wind turbines by dimples on blades: Numerical investigation" [21], the authors created holes on the blade surface to increase the lift force of the turbine blade, etc. Currently, most research groups in the world are focusing on changing the design of the turbine blade, designing the blade to exploit the kinetic energy of the wind most optimally. This is the most important content, contributing decisively to the problem of improving the operating efficiency of wind turbines.

In order to exploit more wind power, turbine blades are increasingly being researched and manufactured to be larger. However, we must also pay attention to the problem of the compatibility between the kinetic energy of the wind and the size of the turbine blade. This is also a very important issue to ensure the efficient operation of wind turbines. Some studies on the investigation of blade type and blade size for different wind speed conditions can be found in the article

“High-resolution direct numerical simulations of flow structure and aerodynamic performance of wind turbine airfoil at wide range of Reynolds numbers” [22], or in the article “Airfoil type and blade size effects on the aerodynamic performance of small-scale wind turbines: Computational fluid dynamics investigation” [23]. This investigation plays a very important role, however, if real models are built for testing and investigation, it will be very expensive. Therefore, research groups often use CFD analysis method, which is a very modern method and gives highly accurate results.

Through brief analysis of a number of research topics and scientific works published domestically and internationally in recent times, the author has noted some values in terms of both content and research methods needed to improve the operational efficiency of wind turbines in Vietnam. The research contents that are still lacking include:

- Research and assessment of wind energy potential of the entire territory and islands of Vietnam, thereby providing a basis for making macro forecasts on the development potential and contribution of wind power. This content has been researched by many groups and achieved many clear and reliable results.

- Research and detailed assessment of wind resource characteristics and the influence of terrain in wind farm construction areas, thereby determining optimal installation locations for wind turbines. This content has not yet received much attention and research from domestic investors and scientists.

- Research on the suitability and improvement of aerodynamic performance of wind turbine blades under operating conditions with wind speeds in each specific area. These studies are often divided into two groups: research on changing the design of the blade model, and research on changing the configuration and size of the entire wind turbine blade. This content has not yet received much attention and research from domestic investors and scientists.

- Research on the design or selection of different types of generators to solve problems related to grid connection. This content has not yet received much attention and research from domestic investors and scientists. However, this content is not studied in depth in this thesis.

- Research on the recyclability of the main components of wind turbines after they have expired and stopped operating. This content has not yet received much attention and research from domestic investors and scientists. However, this content is not studied in depth in this thesis.

Obviously, the author has inherited the research content and research methods from domestic and foreign research groups. However, there are still some contents that have not been studied clearly and accurately, such as the content on evaluating wind source characteristics according to the terrain of the specific construction area, the content on designing to improve aerodynamic efficiency and the installation configuration of wind turbines according to different specific conditions of the farm. Therefore, this thesis will conduct in-depth research on the above two contents. Regarding the research method, domestic publications often use models and methods that have been popular in the world. Therefore, the accuracy is still limited. This thesis will mainly use the CFD method combined with the GIS method to conduct simulation research. The CFD method is a method that is favored by many countries because of its clarity and high accuracy. GIS methods provide detailed terrain and infrastructure data, making farm configuration location selection intuitive and practical.

In the wind farm scope, to forecast or calculate the generating capacity or AEP, it is necessary to perform two main tasks: calculating the change in wind speed over a long period of time at the height corresponding to the turbine HUB and determining the wind energy losses caused by terrain and turbines during operation. In which, terrain factors, design and installation configuration of turbines have an impact on the characteristics of wind resources. Therefore, to

accurately determine the AEP value, it is necessary to consider the three most important input factors: wind resource, turbine type and terrain.

- Methods for forecasting changes in wind speed in the long term include:

+ Physical simulation method: Method of gradually reducing the scale from global, continental, regional, local, wind farm area based on numerical weather forecasting models. The numerical weather forecasting models can directly use real-time satellite image data or use reanalysis data libraries. This method uses a lot of data on terrain roughness, temperature, pressure, humidity, etc. as input data for physical equations [24], [25], [25], [27]. These physical equation systems can then be solved using many different techniques. In this thesis, the RANS technique will be used to solve the physical conservation equation systems for CFD models. This method is used to calculate the characteristics of terrain, wind source, and interactions with turbines on a farm. Therefore, this method requires the implementer to have high expertise and experience, along with a high-configuration computer system.

+ Statistical methods: This method is based on large historical data to make forecasts, not based on specific actual conditions. In the past, this method was often implemented according to time series analysis to construct linear and nonlinear functions. Then, based on the regression techniques Auto-Regressive Moving Average, Auto-Regressive Integrated Moving Average, and Support Vector Regression to make forecasts [28], [29], [30]. In recent years, this method is often implemented with artificial intelligence models such as neural networks, neuron-fuzzy networks, etc. In this thesis, the statistical method is used to forecast the wind speed frequency distribution functions according to different locations and heights in the farm area.

+ Machine learning or deep learning methods: AI-based forecasting methods include Extreme Learning Machines, Light Gradient Boosting Machine, Artificial Neural Network, Convolutional Neural Network, Recurrent Neural

Network, Long Short-term Memory Network [29], [31]. These models are based on relationships between historical power, wind speed and direction, and meteorological variables to make future forecasts. These models need to be fed with more historical data to get more accurate forecasts. This requires sufficient historical data for the wind farm area to be able to make reliable forecasts. In addition, the forecast models for this plant cannot be used for other plants. Therefore, these methods are facing major limitations because wind power plants in Vietnam have not been in operation for long time. Therefore, machine learning and deep learning methods are not used in this thesis. However, they will be developed in near future studies.

+ Spatial correlation method: Many mathematical models are also involved in the problem of forecasting wind speed and direction for specific terrains, such as the spatial correlation model. This model helps determine wind speed values at different locations from a specified reference point. From there, forecast models can be given for an area based on measurements and observations in another area [32]. This method can also be integrated into artificial intelligence models Artificial Neural Network, Local Feedback Dynamic Fuzzy Neural Network, Adaptive Neuro-Fuzzy Inference System [29]. This method is also not used in this thesis because of insufficient real-world data.

+ Combined method: Recently, combined forecasting studies are increasingly being developed to combine the strengths of each method. Some prominent combined models are CFD and Artificial Neural Network [33]; combines AI models such as XGBOOST, Multi-Layer Perceptron with Bayesian Optimization, Gradient Boosting Regression Tree, Ensemble (Gradient Boosting and XGBOOST), and CNN Long Short-Term Memory [29], [31], etc. This method has many advantages compared to using a single method. Therefore, the combined method is used as the basic framework. This thesis uses a combination of CFD with theoretical functions to determine the quantities related to the AEP objective function.

- Wind energy losses due to terrain and turbines: In addition to wind resource data, the input factors for this analysis include: Topography of the site and surrounding area; Wind farm configuration and turbine HUB height; Wind turbine operating characteristics such as power curve and thrust curve versus wind speeds; Air density and turbulence intensity of the incoming flow at the turbine blade locations. The combined CFD and theoretical functions are also further used to determine the interactions and wind energy losses due to terrain and turbines. GIS data is also used to provide topographical characteristics of the wind farm, providing input data for the combined CFD models.

This thesis conducts research on design models to improve the efficiency of wind energy exploitation of turbine blades and installation configuration of onshore wind farms under specific conditions in Vietnam. The main research contents include:

- Research on terrain, infrastructure, and onshore wind energy potential in planned planning areas. From there, identify strategic and optimal locations for wind farm development. The obtained results will be the input basis for developing turbine blade designs and installation configurations in the farms.

- Research and build a turbine blade design model according to the characteristics of wind resources in wind farm development areas. From there, propose turbine blade designs for the largest power coefficient.

- Research and build a turbine installation configuration design model in wind farm areas to obtain the largest AEP and reasonable LCOE.

These research contents will contribute mainly to the important stages for developing onshore wind power projects in Vietnam, which is the “Planning and Signing a Power Purchase Agreement”. The thesis uses a combination of physical methods, statistical methods through numerical simulation techniques and analytical calculations to solve the research contents.

Summary:

In order for onshore wind power projects in Vietnam to achieve high efficiency, it is necessary to ensure the AEP value is maximized and the LCOE value is consistent with the current electricity purchase price. To calculate AEP and LCOE values, it is necessary to have calculating methods based on specific conditions of terrain, wind resources, and turbine types for each specific farm in the long term. Research on these contents have not been conducted in Vietnam. This is a research gap and this thesis conducted research to fill this gap.

The state-of-the-art methods such as machine learning and deep learning are very good forecasting capabilities. However, the limitation of these methods is that they require large enough historical data to train the AI-based models. Therefore, these methods are currently not effective for wind power plants in Vietnam.

Therefore, the thesis used a combination of physical and statistical methods through GIS, CFD, PM analysis models and BEM, BOM, Jensen theories to build turbine blade profile and installation configuration design models of wind farms for the highest efficiency of wind energy exploitation. The detailed theoretical basis of these methods and theories is presented in Chapter II.

CHAPTER II. METHODOLOGY

This thesis studies 02 main contents including: Research on the turbine blade profile design model according to the characteristics of wind resources in wind farm areas. From there, the blade profile designs for the largest power coefficients are proposed; Research on the turbine installation configuration design model in wind farm areas with the goal of obtaining the largest AEP values and reasonable LCOE values.

To conduct the above main research contents, some analytical theories and simulation models need to be used including:

- GIS and CFD models to study, evaluate and select potential regions for onshore wind farms. The results from this analytical model will determine the terrain and wind resource characteristics such as terrain height and roughness, average wind speed and turbulence intensity to serve as input parameters for the turbine blade profile and installation configuration design models.

- BEM and BOM analytical theories combined with PM, LLFVWM and CFD simulation models to study the blade profiles and operating parameters of wind turbines according to wind resource characteristics with the goal of obtaining the largest power coefficients.

- BEM and Jensen analytical theories combined with GIS and CFD models to study the design of turbine installation configurations in wind farm areas with the goal of obtaining the largest AEP values and reasonable LCOE values.

II.1. GIS and CFD models

GIS is a model that provides topography data, maps of terrain and infrastructure with high accuracy based on satellite images. Therefore, this model is essential to provide 3D maps of complex objects such as urban or mountainous areas. In recent years, GIS models have been widely used in studies on site selection for wind farms [34], [35], [36]. In this study, BlenderGIS and QGIS are used as software tools to provide 3D maps of the wind farms. BlenderGIS and

QGIS are open softwares that are fully featured and easy to use for researchers who are not specialized in digital maps , [37].

CFD is a model that simulates the motion, interaction, heat transfer or reaction processes of fluids based on conservation equations such as mass conservation, momentum conservation and energy conservation. This model is commonly used in fields such as aviation, aerospace and energy systems. The conservation equations that govern fluid processes are commonly known as the Navier-Stokes equations and are often implemented in the form of partial differential equations. For example, mass conservation is often expressed through the Continuity equation; Momentum conservation is expressed through Newton's 2nd Law; Energy conservation is expressed through the 1st Thermodynamics Law as expressed in equations (2.1) - (2.3) [38], [39].

The Continuity equation:

$$\frac{\partial \rho}{\partial t} + \nabla . \left(\rho \vec{U} \right) = 0 \tag{2.1}$$

The Newton's 2nd Law:

$$\frac{\partial \vec{U}}{\partial t} + \vec{U} . \nabla \vec{U} = -\frac{\nabla p}{\rho} + \nu \nabla^2 \vec{U} + \vec{f}_b \tag{2.2}$$

The 1st Thermodynamics Law:

$$\frac{\partial \left(\rho h_{tot} \right)}{\partial t} - \frac{\partial p}{\partial t} + \nabla . \left(\rho \vec{U} h_{tot} \right) = \nabla . \left(\lambda \nabla T \right) + \nabla . \left(\vec{U} . \tau \right) + S_E \tag{2.3}$$

The conservation equations (2.1) - (2.3) are often solved through the concept of the Reynolds-Averaged Navier-Stokes (RANS) equations by Direct Numerical Simulation (DNS) method. In the field of wind energy, the flow of air is often turbulent. Therefore, turbulent flow models are often used to determine more accurately the values of wind speed and pressure at each point in space. Among them, the $k - \varepsilon$ turbulent flow model is most commonly used and has

been verified by many previous research groups [39], [40]. The turbulent flow equation system in this model is represented as in equation (2.4):

$$\begin{cases} \dfrac{\partial k}{\partial t} + U_j \dfrac{\partial k}{\partial x_j} - \dfrac{\partial}{\partial x_i}\left(\dfrac{K}{\sigma_k} \dfrac{\partial k}{\partial x_i} \right) = Ps - \varepsilon + f_b \\ \dfrac{\partial \varepsilon}{\partial t} + U_j \dfrac{\partial \varepsilon}{\partial x_j} - \dfrac{\partial}{\partial x_i}\left(\dfrac{K}{\sigma_\varepsilon} \dfrac{\partial k}{\partial x_i} \right) = \dfrac{\varepsilon}{k}\left(C_{\varepsilon 1} Ps - C_{\varepsilon 2}\varepsilon + C_{\varepsilon 3} f_b \right) \end{cases} \quad (2.4)$$

In which: x_i are the coordinates: $x_1 = x$, $x_2 = y$, $x_3 = z$; $\sigma_k = 1.0$, $\sigma_\varepsilon = 1.3$ are the Prandtl constants; $C_{\varepsilon 1} = 1.21, C_{\varepsilon 2} = 1.92$, $C_{\varepsilon 3} = 1.0$ are the coefficients of the model.

By solving the system of equations (4), the value of K and l are determined as in equation (2.5) with $C_\mu = 0.03$ for the flow of air in the surface layer [41], [42], [43]:

$$\begin{cases} K = C_\mu \dfrac{k^2}{\varepsilon} \\ l = C_\mu^{3/4} \dfrac{k^{3/2}}{\varepsilon} \end{cases} \quad (2.5)$$

II.2. BEM and BOM theories

The theory of determining the power of horizontal axis wind turbines was proposed by Betz and Glauert in the 1930s. Initially, the characteristics of the turbine were determined based on the moment theory and the blade element theory. Then, these two theories were combined into the BEM theory. Nowadays, the BEM theory is widely used in the aerodynamic design and performance analysis of horizontal axis wind turbine rotors.

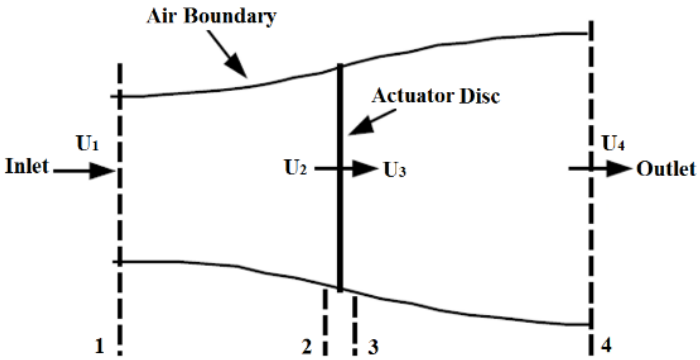

Figure 2.1. Illustration of the BEM theory.

The BEM theory assumes that the air flow will move through a control volume, which is limited by cylindrical surfaces. The turbine rotor is represented by an actuator disc as shown in Figure 2.1. The air flow moving through the control volume is assumed to be incompressible, uniform and steady [44], [45].

This theory also assumes that the number of turbine blades is infinite, the force acting uniformly on the entire actuator disc, and no vortex formation behind the turbine when rotating. Considering the above system as closed and using the momentum conservation law, the force acting on this turbine can be determined as in equation (2.6):

$$Th = U_1\left(\rho A_1 U_1\right) - U_4\left(\rho A_4 U_4\right) \tag{2.6}$$

Under steady flow conditions, the mass conservation law allows determining the air flow rate as in equation (2.7):

$$\dot{m} = \rho A_1 U_1 = \rho A_4 U_4 \tag{2.7}$$

Combining equation (2.7) into equation (6), the force acting on this turbine can be determined as in equation (2.8):

$$Th = \dot{m}\left(U_1 - U_4\right) \tag{2.8}$$

Applying Bernoulli's law to the air flow in front of the turbine:

$$p_1 + \frac{1}{2}\rho U_1^2 = p_2 + \frac{1}{2}\rho U_2^2 \tag{2.9}$$

Applying Bernoulli's law to the air flow behind the turbine:

$$p_3 + \frac{1}{2}\rho U_3^2 = p_4 + \frac{1}{2}\rho U_4^2 \tag{2.10}$$

Because the pressure at the inlet and outlet is equal to the ambient pressure, $p_1=p_4$, the air flow rate in front of the turbine and behind the turbine are equal, $U_2=U_3$. From there, the force acting on one side of the turbine is determined as in equation (2.11):

$$T = A_2\left(p_2 - p_3\right) = \frac{1}{2}\rho A_2\left(U_1^2 - U_4^2\right) \tag{2.11}$$

Combining equation (2.8) and equation (2.11), the wind speed behind the turbine rotor is determined as in equation (2.12):

$$U_2 = \frac{U_1 + U_4}{2} \tag{2.12}$$

Let a be the axial induction factor of the air flow, the value of a is determined through the change of wind speed as in equation (2.13):

$$a = \frac{U_1 - U_2}{U_1} \tag{2.13}$$

Finally, the wind power exerted on the turbine rotor is determined as in equation (2.14):

$$P = Th \times U_2 = \frac{1}{2}\rho A_2\left(U_1^2 - U_4^2\right)U_2 = \frac{1}{2}\rho A_2 U_1^3 4a\left(1-a\right)^2 \tag{2.14}$$

Let C_P be the power coefficient, which is the ratio of the power generated by the turbine to the power of the freestream before reaching the rotor plane. The value of C_P is determined as in equation (2.15):

$$C_P = \frac{P}{\frac{1}{2}\rho A_2 U_1^3} = 4a\left(1-a\right)^2 \tag{2.15}$$

Deriving equation (2.15) will find the maximum value of C_P, C_P=16/27 at a=1/3. This means that the best turbine rotor design will have a flow velocity at the rotor front plane that must be 2/3 of the freestream velocity and the highest wind energy extraction efficiency of the wind turbine that can be achieved is only 59.26% [45].

At this stage, the thrust force acting on the turbine rotor can also be determined according to a as follows:

$$Th = \frac{1}{2}\rho A_2 U_1^2 4a(1-a) \tag{2.16}$$

Let C_{Th} be the thrust coefficient, which is the ratio of the thrust force on the turbine rotor plane to the thrust force of the inlet freestream flow:

$$C_{Th} = 4a(1-a) \tag{2.17}$$

The wind power generated from the turbine rotor will be converted into output electrical power through the mechanical systems, gearbox and generator. From here, the output electrical power of the horizontal axis wind turbine can be determined as in equation (2.18):

$$P_e = \frac{1}{2}\rho A_2 U_1^3 C_P \eta_m \eta_g \tag{2.18}$$

In fact, the number of blades of the industry turbine is limited due to the limitation of installation space on the HUB. The most common number of blades is 3 blades. When considering the number of turbine blades as finite, the maximum power coefficient of the entire rotor is determined by the Wilson theory as in equation (2.19):

$$C_{P,\max} = \frac{16}{27} \times TSR \times \left[TSR + \frac{1.32 + \left(\frac{TSR-8}{20} \right)^2}{B^{2/3}} \right]^{-1} - \frac{0.57 \times TSR^2}{\frac{C_L}{C_D} \times \left(TSR + \frac{1}{2B} \right)} \tag{2.19}$$

$$TSR = \frac{\omega R}{U_1} \tag{2.20}$$

From equation (2.19), the maximum power coefficient of the turbine needs to be considered in relation to the number of blades, the tip speed ratio, and especially the ratio between the lift coefficient and the drag coefficient of the entire blade. Equation (2.20) shows that the power coefficient also depends on the rotor rotation speed during actual operation.

The ratio between the lift coefficient and the drag coefficient of the entire blade depends on the profile design, the twist angle and the length of each different section on the blade. The BOM theory is used to describe the dependence of the airfoil length, thickness, and twist angle, the tip speed ratio on the overall blade length and the total number of blades used to form a rotor. This relationship is expressed as in equations (2.21) - (2.22) [46], [47], [48], [49]:

The airfoil length at a distance r from the rotor center is determined as in equation (2.21):

$$C(r) = \frac{16\pi R}{9B\dfrac{C_l}{C_d}} \frac{1}{TSR\sqrt{TSR^2\left(\dfrac{r}{R}\right)^2 + \dfrac{4}{9}}} \tag{2.21}$$

The twist angle of the ith airfoil section at a distance r from the rotor center is determined as in equation (2.22):

$$\beta^i(r) = \arctan\left(\frac{2R}{3rTSR}\right) - AoA^i_{\max} \tag{2.22}$$

II.3. PM, FIDM and LLFVWM methods

II.3.1. Panel method

The profile of an airfoil design can be determined through characteristic quantities such as maximum thickness, maximum thickness position, maximum camber and maximum camber position as shown in Figure 2.2.

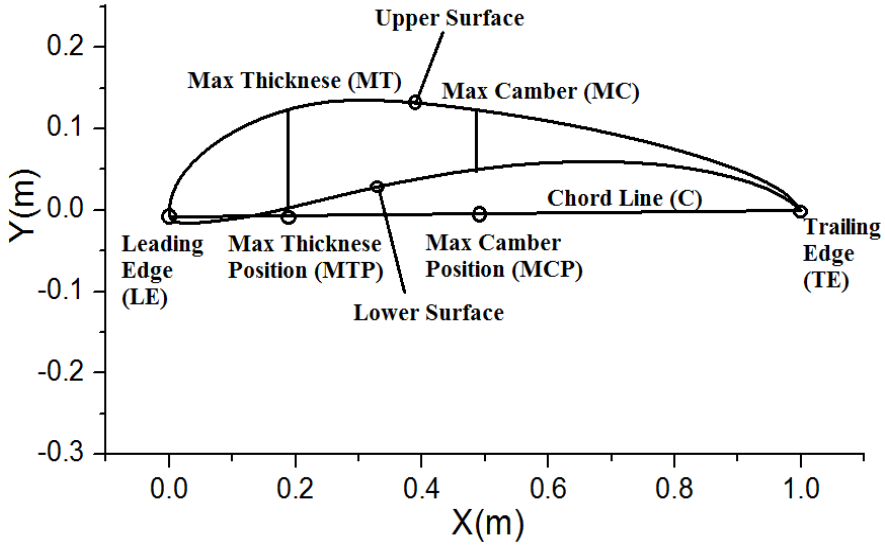

Figure 2.2. Main parameters of an airfoil profile

The PM method is used to conduct aerodynamic analysis of an airfoil model in two-dimensional space. The PM method divides the geometry of the airfoil into many equal parts or many equal panels. The number of panels depends on the requirements of the specific problem. Since each blade design is made up of many different airfoil parts, it is necessary to find the appropriate number of panels for each specific type of airfoil model. Usually, the number of panels is chosen from 90 to 250 panels. The mathematical model of PM is explained by M. Drela [50], the geometry of the airfoil model when divided into panels and determining the vortex points is illustrated in Figure 2.3.

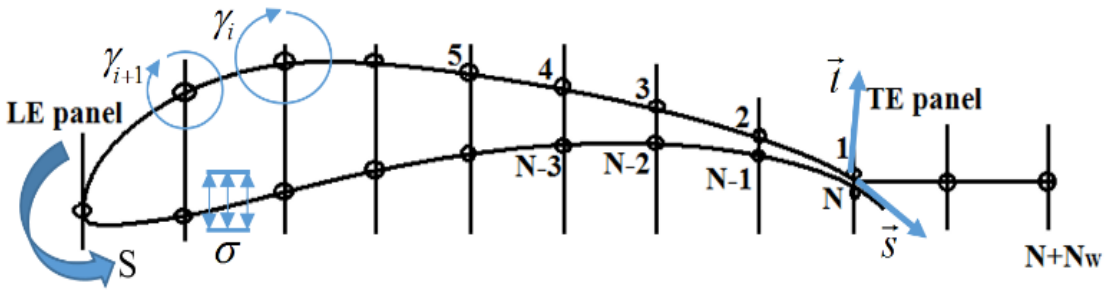

Figure 2.3. Illustrates the process of dividing the airfoil model

After determining the appropriate number of panels, the contact points between the panels and the airfoil surface will be the important points to determine the interaction processes of the wind with the airfoil surface. These interactions will be determined from the kinetic energy of the incoming flow with different

AoAs at different points. The incoming flow function at point (x, y) is determined as in equation (2.23) [50]:

$$\Psi(x,y) = u_\infty y - v_\infty x + \frac{1}{2\pi}\int_s \gamma(s)\ln r(s;x,y)ds + \frac{1}{2\pi}\int_s \sigma(s)\theta(s;x,y)ds \qquad (2.23)$$

In which: $u_\infty = U_1\cos(AoA), v_\infty = U_1\sin(AoA)$ are the velocity components of the incoming flow at any point (x,y) along the ox and oy axes.

The vorticity values at airfoil surface points are determined as in equation (2.24):

$$\gamma_i = \gamma_{0i}\cos(AoA_i) + \gamma_{90i}\sin(AoA_i) \qquad (2.24)$$

Finally, the lift coefficient, drag coefficient and pressure coefficient of the airfoil model are determined as in equation (2.25) [50], [51]. These quantities are important parameters to determine the wind energy exploitation efficiency of each airfoil design.

$$C_l = \frac{\sum_{i=1}^{N}\rho_i v_{\infty i}\gamma_i}{\frac{1}{2}\rho q_\infty^2} \;;\; C_d = \frac{\sum_{i=1}^{N}\rho_i u_{\infty i}\gamma_i}{\frac{1}{2}\rho q_\infty^2};\; C_p = 1 - \left(\frac{\sum_{i=1}^{N}\gamma_i}{q_\infty}\right)^2 \qquad (2.25)$$

II.3.2. Full-inverse design method

When the analysis of the airfoil aerodynamics model with PM has done, the obtained results will be the values of the quantities as shown in equation (2.25). This means that the geometry of the airfoil pattern is directly related to the quantities C_l, C_d and C_p. From there, if the wind velocity or C_p function is modified, the geometry of the corresponding airfoil pattern will be obtained, this is called inverse design.

The inverse design method is divided into two types, namely partial inverse design and full inverse design. The partial inverse design allows to edit wind velocity or the C_p distribution in any part of the airfoil pattern, then redesigning the corresponding part of the airfoil pattern. Similarly, full inverse design allows

to adjust the wind velocity or C_p distribution of part or whole pattern of the airfoil, then redesigning the entire airfoil pattern. Both these inverse design methods are based on conformal mapping method [50], [52], and this paper uses full inverse design method. Figure 2.4 illustrates the process of editing the wind velocity distribution on the airfoil surface, and then creating a new airfoil configuration. The black line is the value of the original airfoil pattern, the blue line is the modified values for the new one.

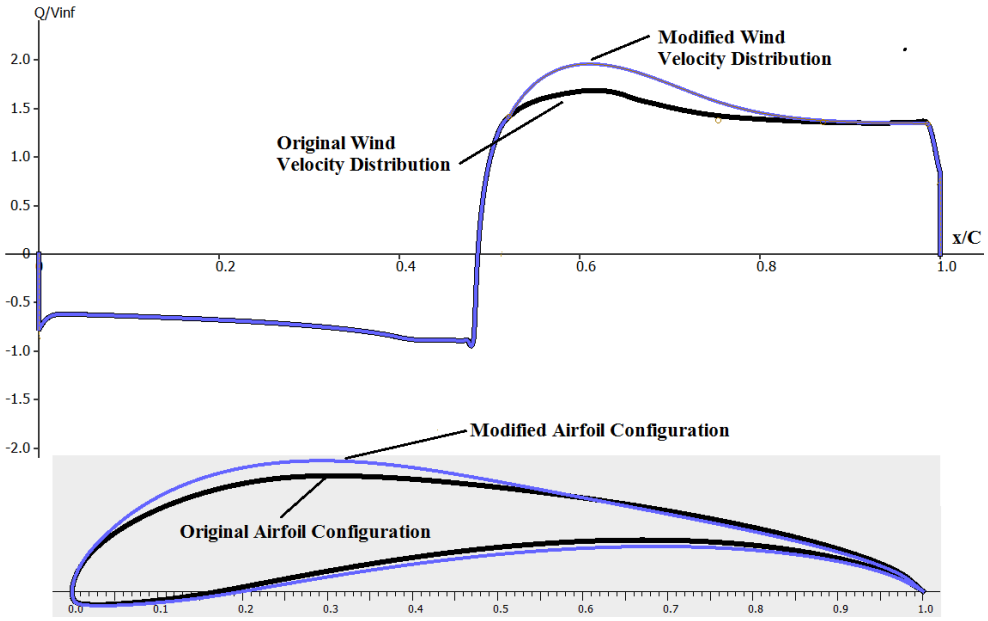

Figure 2.4. The airfoil redesigning process by modification of wind velocity distribution.

After editing the wind velocity distribution or C_p distribution, the new corresponding airfoil pattern will be received, but the parameters of the airfoil pattern may not meet the requirements. To complete the new pattern parameters, the MT, MTP, MC and MCP values can be changed by entering exact numbers. Then all new models will be analyzed by PM method to find out the airfoil model with the largest C_l/C_{dmax}.

II.3.3. Lifting line free vortex wake method

Qblade is a multiphysics software, that is widely used in preliminary design of horizontal and vertical axis wind turbine systems on both onshore and offshore. Qblade software uses the LLFVWM method to determine the aerodynamic

parameters of turbine blade. Unlike the wake approximation as in the traditional BEM method, the LLFVWM method will model explicitly the rotor wake through Lagrangian vortex elements. Therefore, the analysis results of wake effects on rotor using LLFVWM give higher accuracy when compared with BEM [53].

In Qblade software, the blades will be divided into sections corresponding to the airfoil models and designed dimensions. Initially, the forces acting on the blades will be determined by the LLFVWM method through two dimensional sectional airfoil polar data, and the shed from the blades will be explicitly resolved. The two dimensional sectional airfoil polar data will be determined by the panel method (PM) [50] for a specified range of angle of attack (AoA) values, and then extrapolated to the entire 360° angle. The model of a blade in Qblade software as shown in Figure 2.5.

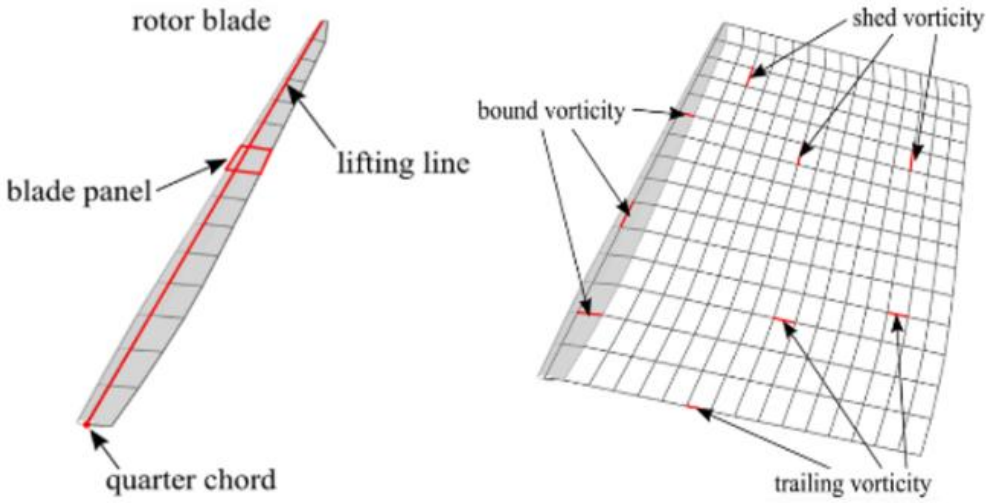

Figure 2.5. A blade and wake model with the LLFVWM [53]

Each blade will be represented by a lift line located at the chord quarter of the 2D airfoil model. The entire blade will be divided into a number of panels, each panel is represented by a vortex ring which consists of four straight vortex filaments as shown in Figure 2.5. The circulation of the bound vortex lines is calculated from the relative inflow velocity. The lift and drag coefficients that are obtained from tabulated airfoil data. The sectional circulation is calculated

according to the Kutta-Joukowski theorem, then the i[th] sectional lift force at the AoA is determined by the equation (2.26) [53]:

$$\partial F_{Li}(AoA) = \rho V_{rel} \partial \Gamma_i \tag{2.26}$$

Then, the aerodynamic characteristics of the entire blade such as lift force, drag force and other secondary effects will be determined in detail through a number of different mathematical models such as OYE or IAG. Previously, the model describing dynamic stall in Qblade could be implemented by using either the unsteady LLFVWM or BEM via the OYE Model. However, this model only calculates the dynamics of separated flow of airfoil. Additionally, the AoA values is only determined in the range from -50^o to 50^o. Recently, the IAG dynamic stall model has been developed and widely used. This model replaces the previous models in Qblade. In the group's latest research, the authors have proposed an improved IAG mathematical model and compared it with other models and experiments based on airfoil models such as S801, S809 and S814. The IAG model in a state-space will divide the flow into three states: attached flow, separated flow and vortex lift state. Finally, the lift and drag coefficients of the blade's sections in space are determined as equations (2.27) and (2.28) [54]:

$$C_{Li}^D = C_{Ni}^D \cos(\mathrm{AoA}_i) - C_{Ti}^D \sin(\mathrm{AoA}_i) \tag{2.27}$$

$$\begin{aligned} C_{Di}^D &= C_{Di}^{VI} + (AoA_i - AoA_{ei}) C_{Ni}^C \\ &+ \left(C_{Di}^{VI} - C_{D0}^{VI}\right)\left[\left(\frac{1-\sqrt{x_4(t)}}{2}\right)^2 - \left(\frac{1-\sqrt{f^{VI}}}{2}\right)^2\right] + x_5(t)\sin\alpha_i \end{aligned} \tag{2.28}$$

Where: $C_{Ni}^D = C_{Ni}^f + C_{Ni}^V$ is the normal force; $C_{Ti}^D = C_T^{VI}(AoA_{fi})$ is the tangential force; $C_{Di}^{VI}, C_{D0}^{VI}, f^{VI}$ are the static values of drag coefficient, drag level at the zero normal force AoA and static separation position, respectively; x4(t) is the unsteady trailing edge separation point; x5(t) is the normal force due to the vortex lift effect.

The results published by this group show that the current IAG model in Qblade software has helped to overcome the limitations of previous models related to dynamic stall of airfoil patterns. This new model can cover the effects of unsteady flow parameters, airfoil thickness, large changes in Reynolds number, AoA changes from -180^{o} to 180^{o} and also the problem of surface roughness of the airfoil models. Consequently, the aerodynamic analysis results of wind turbine blades using Qblade software are highly accurate and reliable.

II.4. Jensen, AEP, WL and LCOE theories

Once a wind farm has been sited, turbines will be installed in different configurations depending on factors such as terrain, infrastructure, wind speed, wind speed frequency and main wind direction. Some issues that need to be carefully considered include the type of turbine that must be suitable for the wind energy potential and how to arrange these turbines to minimize the effects on each other during operation. Of these, the wake effects are the most concern. Wind energy loss from the wake effects can come from the roughness of the terrain or from the operation of the turbines. The theory of calculating the wake effects is intended to determine the effects on the output power of the turbines when their distance is different. When the blades of the front turbine rotate, it will create wake flows behind. This wake region is gradually expanded with distance behind that turbine as shown in Figure 2.6. The wake will cause an increase in turbulence intensity and reduce the air flow velocity to the behind turbines [55].

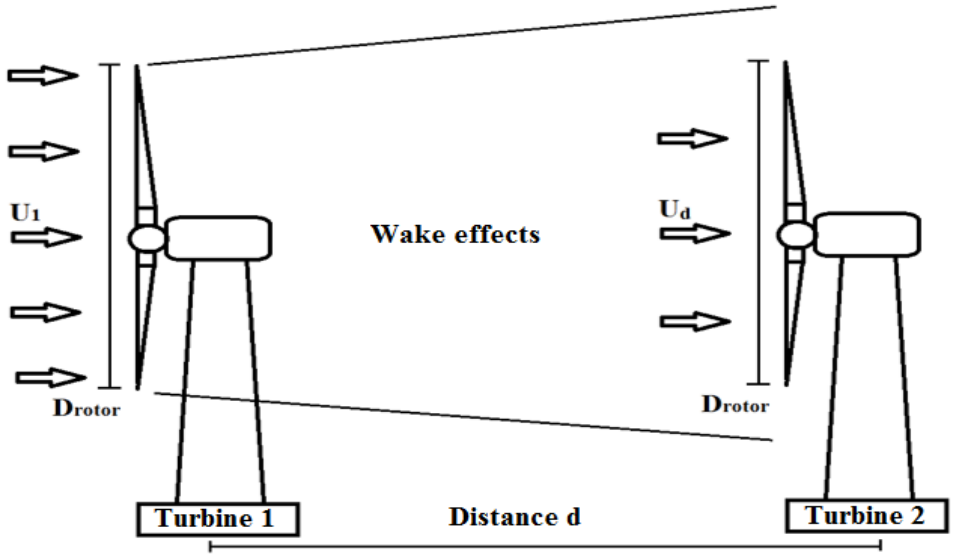

Figure 2.6. Illustration of the wake effect caused by a turbine

When considering the wake effects on the behind turbines, the two main contributing components are the wind velocity deficit and the turbulence intensity. The wind speeds at these different locations are affected by wake due to both the forward turbines and the terrain slope. Obviously, the value of U_d can be determined through some approximate assumptions for the terrain type and turbine type. However, in this study, the exact values of U_d will be determined by a modern method based on a combined GIS - CFD model. The balance equation between the vortex moment and the wind velocity deficit is determined according to Jensen theory as in equation (2.29) [56], [57]:

$$U_d = U_1 \left[1 - \frac{a}{\alpha_d \dfrac{d}{D_{\text{rotor}}}} \right] \tag{2.29}$$

Because each area has a different terrain slope, the rate of change of wind speed with terrain slope (r_{cw}) needs to be determined by the combined GIS - CFD method. r_{cw} is the rate of change in wind speed caused by the surface roughness of the wind farm terrain. A given terrain area will have a function of r_{cw} along the main wind direction (along the turbine rows). Based on the function of r_{cw}, the change in wind speed at different locations in the same row can be

determined. From there, it is only necessary to determine the wind speed at one point in the farm area to interpolate the wind speed at other points. This helps to accurately determine the wind speed at each point where turbines are expected to be installed in the farm area. The r_{cw} function can be determined by experimental measurements, or using the CFD simulation method. In this thesis, r_{cw} is determined by the GIS - CFD model. For a terrain area, it is only necessary to build a GIS - CFD model once using the average wind speed to determine the r_{cw} function. The wind speed at the behind turbine at a distance will be multiplied by r_{cw} as shown in equation (2.30):

$$U_d = r_{cw} U_1 \left[1 - \frac{a}{\alpha_d \dfrac{d}{D_{\text{rotor}}}} \right] \tag{2.30}$$

Then, the wind velocity deficit (VD) at point d behind the first rotor is determined as in equation (2.31):

$$VD = \left(1 - \frac{U_d}{U_1} \right) \times 100\% = \left(\frac{a}{\alpha_d \dfrac{d}{D_{rotor}}} \right) \times 100\% \tag{2.31}$$

With α_d is a decay coefficient, $\alpha_d = 0.075$ for onshore wind farms [57].

The turbines are typically installed in rows and each farm will have multiple rows of turbines depending on the actual conditions. The annual electricity production of the turbines can also be determined according to equation (2.32) [58], [59]:

$$AEP = 8760 \sum_{i=1}^{n} \sum_{j=1}^{m} \left(Pe_j^i \times f_j^i \right) \tag{2.32}$$

Where: n is the number of turbine rows; m is the number of wind speed intervals; Pe_j^i is the turbine's output power for wind speed interval j at row i,

kW; f_j^i is the Weibull distribution function value of wind speed interval j at row i.

The Weibull distribution function is expressed as in the equation (2.33):

$$f(U) = \left(\frac{\mathrm{W}}{S}\right)\left(\frac{U}{S}\right)^{\mathrm{W-1}} E\,\mathrm{xp}\left(-\left(\frac{U}{S}\right)^{\mathrm{W}}\right) \tag{2.33}$$

With W and S are the width and scale parameters of the wind speed distribution, respectively.

The parameter that causes the largest error for AEP is the wind speed frequency. Therefore, the error of AEP will be determined by the error propagation method through the output power and Weibull distribution function as follows:

$$\Delta AEP = 8760\sum_{i=1}^{n}\sum_{j=1}^{m}\left(\Delta Pe_j^i f_j^i + Pe_j^i \Delta f_j^i\right) \tag{2.34}$$

With:

$$\Delta Pe_j^i = \frac{1}{2}\rho\pi R^2 C_p \eta_m \eta_g 3\left(U_j^i\right)^2 \Delta U_j^i \tag{2.35}$$

$$\Delta f_j^i = \frac{\mathrm{W}}{S^2} Exp\left(-\left(\frac{U_j^i}{S}\right)^{\mathrm{W}}\right)\left[\left(\mathrm{W}-1\right)\left(\frac{U_j^i}{S}\right)^{\mathrm{W-2}} - \mathrm{W}\left(\frac{U_j^i}{S}\right)^{2(\mathrm{W-1})}\right]\Delta U_j^i \tag{2.36}$$

Where: ΔAEP is the absolute error of AEP, kWh/year; Δf_j^i is the absolute error of wind speed frequency at the (i,j) turbine's HUB; ΔU_j^i is the absolute error of wind speed at the (i,j) turbine's HUB, m/s.

The wake loss can be determined as in equation (2.37):

$$\mathrm{W}L = \left(1 - \frac{AEP}{AEP_{no-wake}}\right)\times 100\% \tag{2.37}$$

Where: AEP and $AEP_{no-wake}$ are the annual electricity production with and without wake effects, respectively.

LCOE is an important parameter for investors to make investment decisions on any wind power project. In addition, electricity market managers in Vietnam

such as EVN also need to rely on actual LCOE to advise the Ministry of Industry and Trade to issue electricity purchase prices for the power purchase agreements. LCOE calculation models need to consider many factors such as land rental, equipment purchase, transportation, installation, operation, maintenance, etc. However, many published studies have shown that the costs should be grouped into two parts: capital investment cost (CapEx) and operating cost (OpEx). The LCOE value for an onshore wind farm can be determined as shown in equation (2.38) [60], [61]:

$$LCOE = \frac{CapEx + \sum_{i=1}^{T} OpEx_i \left(1+rd\right)^{-i}}{\sum_{i=1}^{T} AEP_i \left(1+rd\right)^{-i}} \quad (2.38)$$

II.5. Research methods

This thesis uses a combination of physical and statistical methods as the basis for analytical calculations and numerical simulation models. These models will be combined to create the models for designing turbine blade profiles and installation configurations in wind farms. The powerful features of the methods will be exploited through the specific models proposed in the thesis. In addition, a number of other methods are also used to support the construction of design models, specifically including:

- Methods of searching, collecting, and processing information and data online: This method is used to solve problems related to data sources such as terrain characteristics, infrastructure, wind resources, design parameters of turbines; theoretical basis of BEM, BOM, AEP, WL and LCOE theories; theoretical basis and data library of GIS, CFD, PM, LLFVWM analytical models.

- Digital map construction method: The characteristics of terrain, infrastructure, wind resources in areas of interest will be built and displayed on digital maps based on software tools BlenderGIS and QGIS or Ansys CFX and

Fluent. From there, create 2D, 3D models of the objects to study, evaluate, select the most suitable locations.

- Digital simulation method: The 2D, 3D models of the onshore wind farm areas will be used to simulate wind interaction processes under different conditions. From there, the interaction processes, the influence of eddies, and energy losses when the wind flow blows through these areas will be determined. These results will be used to calculate the operating parameters of different turbines to evaluate and select the most optimal locations to install turbines in the surveyed areas.

- Analytical calculation method:

+ BEM, BOM theories combined with PM, FIDM, LLFVWM, CFD models are used to study and design optimal wind turbine blade profiles according to terrain characteristics and wind resources in the surveyed areas. From there, the most suitable optimal turbine blade profile designs for the surveyed areas will be determined.

+ BEM, Jensen, Weibull theories combined with GIS, CFD models are used to study the optimal turbine installation configurations in the wind farm development areas to obtain the largest AEP values and reasonable LCOE values. Finally, the optimal turbine installation configurations for the entire wind farm development areas will be determined.

Summary:

This thesis uses physical and statistical theories such as the laws of conservation of mass, energy, momentum through BEM, BOM, Jensen, Weibull to calculate the aerodynamic parameters of turbine blades and the values of AEP, WL, LCOE for wind farms.

Numerical simulation and analytical models such as GIS, CFD, PM, FIDM, LLFVWM are used to carry out the stages in building the models for designing turbine blade profiles and installation configurations of onshore wind farms.

CHAPTER III. A PROPOSED MODEL FOR DESIGNING WIND TURBINE BLADE PROFILES

III.1. Changes in wind speed according to terrain and altitude

Vietnam has a territory stretching from North to South, the terrain is mainly mountainous. The terrain elevation increases gradually from East to West. Wind direction changes seasonally and regionally, mainly from Southwest and Southeast, sometimes from Northeast.

When the air flow moves, the characteristics of the wind resources will depend greatly on the terrain. Because air is a type of fluid, the properties and shape of the fluid generally depend on the environment around them. The moving air flow will change its state continuously with three forms: laminar flow, transition flow and turbulent flow. At each state, the important properties such as direction, flow, density, viscosity, etc. will change accordingly. Therefore, with the same initial wind resources, but when moving to different terrain areas, almost all of their properties will be changed. Therefore, it is necessary to have detailed and specific research for each area according to the terrain characteristics and wind resource to ensure that all processes occurring are calculated in advance and ensure that the turbines will exploit the most energy efficient during the entire operating life of the wind farms.

In order to accurately describe the air flow processes, some important initial parameters need to be clarified such as: Direction, speed and turbulence intensity of the incoming flow; The surrounding material layer, in direct contact with the flow, is often called the Boundary Layer. At the contact surface with the Boundary Layer, the flow speed will be zero. The roughness of the Boundary Layer will greatly affect the formation of friction with the air layer in direct contact, thereby creating turbulent, eddies, and opposite-direction flow regions as illustrated in Figure 3.1. This leads to loss of flow energy and other problems such as vibration (fatigue problem), noise (health problem) for the turbines during operation. It is

necessary to clearly determine the width of this interaction zone to avoid unnecessary impacts and losses on the actual operation of the turbines.

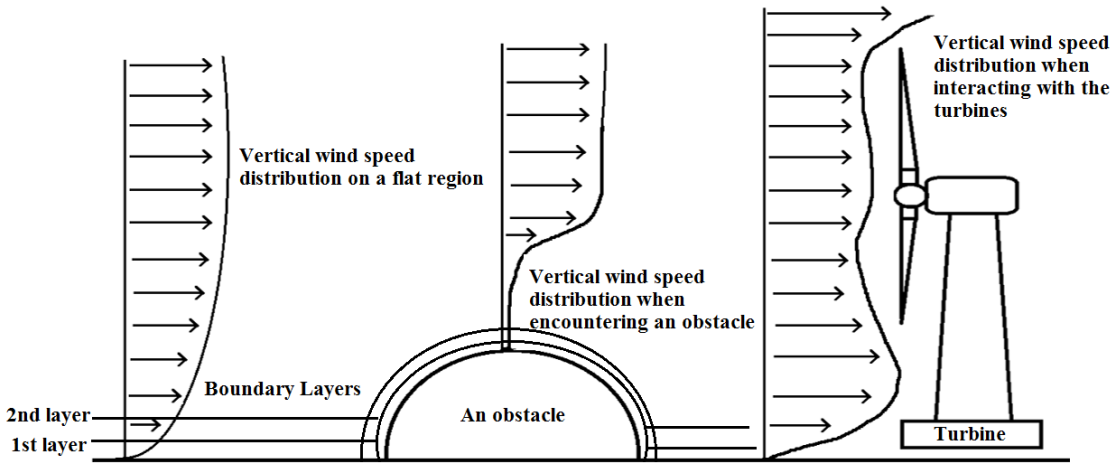

Figure 3.1. Illustration of the wind speed distributions

Wind turbines are usually located 100 m above ground level, so the wind speed distribution functions with height need to be determined as accurately as possible. The wind speed distribution with different heights and terrains is often described by the Hellmann wind speed ratio function as shown in equation (3.1) [45]:

$$\frac{U_h}{U_{h_0}} = \left(\frac{h}{h_0} \right)^{\alpha} \tag{3.1}$$

The values of the Hellmann coefficient vary with different terrain types over a wide range. If considering at each point in a narrow range, it is necessary to use actual measurement systems or CFD numerical simulation models to determine the exact Hellmann coefficient values.

In addition, wind flow often exists in a turbulent state. The turbulent flow state is characterized by the turbulence intensity as defined in equations (3.2) - (3.4) [45]:

$$TI = \frac{\sigma_{\bar{U}}}{\bar{U}} \tag{3.2}$$

$$\overline{U} = \frac{1}{N_s}\sum_{i=1}^{N_s} u_i \tag{3.3}$$

$$\sigma_{\overline{U}} = \sqrt{\frac{1}{N_s - 1}\sum_{i=1}^{N_s}\left(u_i - \overline{U}\right)^2} \tag{3.4}$$

Where N_s is the number of data recordings; u_i is the wind speed recorded at each measurement, m/s.

Vietnam's territory is mainly mountainous, with large differences in altitude. Therefore, it is necessary to conduct research for each area where the farm is planned to be built in order to determine the most accurate wind speed distribution.

In this study, the mountainous area of Ninh Phuoc commune, bordering the two former provinces of Ninh Thuan and Binh Thuan, which has a large wind source, was selected for building a wind farm model. To accurately model the terrain of this area, it is necessary to use Google Earth satellite image data. This data is integrated into the BlenderGIS or QGIS software tools. The softwares will be used to collect and create 2D or 3D topographic map data of this area. Then, the 3D terrain map will be converted to the format of Ansys CFX or Fluent softwares to carry out boundary condition settings, initial conditions, turbulence models and analyze aerodynamic quantities based on the CFD method. The interaction processes of incoming flow with terrain obstacles will be shown in images, graphs, wind speed distribution functions according to heights at diffirent points such as valleys, slopes, mountain peaks, etc. From there, we can determine the best locations for selecting and installing wind turbines.

The flowchart analyzing terrain characteristics and wind resources in the area corresponding to a wind farm is shown in Figure 3.2.

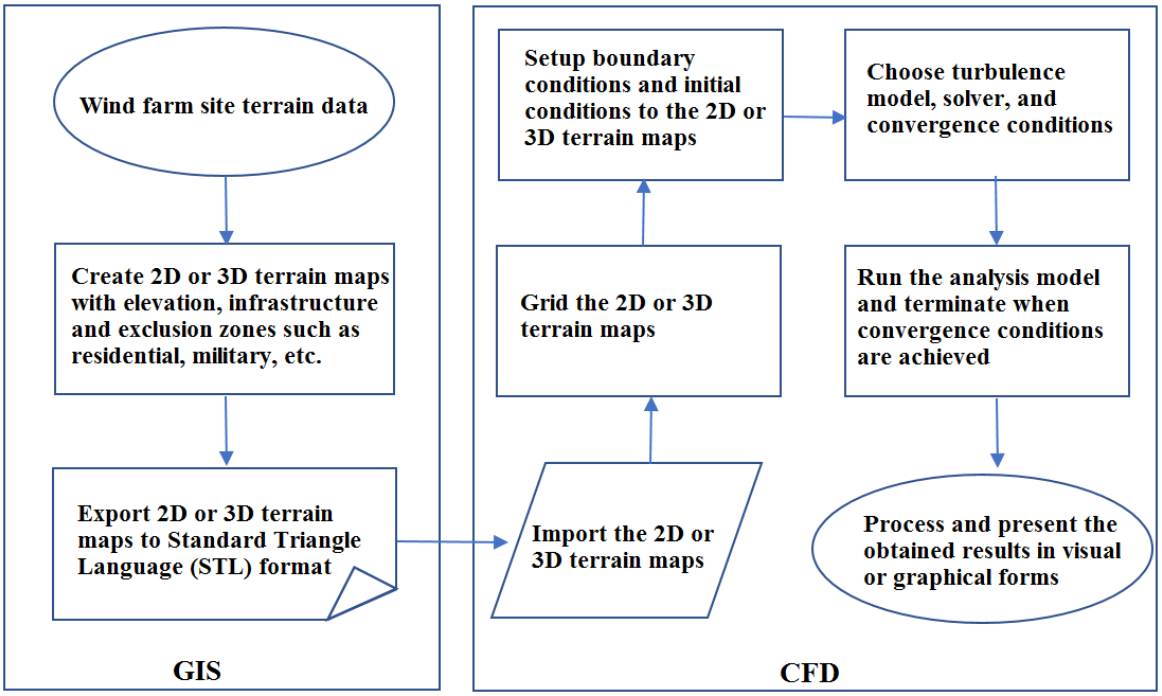

Figure 3.2. The flowchart analyzes terrain characteristics and wind resources

Following the steps in Figure 8, the terrain and infrastructure data of the Ninh Phuoc commune area were firstly modeled using BlenderGIS software and then transferred to Ansys CFX software for completion. The model has a rectangular shape with a width of 12,040 m, a length of 16,882 m and a height of 936 m above sea level as shown in Figure 3.3.

(a)

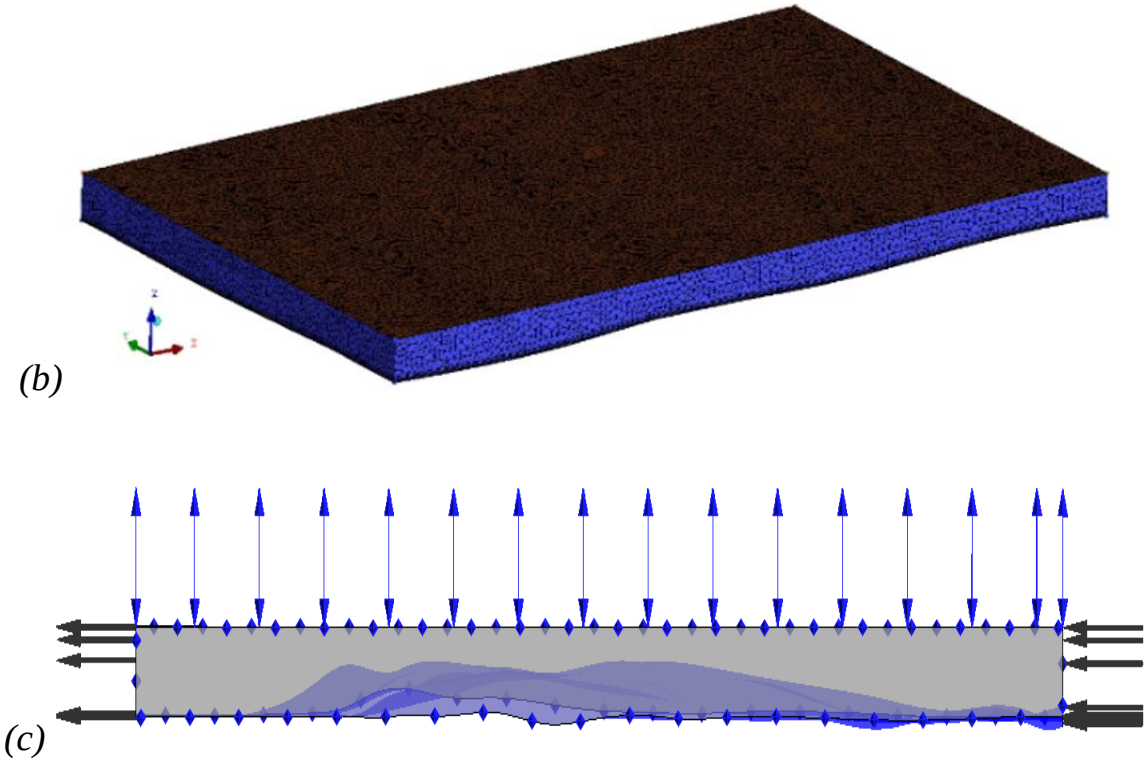

Figure 3.3. Modeling the terrain of the wind farm development area on BlenderGIS (a) and Ansys CFX (b),(c)

The model was then divided into smaller spaces to apply the numerical solution methods, the grid size was 200 m, meaning that the spatial resolution in the horizontal plane was 200 m. The grid type used was a combination of Quadrilateral and Hexagonal grids. The boundary mesh layer in contact with the ground surface has a thickness of 10 m, each subsequent layer has a thickness 1.2 times greater than the previous layer, the total number of boundary layers is 5 layers. The total number of meshes of this model is 384,766 meshes, the meshing quality of the entire model is about 0.85.

To determine the initial conditions of the wind speed distribution for the model, data provided by the WorldBank at heights of 10 m, 50 m, 100 m, 150 m and 200 m were exploited. This is a data source presented in atlas form and is widely used in global wind energy studies. These data are shown in Figure 3.4 and Table 3.1 [62].

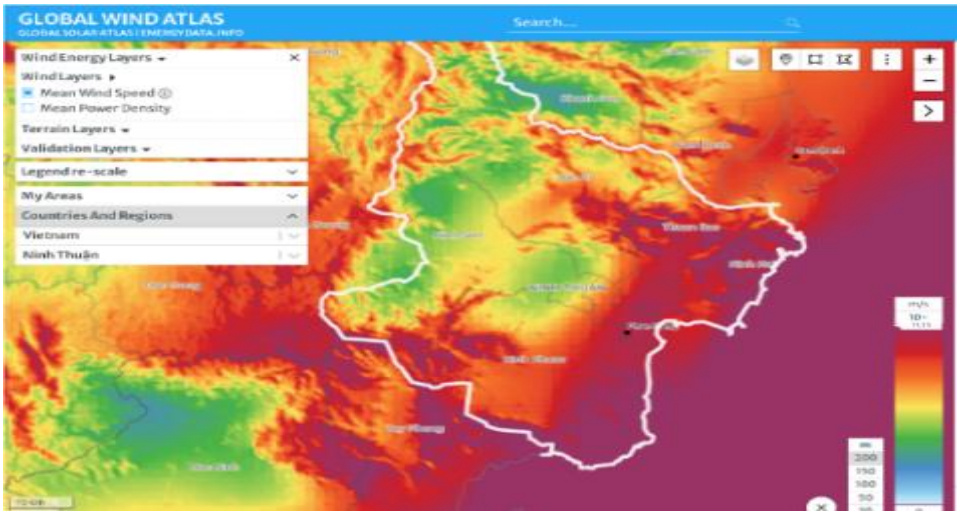

Figure 3.4. Wind resource data provided by the WorldBank

Table 3.1. Average wind speed distribution by height in the Ninh Phuoc area

No.	h, m	$\overline{U}$, m/s
1	10	8.2
2	50	9.5
3	100	10.4
4	150	10.9
5	200	11.3

Model Reliability Assessment:

According to reference [63], the Pacific Northwest National Laboratory conducted wind resource characteristic measurements from November 16, 2010 to March 21, 2012 in northeastern Oregon. This project provided experimental data on wind speed and wind direction in this complex terrain area, according to the altitude of the atmospheric boundary layer. The measurements used anemometers, propellers, and ultrasonics mounted on a 62 m high tower and a wind analysis radar to collect and process the data. The coordinate location of this tower is (45.9551^{o}N, -118.6877^{o}W) as marked in Figure 3.5. The wind resource and terrain data of this area are very complete, so this area was selected to evaluate the reliability of the proposed method.

Figure 3.5. Topography of the area around coordinates (45.9551°N, -118.6877°W).

Following the steps in Figure 3.2, the terrain data of the area around the coordinates (45.9551°N, -118.6877°W) was collected in BlenderGIS and the boundary and initial conditions in Ansys CFX were set up similar to those in Figure 3.3. These parameters have been used in some previously published studies [64], [65]. This model has a total of 994,735 elements and 210,697 nodes. Using a computer configuration with a core i7 processor and 128Gb ram, the analysis run time is about 30 minutes for a model.

The average wind speed values at 5 different altitudes are shown and fitted in Figure 3.6. This theoretical fitting function represents the relationship between wind speed distribution and height for terrain surfaces with different characteristic roughnesses. The theoretical fitting function obtained from Figure 3.6 is shown in equation (3.5) with a Hellmann exponent of 0.12, which is used to establish the height-averaged wind speed value at the input plane of the simulation model:

$$WindSpeed = 6.14 \times \left(\frac{h}{10} \right)^{0.12} \tag{3.5}$$

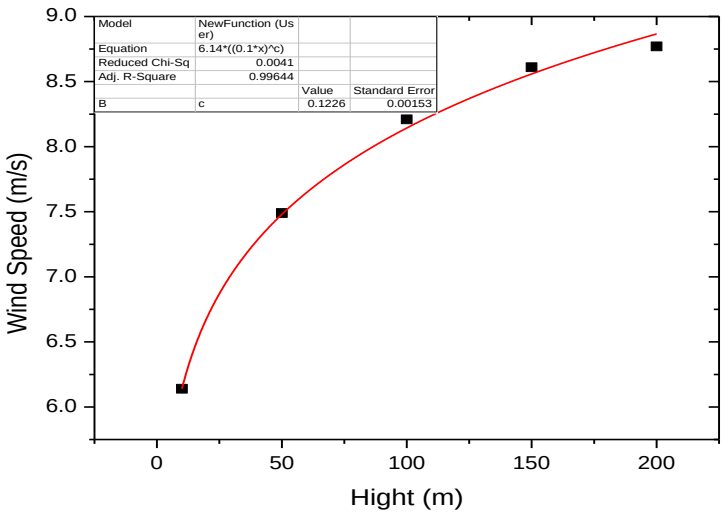

Figure 3.6. Height-averaged wind speed distribution obtained from WorldBank data [62]

From equation (3.5), the average wind speed at 62 m height is calculated to be 7.64 m/s, which is very close to the experimental measurement value of 7.7 m/s by the Pacific Northwest National Laboratory [63]. In this case, the deviation between the values obtained from the model and the experiment is only about 0.8%. This proves that the input data and simulation model built in this study are highly reliable. Furthermore, according to reference [66], the wind speed at an altitude of 80 m in the coordinate region (45.9551°N, -118.6877°W) has a value of about 7.5 m/s to 8.0 m/s as shown in Figure 3.7. This value is very consistent with the values obtained from equation (3.5). This further confirms the reliability of the wind speed distribution function according to altitude used in this research model.

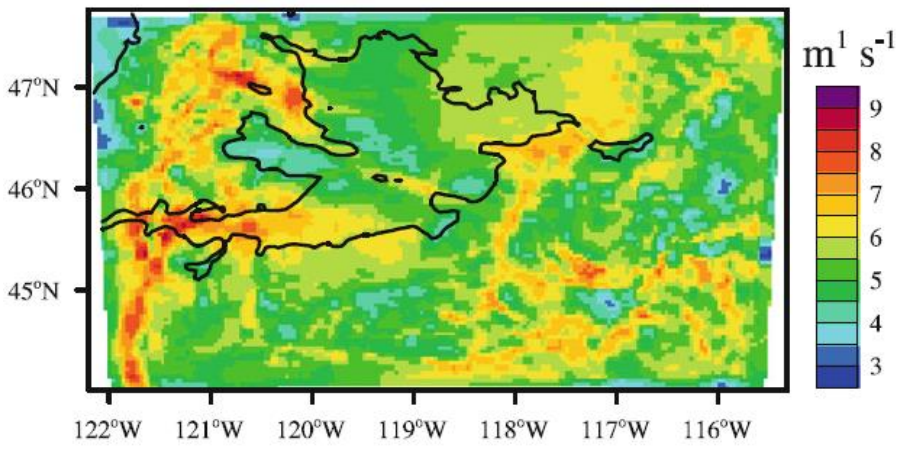

(a)

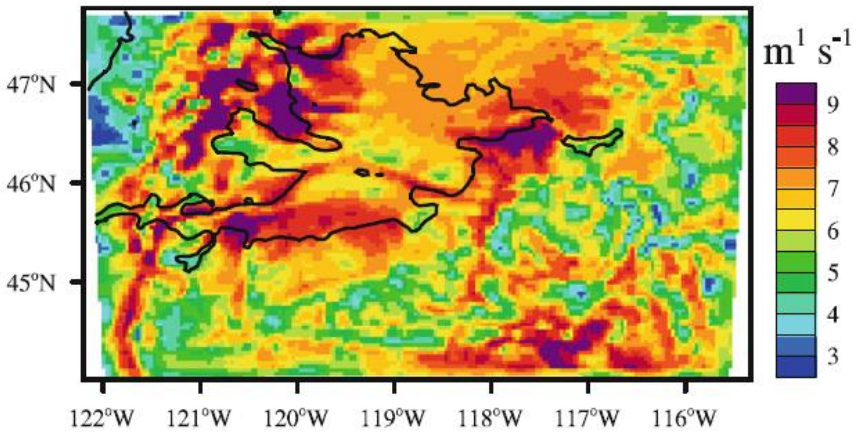

(b)

Figure 3.7. Average wind speed at an altitude of 80 m: (a) Day, (b) Night [66]

After confirming the reliability of the model, the Ninh Thuan model will be run for analysis in steady state with a total of 500 iterations. After the solution process is finished, to have an overview of the wind speed distribution in the entire model, the wind speed distribution in 3D space is processed and shown in Figure 3.8.

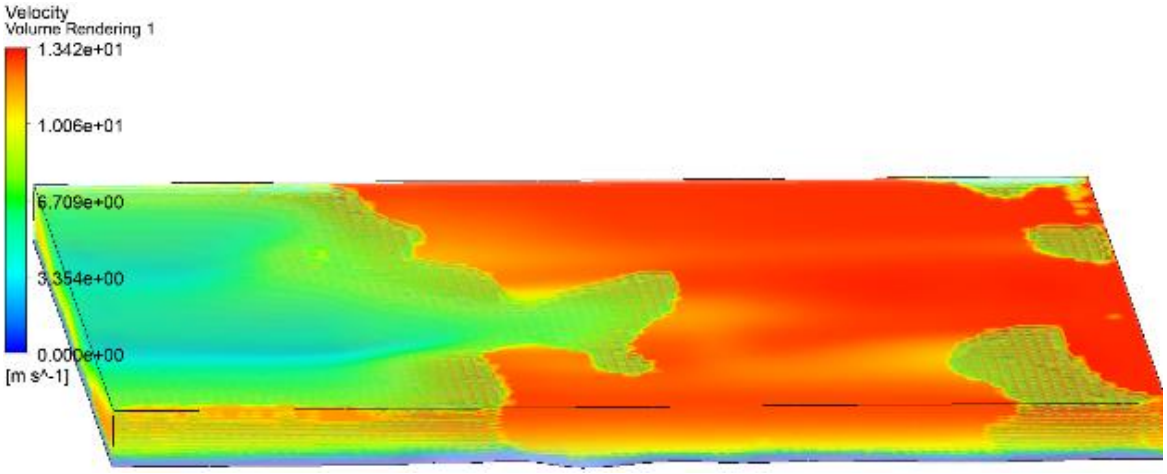

Figure 3.8. Wind speed distribution in 3D space

Figure 3.8 shows that the front mountain slope area, blowing from the East Sea direction, will give higher wind speed values than other areas. On the contrary, the behind mountain slope area, the western slope, gives very low wind speed. The reason for this difference can be roughly explained that when the wind meets the front mountain slope, the space will be narrowed, leading to the wind speed having to increase to ensure the law of mass conservation. In the case of

wind going to the back slope, the wind flow will be formed into vortexes due to friction with the rough terrain surface, from which the wind directions will be canceled out, leading to a significant decrease in the value of wind speed. The wind speed distribution in the cross section at different heights is shown in detail in Figure 3.9.

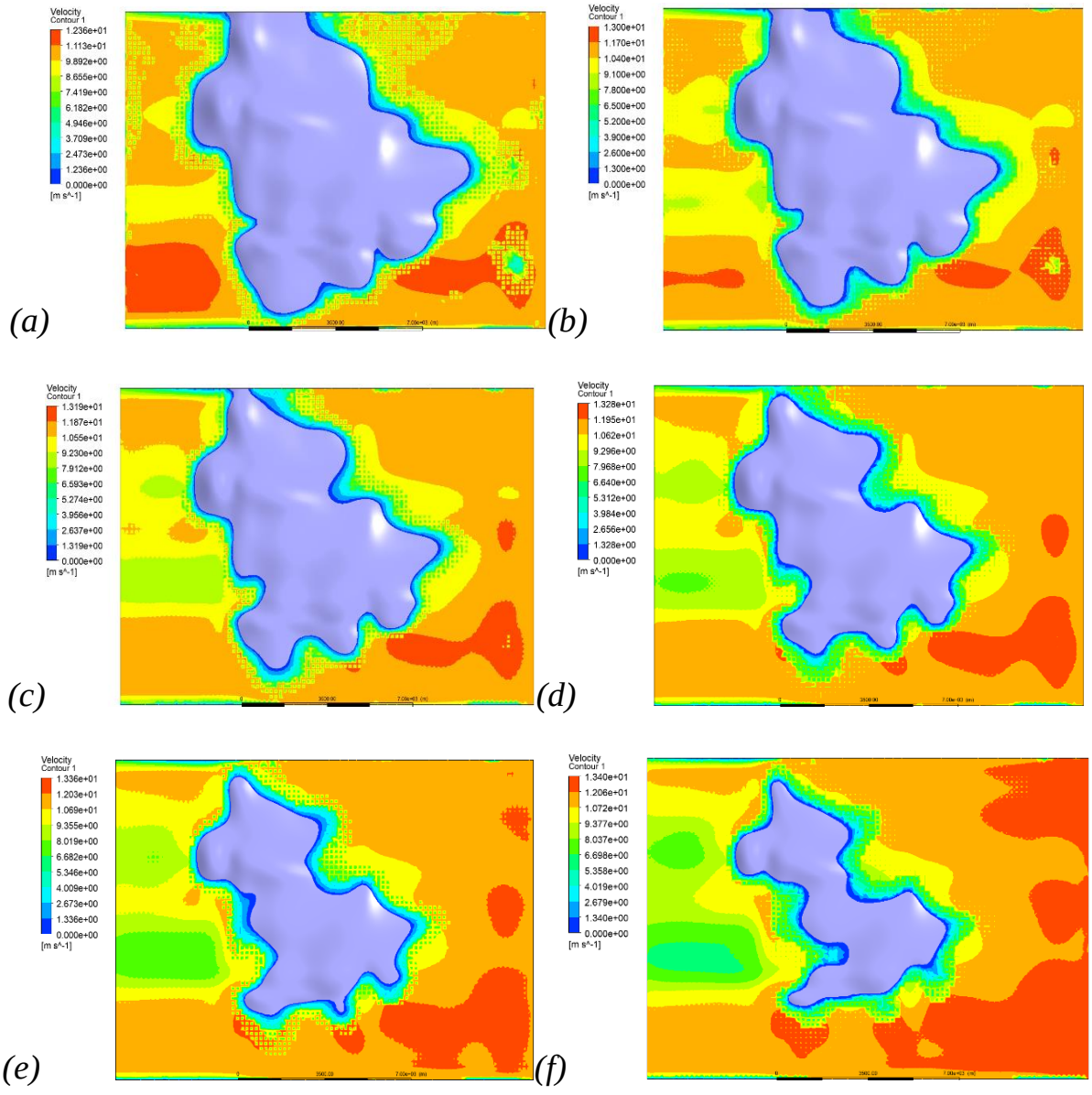

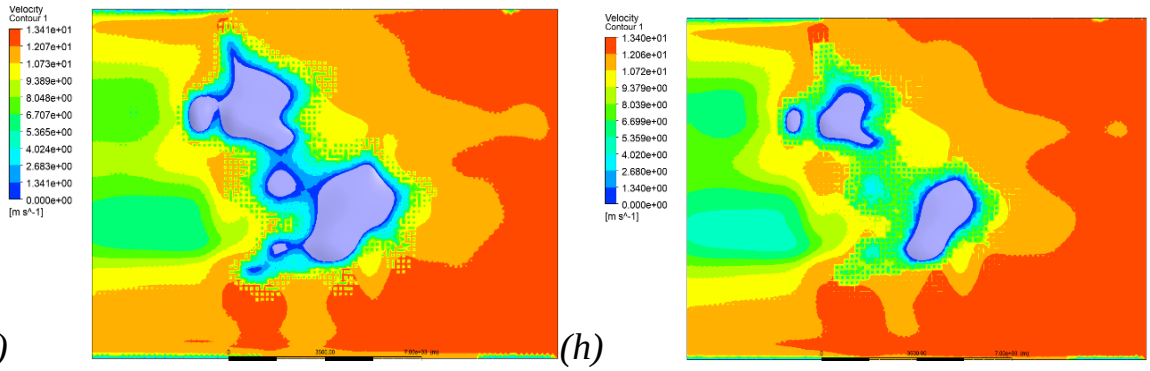

(g) *(h)*

Figure 3.9. Wind speed distribution at different heights: (a) h=166 m, (b) h=216 m, (c) h=266 m, (d) h=316 m, (e) h=366 m, (f) h=416 m, (g) h=466 m and (h) h=516 m.

The detailed wind speed distributions from Figure 3.9 clearly show that the areas from the East to the center of the model have flat terrain, with wind speeds greater than 9.9 m/s. Figure 3.9 (a) shows the eastern region at an altitude of about 160 m with an average wind speed of about 9.0 m/s. This region is adjacent to the sea, has flat terrain and available roads, which is very suitable for building a wind farm. The length of this region is about 12,000 m and the width is about 6,000 m. Assume this region is installed with 4 MW turbines. These turbines are installed in horizontal rows, each turbine is 1,000 m apart, then each row along the width of the model can install 12 columns. The model can be installed with a maximum of 5 rows. The total number of wind turbines that can be installed will reach 60, corresponding to a total installed capacity of 240 MW.

However, Vietnam often has big storms, which can affect the integrity of the turbines throughout their operating life (about 20 years). Therefore, considering the case of a very strong storm wind of level 12 according to the Beaufort wind scale [67], the wind speed reaches from 32.19 m/s to 37.10 m/s. Select the wind speed at the boundary condition of the model as 35.0 m/s and the turbulence intensity as 10% and re-run the model analysis as the steps above. The results obtained are similar to those in Figure 3.10.

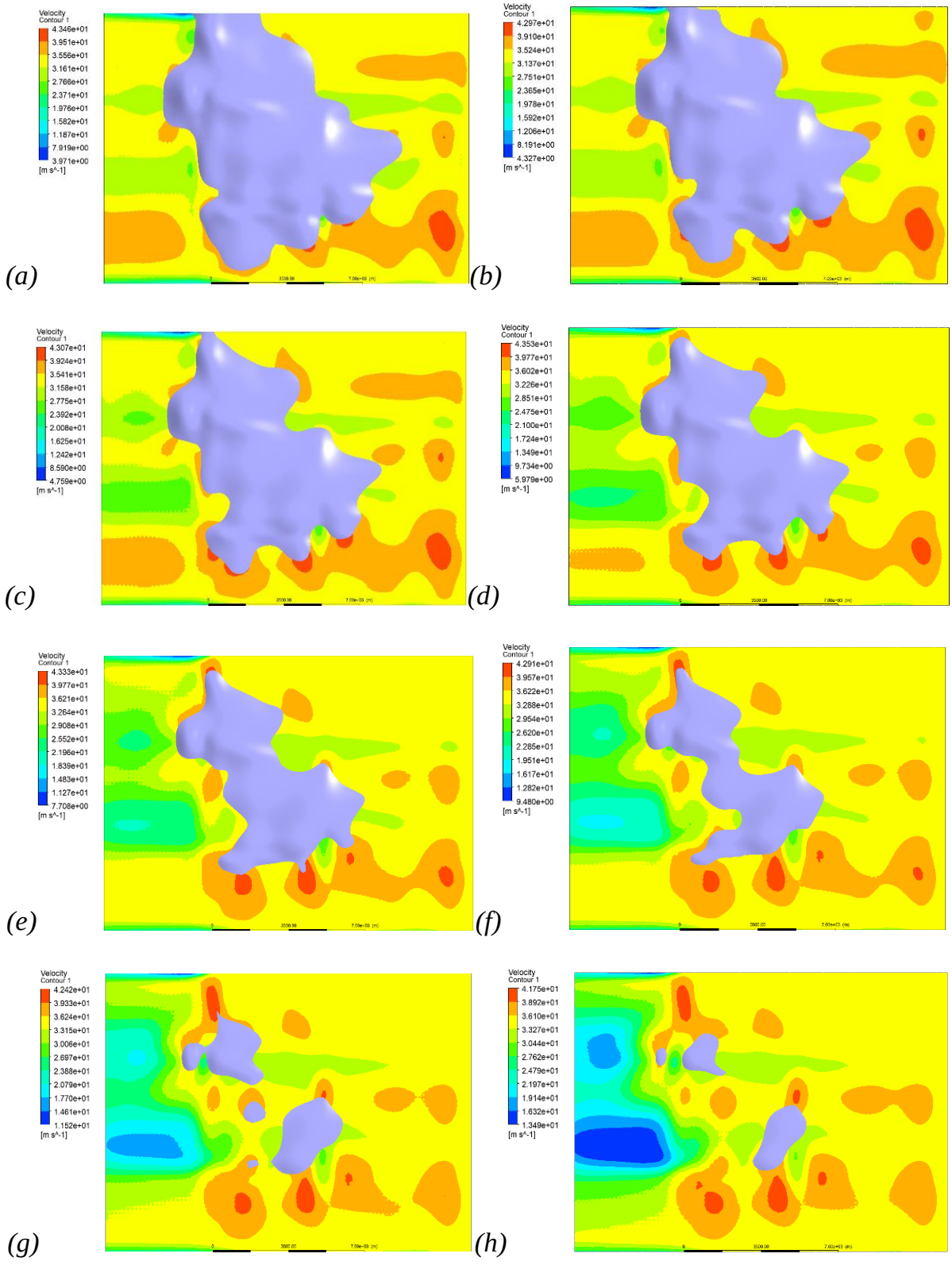

Figure 3.10. Wind speed distribution at heights under storm wind conditions: (a) h=166 m, (b) h=216 m, (c) h=266 m, (d) h=316 m, (e) h=366 m, (f) h=416 m, (g) h=466 m and (h) h=516 m.

From Figure 3.10, when a major storm occurs, the area from the middle part to the southern part of the model is very windy, with wind speeds reaching more than 40.0 m/s. This can cause incidents such as broken turbine blades, causing serious economic and safety losses to the plant. The differences in wind speed distributions on the two sides are mainly due to different terrain. The southwest area has many hills, when the wind blows in from the sea, it will collide with the obstacle of hills, causing changes in direction, the wind will blow stronger, leading to an abnormal increase in wind speeds. These changes will become more obvious as the inlet wind speed increases. On the contrary, the northeast area of the model is flatter, so the wind speeds in this area will always be more stable than the remaining areas. In order to avoid the negative impacts caused by major storms, the area suitable for building turbines is narrowed by half. The most suitable area is the northeastern area of the model with an area of about 3,000 ha.

The GIS-CFD model is used to identify areas with the best wind energy potential. In addition, this model also indicates locations with high risks when storms occur. Due to the influence of the terrain surface, it can create areas with vortexes and abnormally high wind speeds, which can cause serious damage to turbine blades. According to the IEC 61400-1 standard [68], the IA, IB turbines, with a rated wind speed of 10.0 m/s, must withstand gusts of 70.0 m/s for 3 seconds over 50 years. The IIA, IIB turbines, with a rated wind speed of 8.5 m/s, must withstand gusts of 59.5 m/s. The IIIA, IIIB turbines, with a rated wind speed of 7.5 m/s, must withstand gusts of 52.5 m/s. The S-type turbines, with a rated wind speed of 6.0m/s, must withstand gusts of 42.0 m/s.

To ensure compliance with IEC 61400-1 standards, turbine manufacturers need to select appropriate technology and materials. Detailed information on these contents are often not available.

In the thesis, the research objective is to build a turbine blade profile design model to achieve the best wind energy exploitation efficiency when operating at

common wind speeds in Vietnam (4.5-6.5m/s). Through the initial results obtained, the VAST-EPU turbine blades give the highest efficiency with blade lengths of about less than 10.0m. With this size, VAST-EPU blades can be manufactured through 3D printing technology with composite materials. The materials are lightweight and very durable. Therefore, the VAST-EPU turbine blades completely ensure the structural integrity and fatigue load in extreme weather conditions. The detailed research content on these characteristics will be continued in the coming time.

Clearly, the GIS – CFD model proposed in this study can help select the most optimal areas and locations for developing onshore wind power projects in Vietnam. The results obtained from this model include the locations and terrain characteristics of the farms, wind speed distributions according to terrain and altitude, which will be important bases for conducting further studies on blade profile designs and installation configurations of turbines in the farm areas.

III.2. Turbine blade profile design model

The GIS – CFD model allows to determine the terrain characteristics and wind resources at each location in the wind farm development areas. The wind speed distribution function and the turbulence intensity according to height are important bases for selecting or designing suitable wind turbines.

Vietnam has great potential for wind energy, the total onshore wind energy potential is about 221,000 MW, the total offshore wind energy potential is about 600,000 MW. The wind speeds at an altitude of 80 m has a value in the range of 3.0 – 8.0 m/s. However, the wind speeds is mainly from 4.5 – 6.5 m/s, very few areas have wind speeds greater than 6.5 m/s [4]. By 2025, onshore areas with average wind speeds higher than 8.0 m/s have been used or included in the planning. These areas can only generate a very small portion of the capacity. At present, it is necessary to take into account the exploitation of areas with lower wind speeds. This requires studies on the design of wind turbine blade profiles to achieve the highest power coefficient when operating in these low wind speed

areas. From the GIS - CFD model, forecasting the changes of wind speeds according to terrain and height as proposed in Section III.1, the average wind speed values according to terrain and height at each expected location will be accurately determined. This is the practical basis for designing blade profiles for the highest power coefficient values.

The general theoretical basis for calculating the parameters of a wind turbine is the BEM theory. The operating principle of a three-bladed horizontal axis turbine can be summarized as follows: Wind hits the turbine blades, transmitting its kinetic energy to rotate the turbine blades; The turbine blades are connected to a HUB to form a rotor. The rotor is linked to a system of drive shafts, gearbox and generator. When the rotor rotates, it will create mechanical energy to rotate the drive shafts, bringing this energy to rotate the generator, and finally converting it into electrical energy; This electrical energy is led by cable down to a small transformer located at the foot of the tower foundation, then transmitted to the central transformer station of the wind farm. An illustration of the main components of a three-bladed horizontal axis turbine is shown in Figure 3.11.

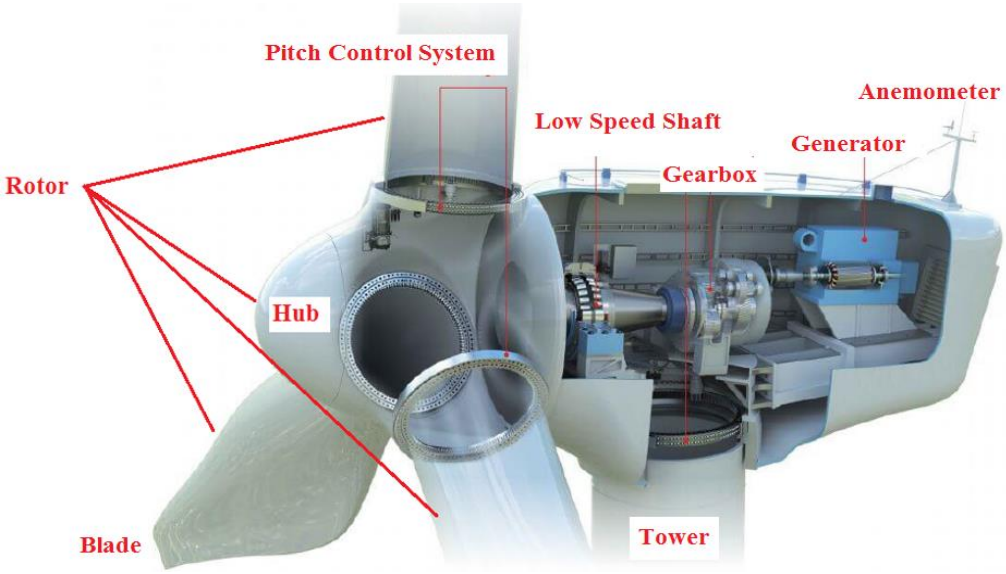

Figure 3.11. Illustration of the main components of a three-bladed horizontal axis turbine

According to the BEM theory, the output electrical power of the wind turbines will depend on factors such as air density, incoming wind speed, blade length, power coefficient, mechanical system efficiency and generator efficiency as detailed in Section II.2. Each turbine design will be associated with a Power – Wind speed characteristic curve to represent the output electrical power value obtained when the turbine operates at the actual wind speed value. This characteristic curve is illustrated in Figure 3.12.

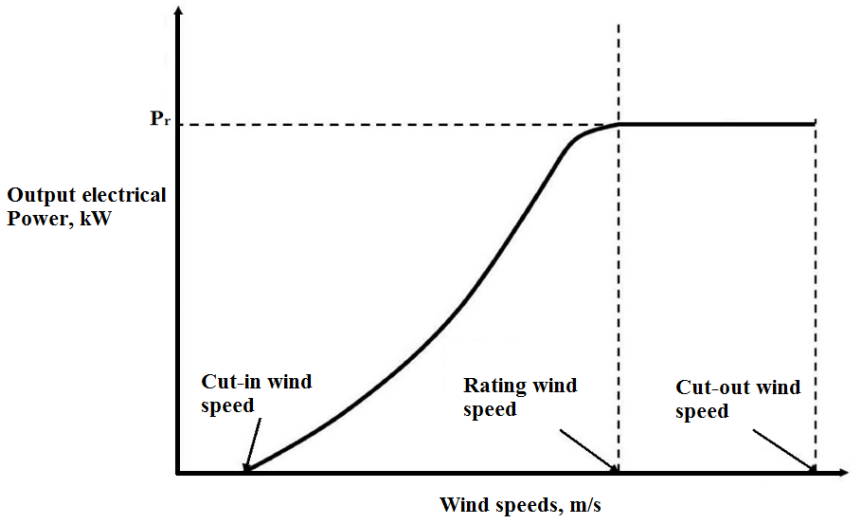

Figure 3.12. Illustration of the Power-Wind speed characteristic curve of the turbine

In fact, there are many turbine designs that have a large rating powers (Pr), but the actual output electrical powers are small. Because, they have to operate in the wind speeds below the design threshold. This causes huge losses not only economic problems but also technical problems related to the mechanical properties of the components and equipment in the turbine. Terrain areas in Vietnam have wind speeds of less than 8 m/s, lower than most of the rating wind speed values of turbines currently popular on the market. In order for wind turbines to achieve the highest operating efficiency, it is necessary to have research, evaluation, and improvement of the design of the components. In which, the improvement design of the turbine blade profiles according to the actual wind speeds is the first and most important issue.

Wind turbine blades are often designed from many different airfoils. The airfoil sections will be placed in different positions, thicknesses, lengths, and twist angles to create a complete blade design. Figure 3.13 illustrates the design of a horizontal axis wind turbine blade.

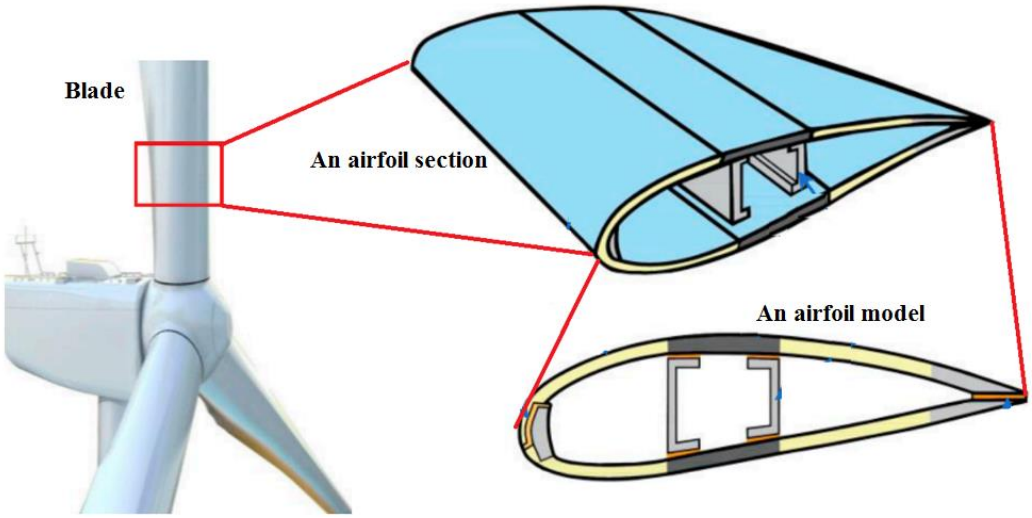

Figure 3.13. Illustrates the design of a horizontal axis wind turbine blade

When the incoming wind interacts with the surfaces of the airfoil sections, depending on the wind speed, AoA, size and surface roughness of the blade, different phenomena will occur as illustrated in Figure 3.14. If the airfoil models are designed in terms of size and AoA values to match the incoming wind speeds, it will create the largest lift force and the smallest drag force, then the C_l/C_d ratio will reach the largest value. On the contrary, if the airfoil size or AoA values are not suitable for the incoming wind characteristics, it will create a lot of drag force and reduce lift force, leading to a low C_l/C_d value.

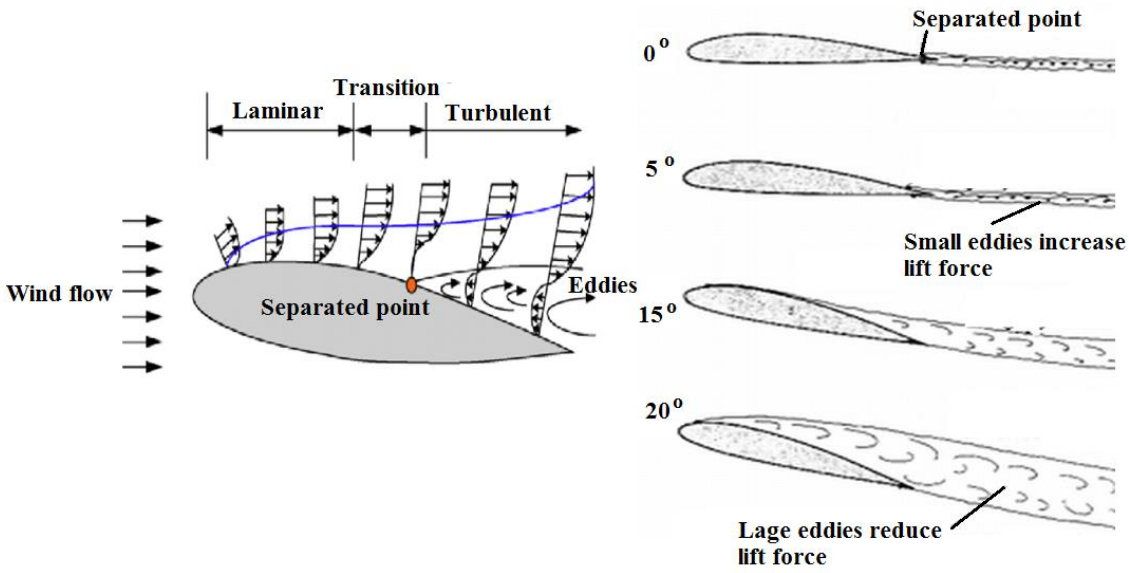

Figure 3.14. Illustration of the interaction processes of incoming flow with an airfoil

When the incoming wind interacts with the turbine blade under an AoA value, each airfoil section will receive the wind at a different angle. The power coefficient of the entire blade will depend on the lift-to-drag ratio of each airfoil section. Therefore, to design a complete blade, it is necessary to study the design of the airfoil models. Then, the selected airfoil sections will be combined to create an optimal blade profile based on the BOM theory. The detailed model for designing the turbine blade profiles proposed is shown in Figure 3.15. The optimal design model of the turbine blade profiles includes 11 steps as follows:

- The 1st step: Select an airfoil model with high wind energy exploitation efficiency - Original airfoil model.

- The 2nd step: Analyze the aerodynamics parameters of the original airfoil model in the wind speed region of interest using the PM. The results are the lift coefficient, drag coefficient, lift to drag coefficient ratio when operating in the wind speed and the graph or function of wind speed distribution or wind pressure on the surface of the original airfoil model.

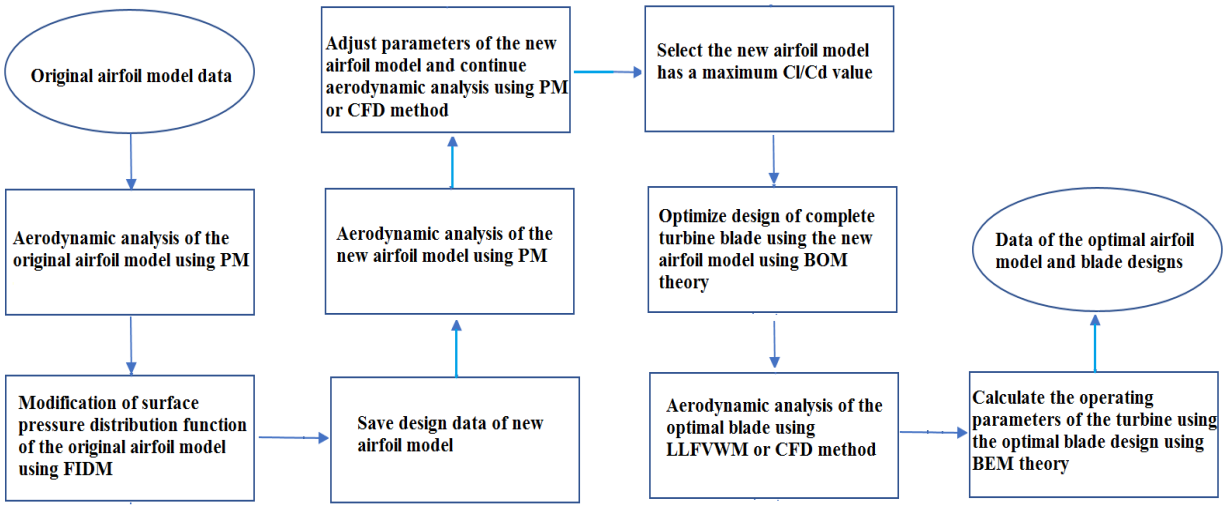

Figure 3.15. The flowchart of the optimal blade design model

- The 3rd step: Modify the graph or wind speed distribution function or wind pressure distribution function on the surface of the original airfoil model to obtain a new graph or pressure distribution function with the largest difference between the upper and lower surfaces of the original airfoil model. The result is to obtain a new wind speed distribution function or new wind pressure distribution function. Then, a new airfoil profile will be created based on the new wind speed distribution function or new wind pressure distribution function using the FIDM.

- The 4th step: Save the data of the new airfoil profile with a suitable name or identification number.

- The 5th step: Analyze the aerodynamics parameters of the new airfoil model in the same wind speeds using the PM. The results are the lift coefficient, drag coefficient, lift to drag coefficient ratio. Compare and evaluate the values obtained from the new airfoil model with the original one.

- The 6th step: Continuously adjust the design parameters of the new airfoil model such as MT, MTP, MC and MCP to obtain the new airfoil model profiles. Then, all the new airfoil models are aerodynamically analyzed using PM or CFD methods. The results are obtained lift coefficients, drag coefficients, lift coefficient to drag coefficient ratios of the new airfoil models in the same wind speeds.

- The 7th step: Compare and evaluate the lift coefficient to drag coefficient ratios of the original airfoil model and the new airfoil models, then select the airfoil model with the largest lift coefficient to drag coefficient ratio. The result is to obtain the optimal airfoil model profile in the wind speed region of interest.

- The 8th step: Use BOM theory to arrange the airfoil models according to different size and twist angle parameters to create complete blade designs. Each complete blade design can use several different airfoil types, but it is also possible to use only the airfoil model with the largest C_l/C_d. The result is the turbine blade profiles.

- The 9th step: These new blade profiles are aerodynamically analyzed using LLFVWM or CFD methods to calculate C_P values at different wind speeds. The blade profile design with the largest C_P value is selected.

- The 10th step: The blade profile with the largest C_P is used to create a 3-blade horizontal axis turbine. The BEM theory is then used to determine the turbine operating parameters such as the output electrical power based on the mechanical system and generator parameters. The result is the operating values of the turbine designs under different conditions.

- The 11th step: Compare the power coefficient values of the turbine designs and select the blade design with the largest C_P value. The result is an optimal turbine blade design in the wind speed region of interest. Finally, the detailed data of the optimal turbine blade design is exported and given a suitable name.The optimal design model of turbine blade profiles as shown in Figure 3.15 is then implemented in this thesis. According to the first step in the optimal design model, some original airfoil models with good wind energy exploitation efficiency and are commonly used in the wind power field are selected such as: NACA6409, S1010, S1223. These airfoil designs represent symmetrical and asymmetrical airfoil models.

From the step 2 to step 7, these airfoil models are analyzed by PM or CFD methods to determine the characteristic aerodynamic quantities under operating conditions with wind speeds in the range of 3.0 - 10.0 m/s. The dimensions of the airfoil models will be brought to the standard length of c=1.0 m, and divided equally into 149 panels when using PM. However, because the main wind speed region in Vietnam is in the range of 4.0 - 6.0 m/s. Therefore, the analysis results with this wind speeds will be presented specifically in this thesis. All 03 original airfoil models were analyzed in the same steps and after comparison and selection, 03 new airfoil models were obtained for the corresponding maximum lift coefficient to drag coefficient ratio. The new optimized models were named based on the research cooperation between Electric Power University and Vietnam Academy of Science and Technology: VAST-EPU-N6409, VAST-EPU-S1010, VAST-EPU-S1223.

Reliability of PM and CFD methods:

The turbine blade profile design model uses PM and CFD methods to determine aerodynamic quantities. The PM method provides faster analysis time than CFD. Therefore, the PM method is used for initial evaluation of the airfoil models. Then, the airfoil models with the best wind energy extraction efficiency will be analyzed by CFD method to obtain more accurate results.

To compare the reliability of PM and CFD, the analyses were conducted with the NACA64A010 models operating at wind speeds of 2.96 m/s, 4.87 m/s and 9.73 m/s, respectively. Then, the results obtained from the simulation models will be compared with the experimental results from the study of Selig et al. [69]. In the analysis models with PM method, the airfoils are divided into 149 panels. The aerodynamic parameters will be determined based on the analytical functions as presented in section II.3.1. In the CFD models, the airfoil is placed in the center, the front surface is a semicircle with a radius of 40c, the space behind is a rectangle with a side length of 60c. The space surrounding the airfoil is shown in Figure 3.16. The chord length of the airfoil is 0.3048 m. The distance from the

leading edge and two side edges to the center of the airfoil is 12.0 m. The distance from the outlet boundary to the center of the airfoil is 18.0 m. The mesh type is a combination of quadrilateral and hexagonal. The mesh size is 0.03 m. The first boundary layer is 0.005 m, the ratio between layers is 1.2 and the number of layers is 11. The chosen solver is RANS, the turbulence model is $k-\varepsilon$, the number of numerical solving iterations is 1,000 for each analysis case.

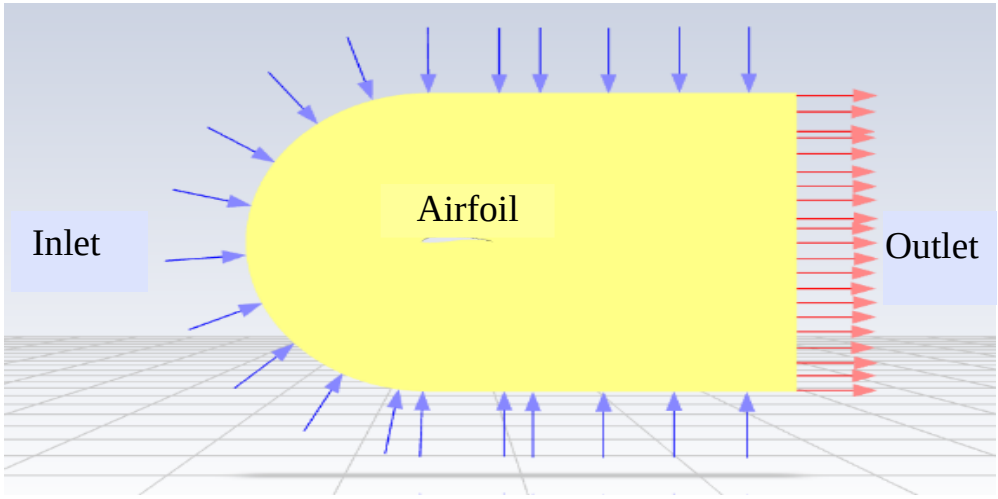

Figure 3.16. CFD model for the airfoil

The results obtained from the PM and CFD models are shown in Figure 3.17, Figure 3.18 and Figure 3.19. The error of the PM method is about 10%, while the error of the CFD method is only about 3%. The results confirmed that the PM method is less reliable than the CFD method. The error of the PM method is larger when the wind speed is larger in the range of approximately 3.0 m/s to 10.0 m/s.

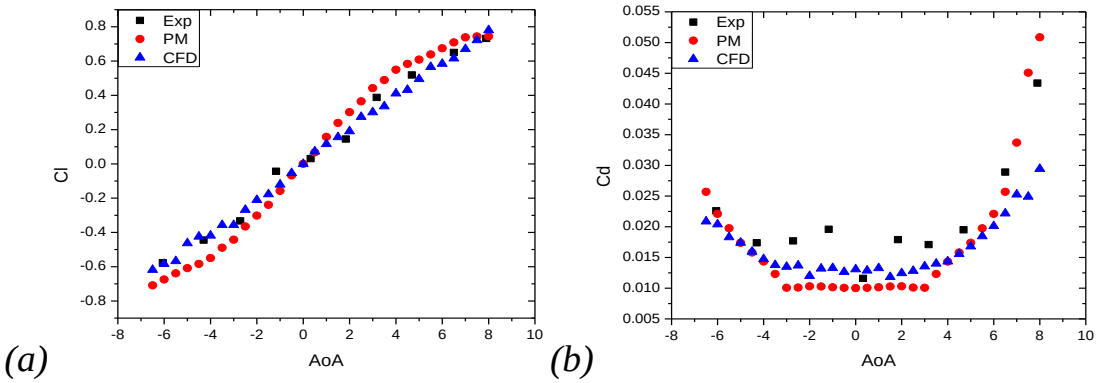

(a) *(b)*

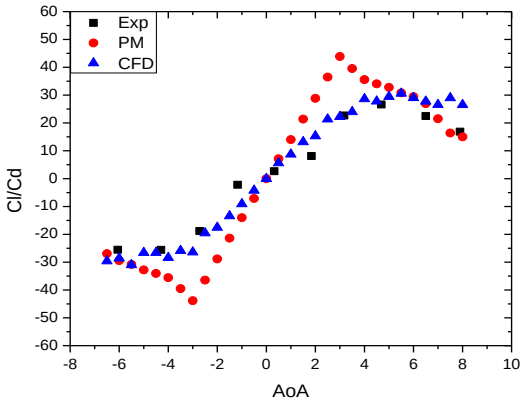

(c)

Figure 3.17. Comparison of aerodynamic parameters of the NACA64A010 when the wind speed is 2.96 m/s: C_l (a); C_d (b); C_l/C_d (c)

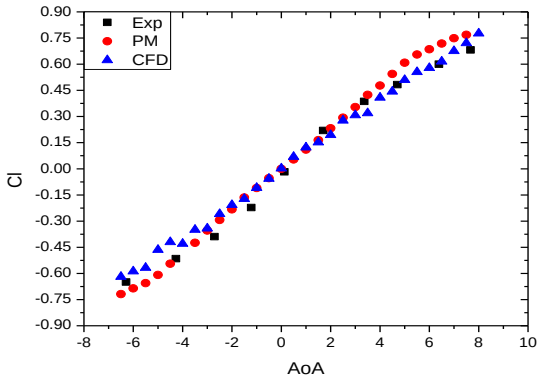

(a)

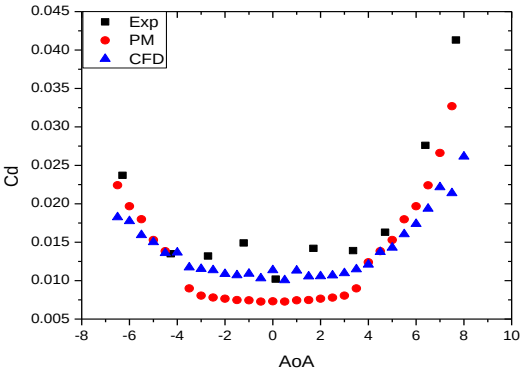

(b)

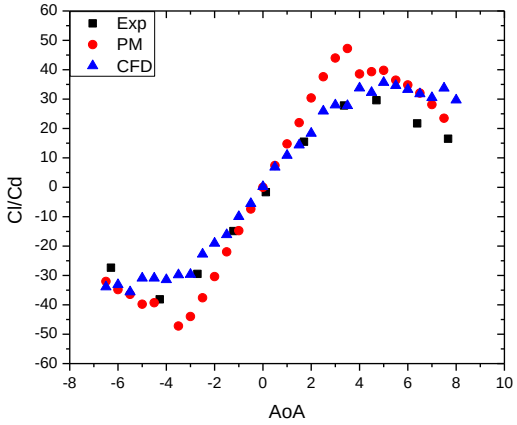

(c)

Figure 3.18. Comparison of aerodynamic parameters of the NACA64A010 when the wind speed is 4.78 m/s: C_l (a); C_d (b); C_l/C_d (c)

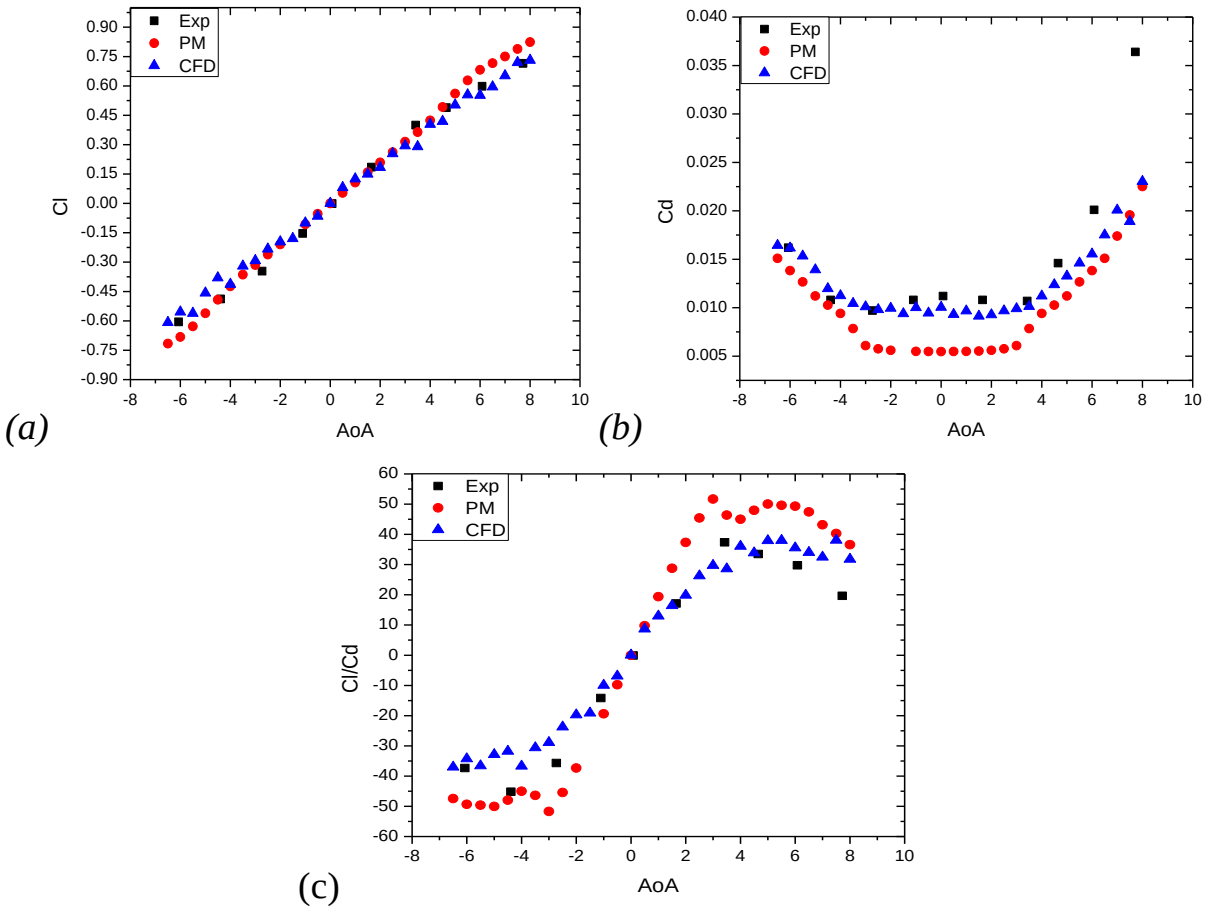

Figure 3.19. Comparison of aerodynamic parameters of the NACA64A010 when the wind speed is 9.73 m/s: C_l (a); C_d (b); C_l/C_d (c)

III.2.1. NACA6409 airfoil model

The basic parameters of the original airfoil model and the optimized new airfoil model obtained from applying the proposed design model are shown in Table 3.2 and Figure 3.20.

Table 3.2. Basic parameters of NACA6409 and VAST-EPU-N6409 models

Parameters	NACA6409	VAST-EPU-N6409
MT	9.00%	10.30%
MTP	30.03%	32.03%
MC	6.0%	7.99%
MCP	40.44%	51.45%

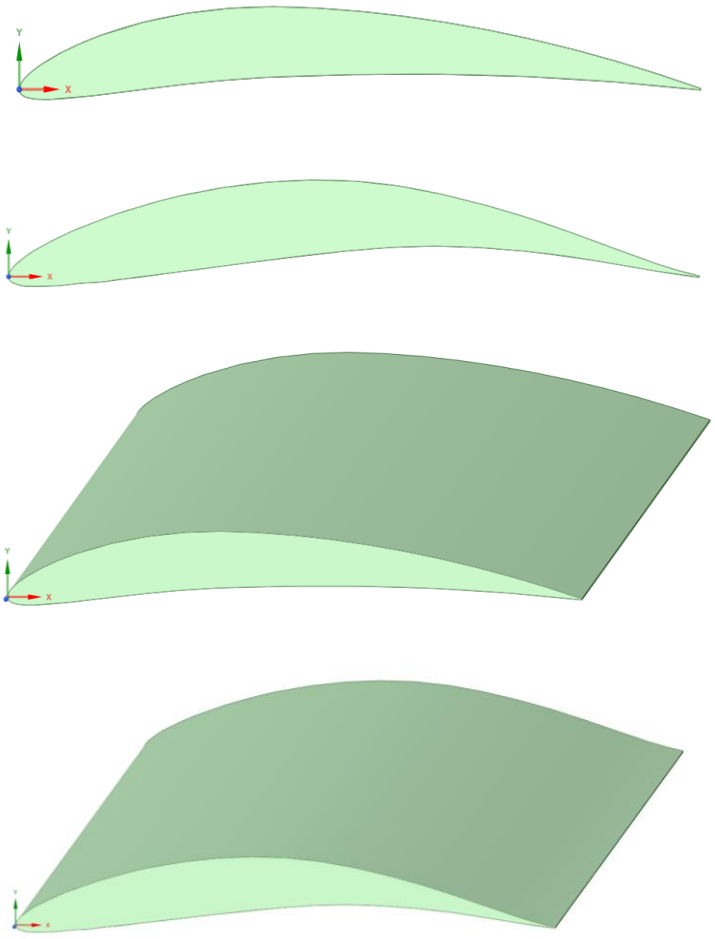

Figure 3.20. Shapes of NACA6409 and VAST-EPU-N6409 airfoil models

After aerodynamic analysis using PM, the obtained values of lift coefficient, drag coefficient, and lift-to-drag coefficient ratio when these two airfoil models operate at a wind speed of 4.0 m/s are shown in Figure 3.21.

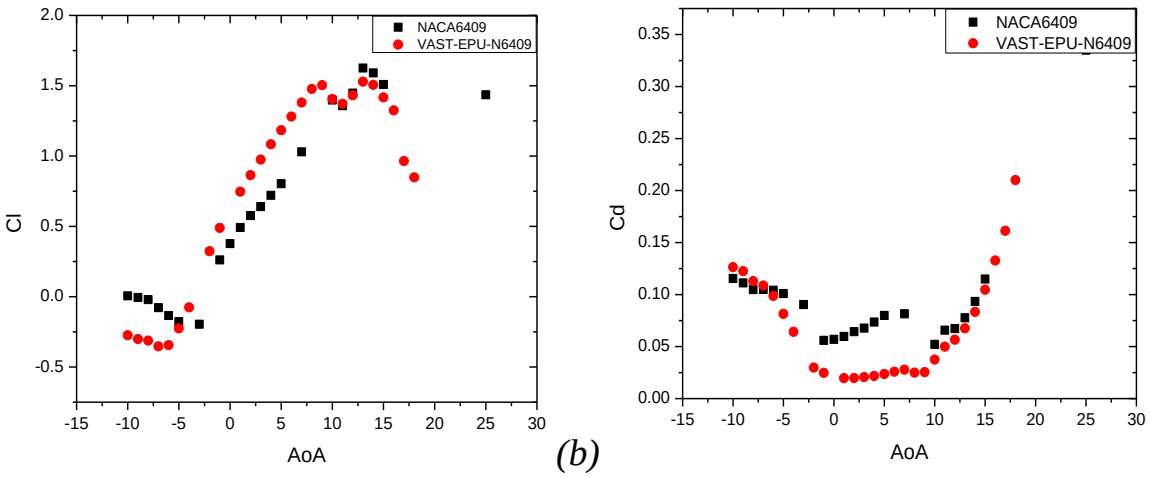

(a) *(b)*

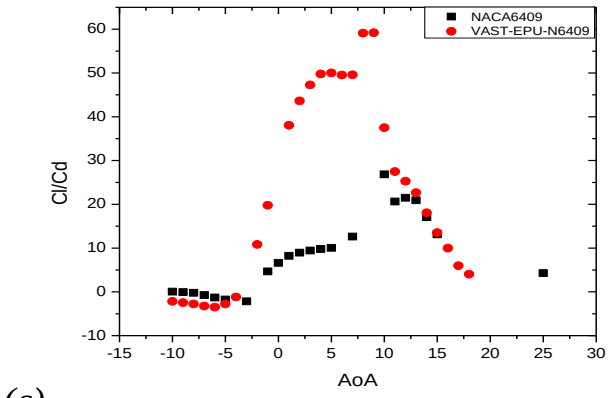

(c)

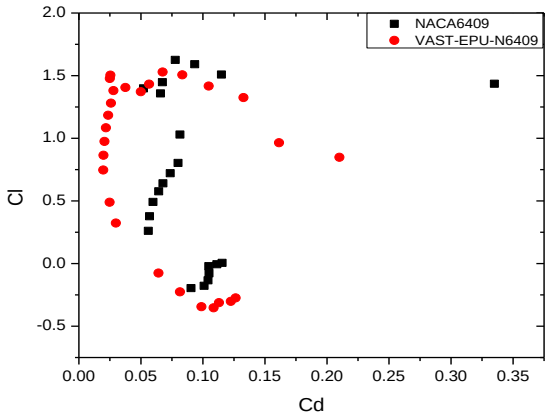

(d)

Figure 3.21. The obtained values of C_l (a), C_d (b), C_l/C_d (c), C_l compared to C_d (d) when operating at a wind speed of 4.0 m/s

Similarly, the graphs showing the obtained values of lift coefficient, drag coefficient, lift to drag coefficient ratio when these two airfoil models operate at a wind speed of 5.0 m/s are shown in Figure 3.22.

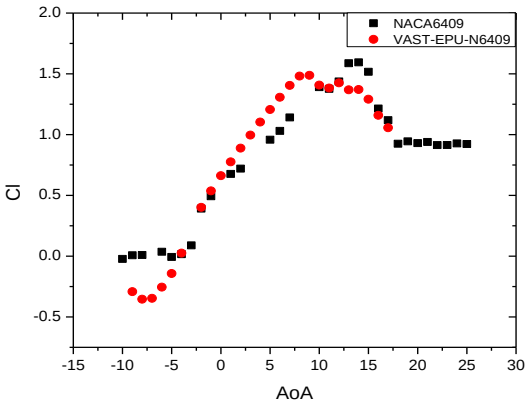

(a)

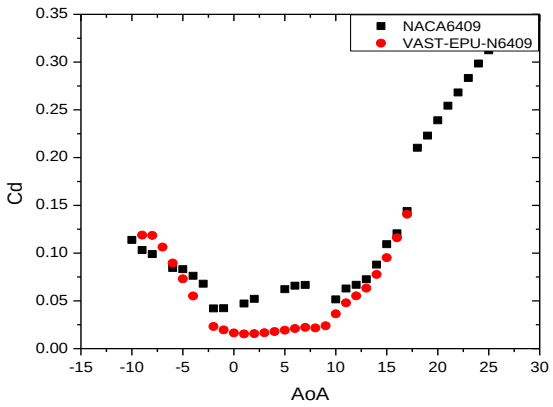

(b)

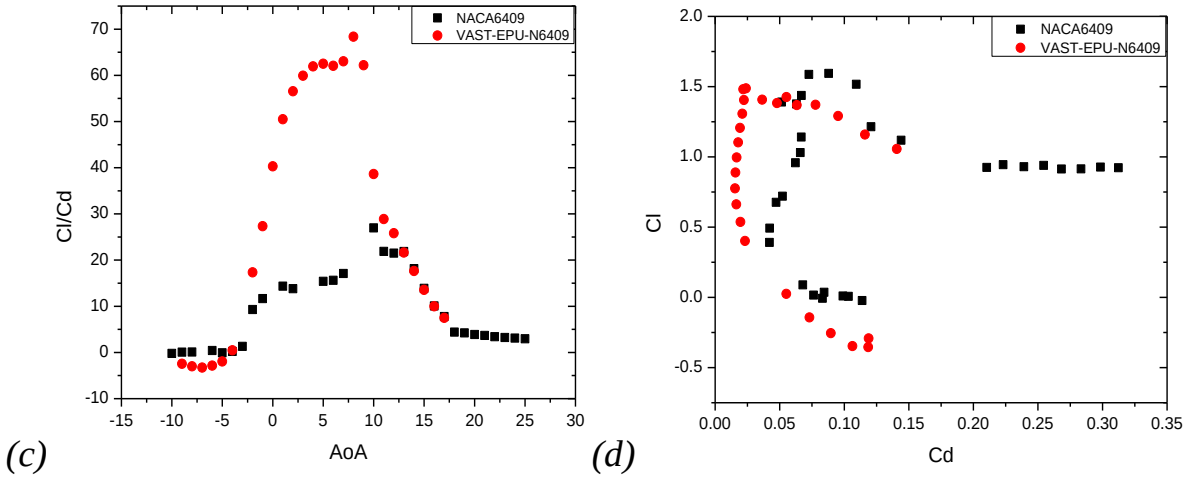

Figure 3.22. The obtained values of C_l (a), C_d (b), C_l/C_d (c), C_l compared to C_d (d) when operating at a wind speed of 5.0 m/s

Finally, the graphs showing the obtained values of lift coefficient, drag coefficient, lift-to-drag coefficient ratio when these two airfoil models operate at a wind speed of 6.0 m/s are shown in Figure 3.23.

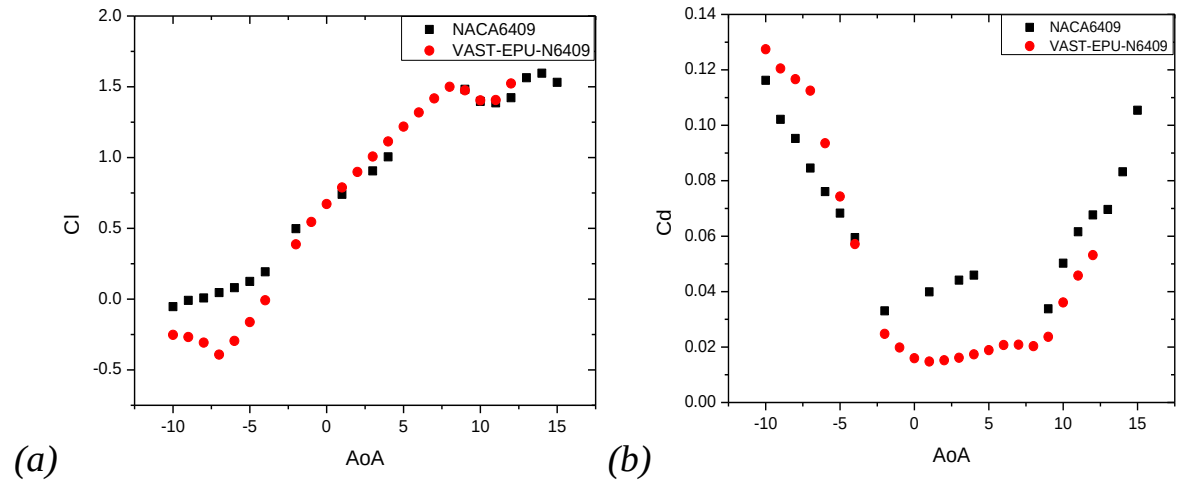

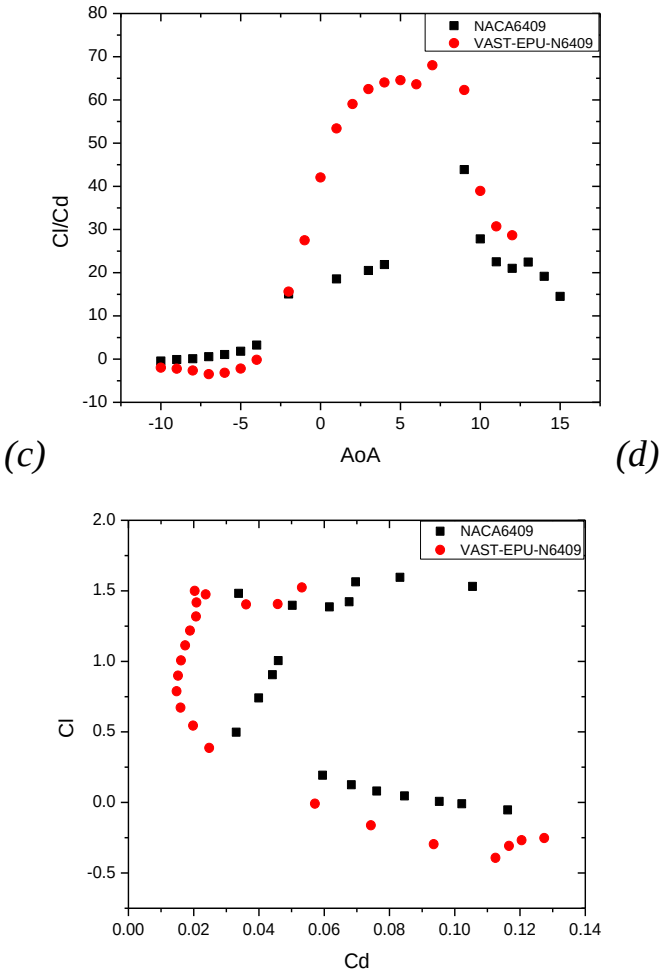

Figure 3.23. The obtained values of C_l (a), C_d (b), C_l/C_d (c), C_l compared to C_d (d) when operating at a wind speed of 6.0 m/s

The results show that the VAST-EPU-N6409 model has a smaller thickness and larger curvature than the NACA6409 model. When operating at wind speeds between 4.0 m/s and 6.0 m/s, the maximum C_l/C_d value of the VAST-EPU-N6409 model is 4.5, 3.0, 1.2 times higher than that of the original model, respectively. This shows that the VAST-EPU-N6409 model has a very high wind energy exploitation efficiency when operating at common wind speed values in Vietnam.

III.2.2. S1010 airfoil model

The basic parameters of the original airfoil model and the optimized new airfoil model obtained from applying the proposed design model are shown in Table 3.3 and Figure 3.24.

Table 3.3. Basic parameters of S1010 and VAST-EPU-S1010 airfoil models

Parameters	S1010	VAST-EPU-S1010

MT	6.02%	8.00%
MTP	23.42%	20.32%
MC	0.00%	5.96%
MCP	0.00%	72.77%

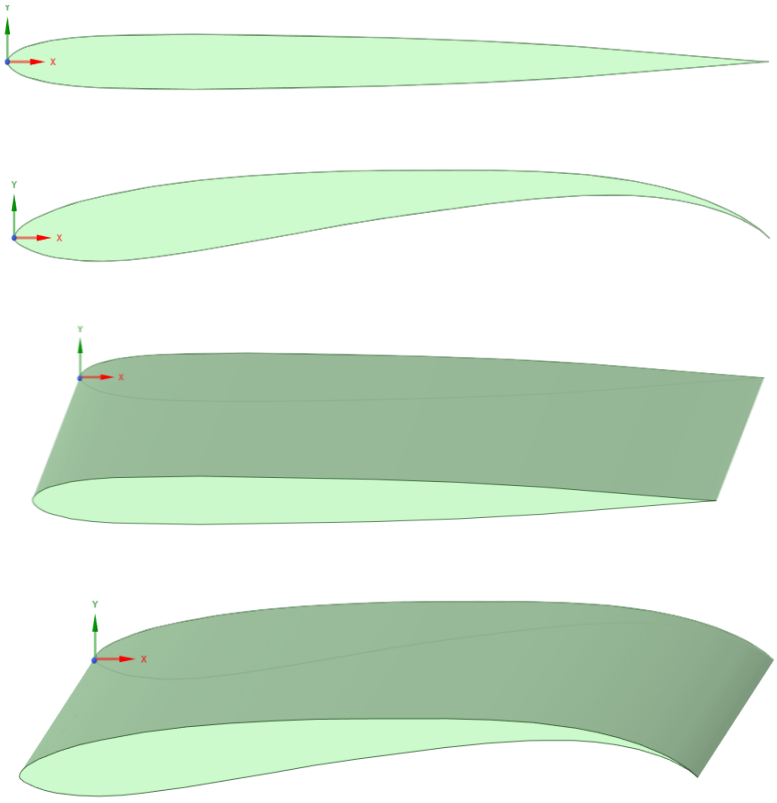

Figure 3.24. Shapes of S1010 and VAST-EPU-S1010 airfoil models

Similarly, the graphs showing the obtained values of lift coefficient, drag coefficient, lift to drag coefficient ratio when these two airfoil models operate at a wind speed of 4.0 m/s are shown in Figure 3.25.

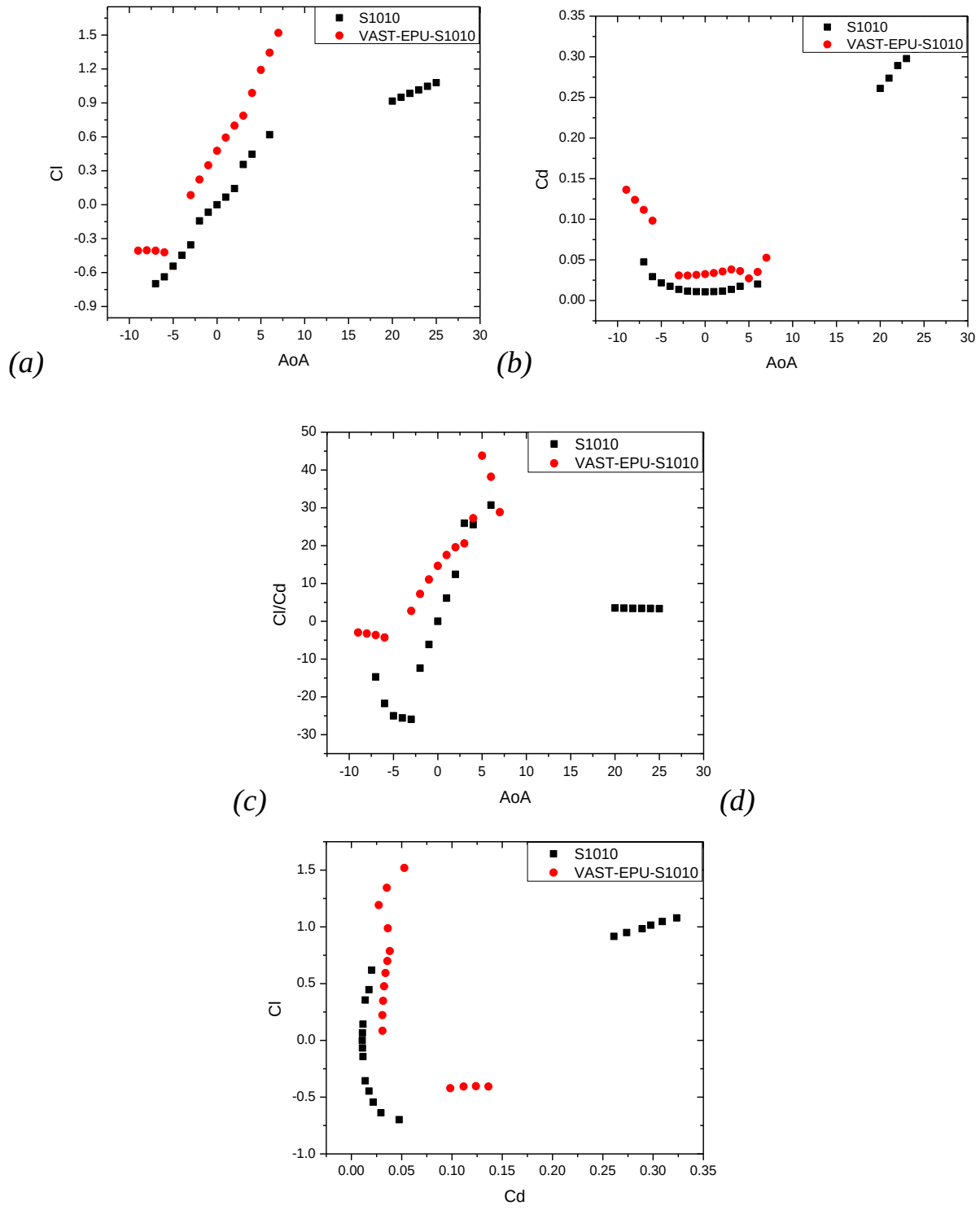

Figure 3.25. The obtained values of C_l (a), C_d (b), C_l/C_d (c), C_l compared to C_d (d) when operating at a wind speed of 4.0 m/s

The graphs showing the obtained values of lift coefficient, drag coefficient, lift to drag coefficient ratio when these two airfoil models operate at a wind speed of 5.0 m/s are shown in Figure 3.26.

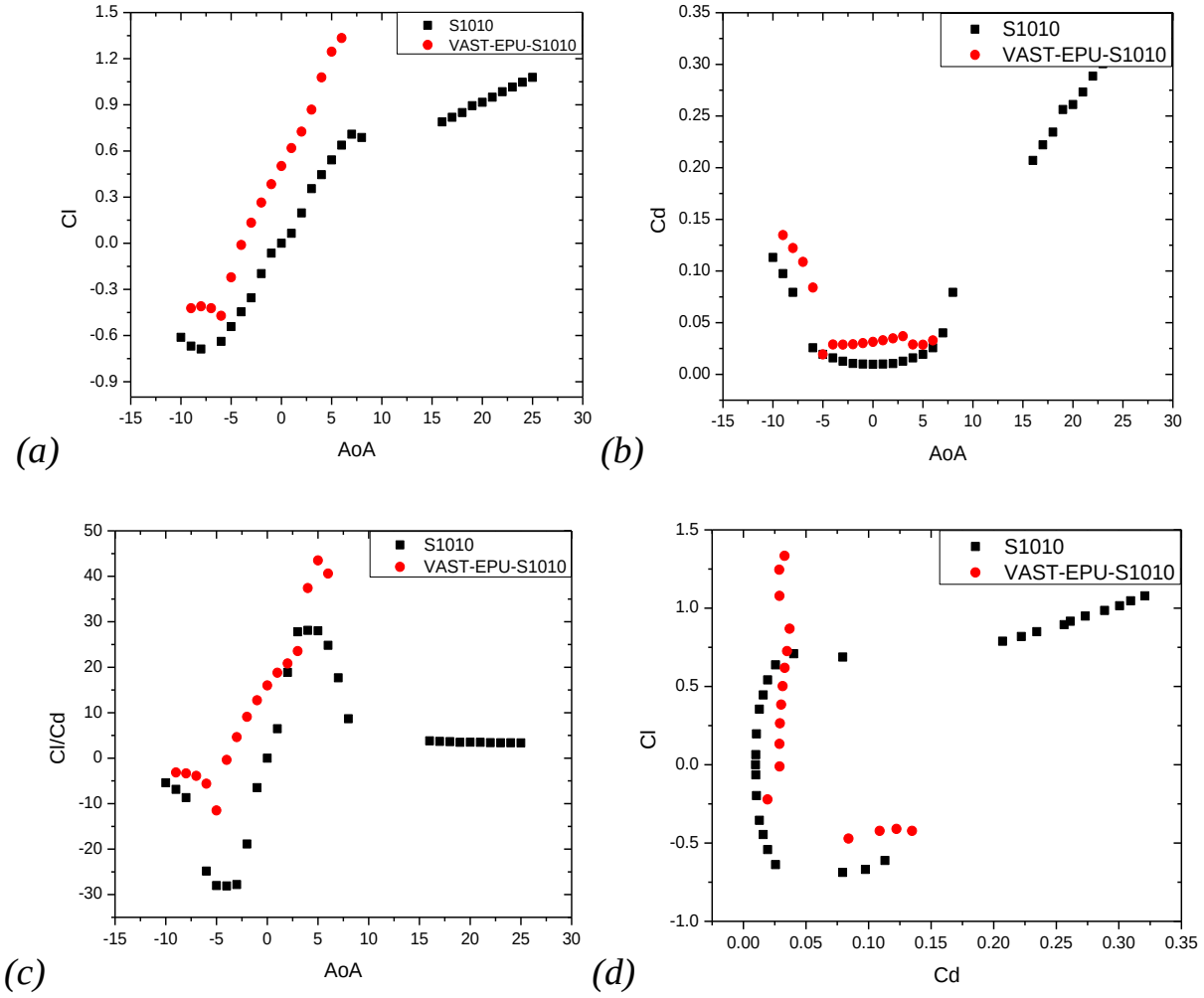

Figure 3.26. The obtained values of C_l (a), C_d (b), C_l/C_d (c), C_l compared to C_d (d) when operating at a wind speed of 5.0 m/s

Finally, the graphs showing the obtained values of lift coefficient, drag coefficient, lift-to-drag coefficient ratio when these two airfoil models operate at a wind speed of 6.0 m/s are shown in Figure 3.27.

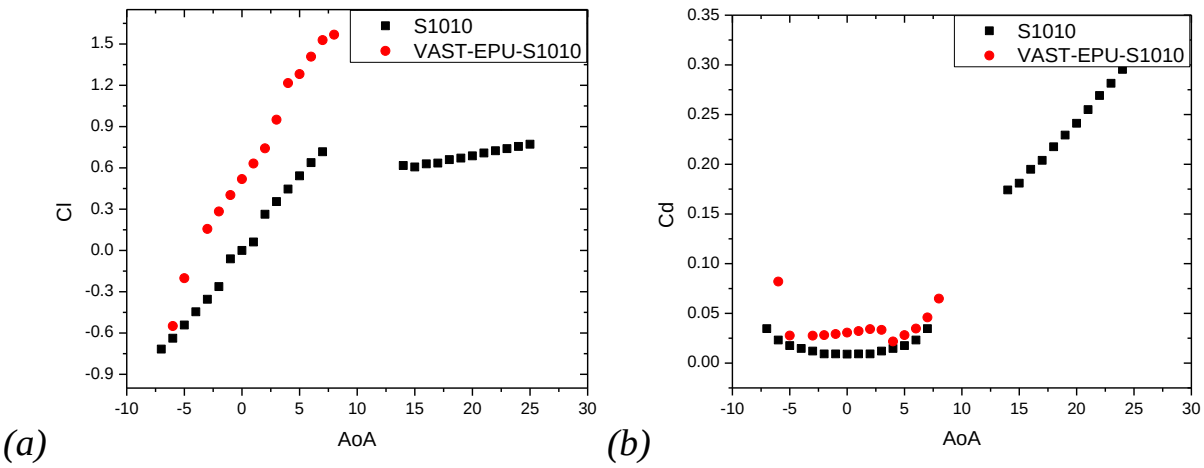

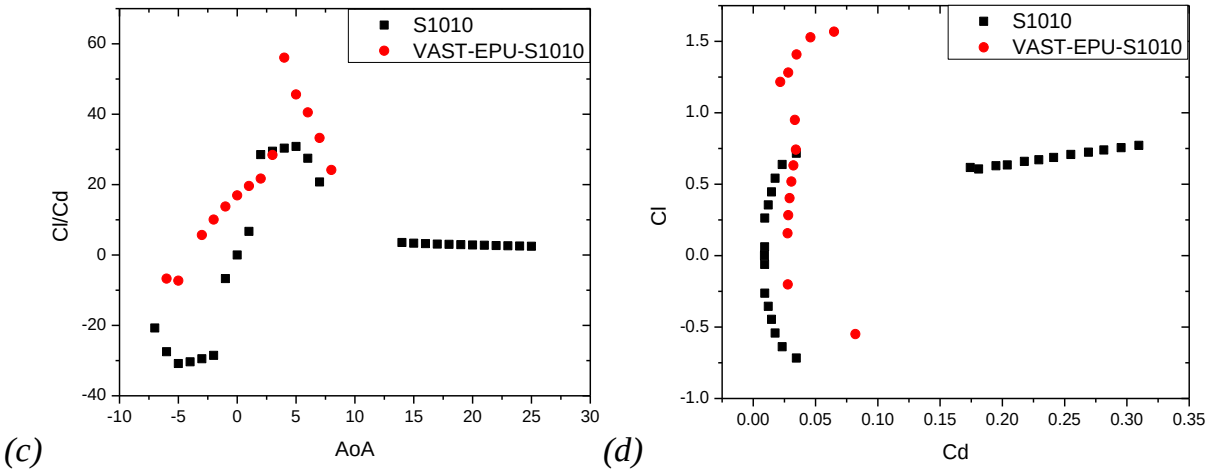

Figure 3.27. The obtained values of C_l (a), C_d (b), C_l/C_d (c), C_l compared to C_d (d) when operating at a wind speed of 6.0 m/s

The results show that the VAST-EPU-S1010 model has a lager thickness and larger curvature than the S1010 model. When operating at wind speeds between 4.0 m/s and 6.0 m/s, the maximum C_l/C_d value of the VAST-EPU-S1010 model is 35.7%, 40.2%, 45.5% higher than S1010 respectively. This shows that the VAST-EPU-S1010 model has a good wind energy exploitation efficiency when operating at common wind speed values in Vietnam.

III.2.3. S1223 airfoil model

The basic parameters of the original airfoil model and the optimized new airfoil model obtained from applying the proposed design model are shown in Table 3.4 and Figure 3.28.

Table 3.4. Basic parameters of S1223 and VAST-EPU-S1223 airfoil models

Parameters	S1223	VAST-EPU-S1223
MT	12.14%	5.0%
MTP	20.12%	19.82%
MC	8.68%	8.16%
MCP	47.45%	48.65%

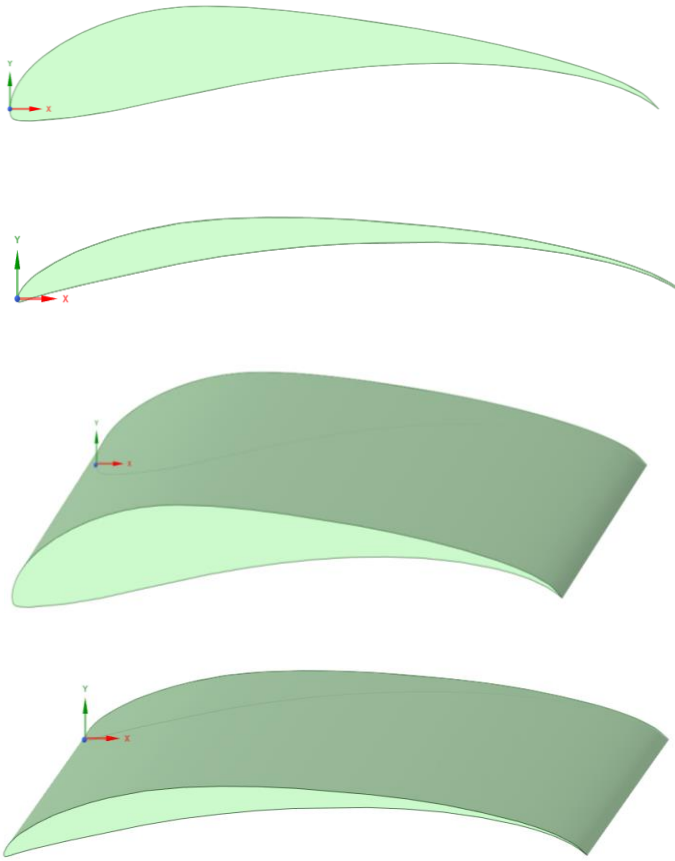

Figure 3.28. Shapes of S1223 and VAST-EPU-S1223 airfoil models

The graphs showing the obtained values of lift coefficient, drag coefficient, lift to drag coefficient ratio when these two airfoil models operate at a wind speed of 4.0 m/s are shown in Figure 3.29.

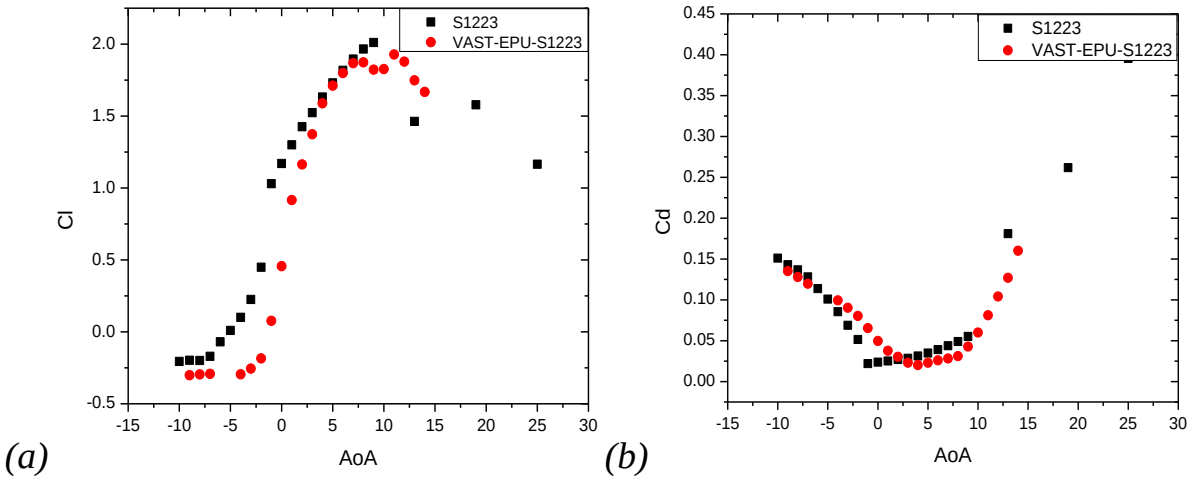

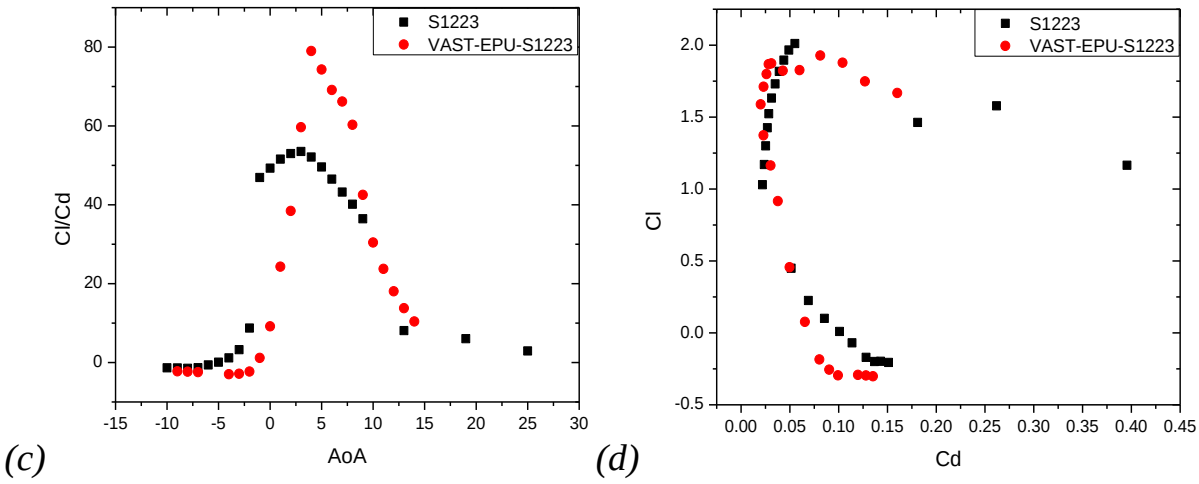

Figure 3.29. The obtained values of C_l (a), C_d (b), C_l/C_d (c), C_l compared to C_d (d) when operating at a wind speed of 4.0 m/s

The graphs showing the obtained values of lift coefficient, drag coefficient, lift to drag coefficient ratio when these two airfoil models operate at a wind speed of 5.0 m/s are shown in Figure 3.30.

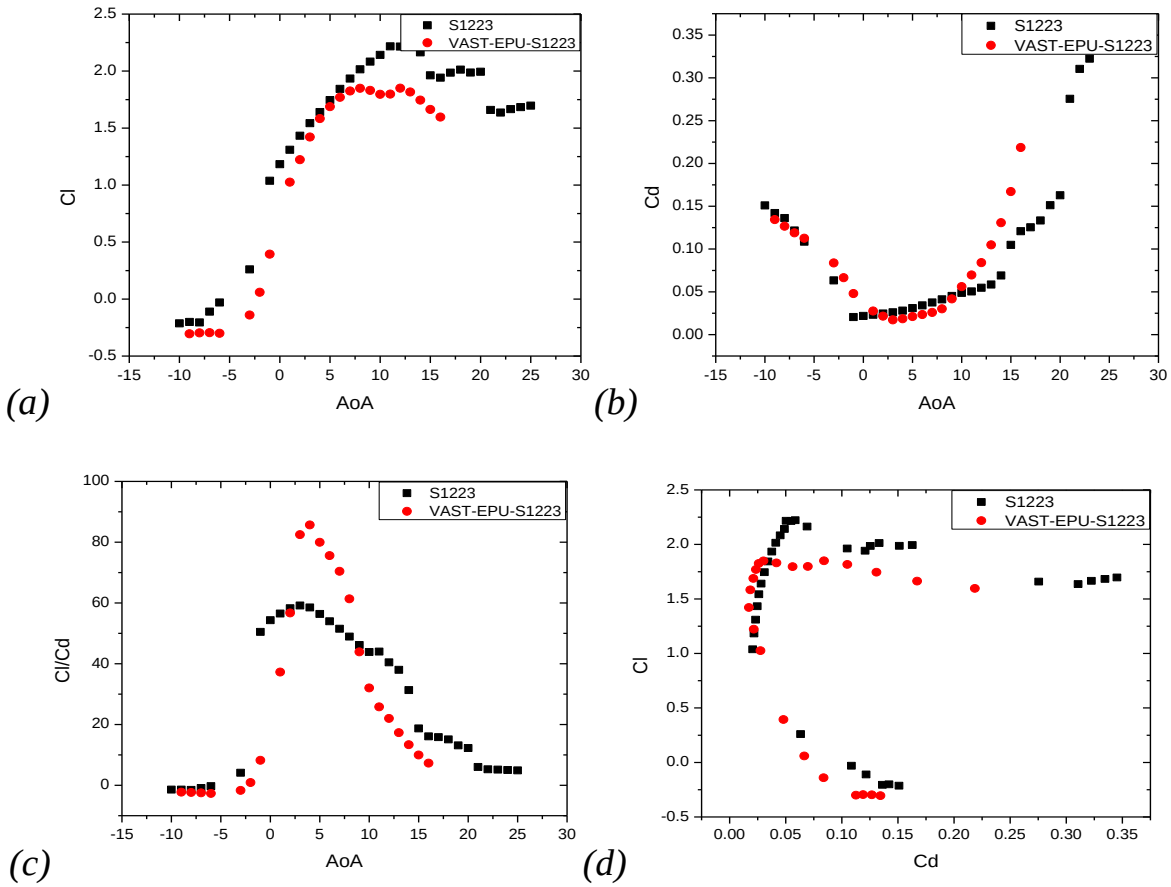

Figure 3.30. The obtained values of C_l (a), C_d (b), C_l/C_d (c), C_l compared to C_d (d) when operating at a wind speed of 5.0 m/s

The graphs showing the obtained values of lift coefficient, drag coefficient, lift to drag coefficient ratio when these two airfoil models operate at a wind speed of 6.0 m/s are shown in Figure 3.31.

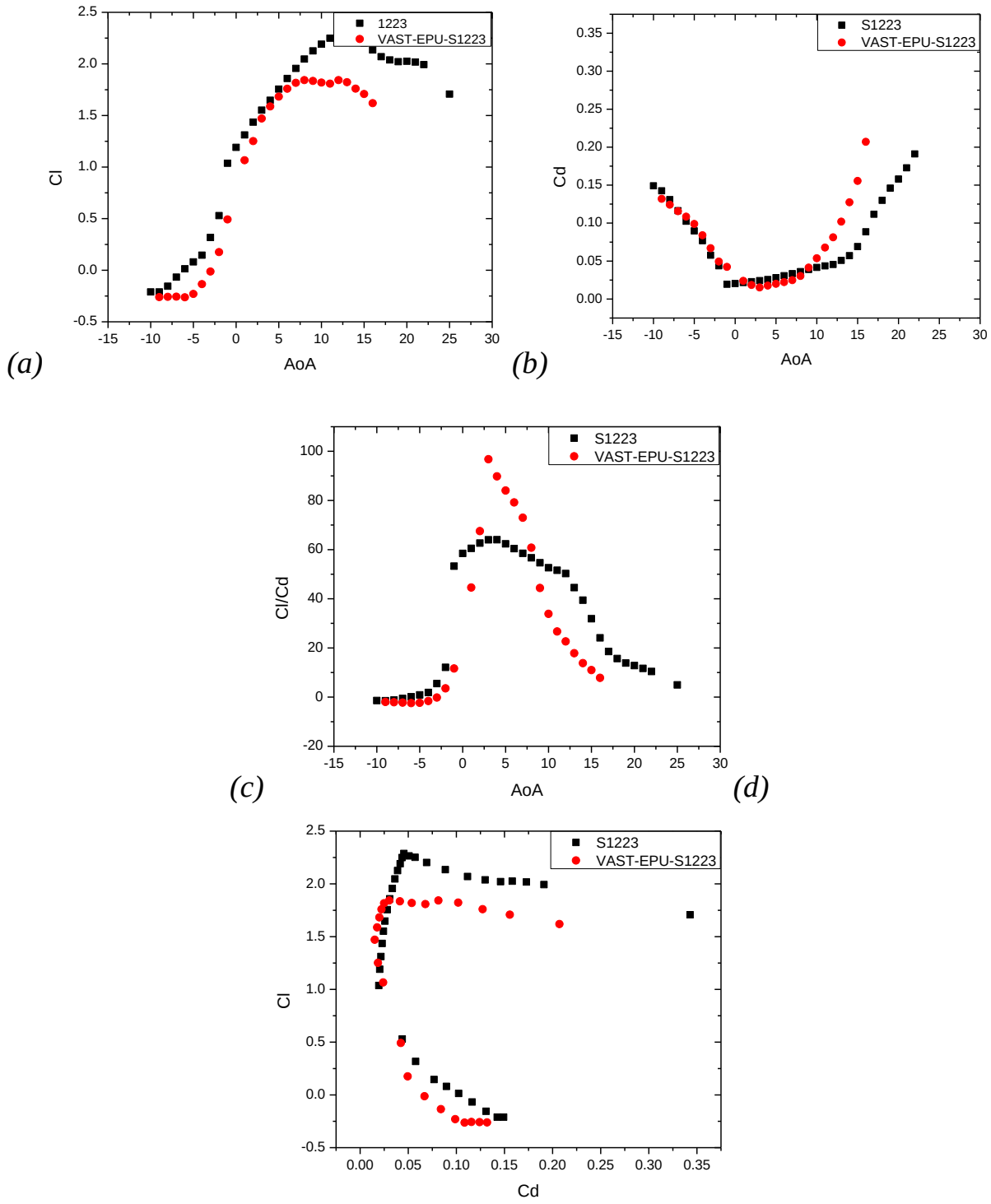

Figure 3.31. The obtained values of C_l (a), C_d (b), C_l/C_d (c), C_l compared to C_d (d) when operating at a wind speed of 6.0 m/s

After analysis and comparison, the most optimal airfoil models were selected and proposed. These new airfoil designs give lift-to-drag coefficient ratios larger than the original airfoil models by about 10% to 50%.

However, from the graphs, it can be seen that at some AoAs, the C_l, C_d values are not obtained. This is because the number of dividing panels is 149 and other boundary conditions make the solution of the equations not converge. If these points are converge, it is necessary to redistribute the number of panels according to each AoA value. However, the lack of some C_l, C_d values at some AoA points does not affect the overall evaluation of the design of the airfoil models. However, this also clearly shows the weakness of PM in the aerodynamic analysis problem for airfoil models.

To overcome the weakness of PM, the airfoil models continue to be analyzed using the CFD method to compare and confirm the reliability of the analyzed data.

The CFD models and implementation steps for the airfoil models are the same. Then, the numerical solution process is performed, the changes of the quantities according to the number of iterations is shown as in Figure 3.32. When the variations are close to constant, it means that the solution process has converged and can be stopped to process the results. In this thesis, the analysis results of the S1010 and VAST-EPU-S1010 airfoil models are presented as a typical example. The results are shown as in Figure 3.33, Figure 3.34, Figure 3.35.

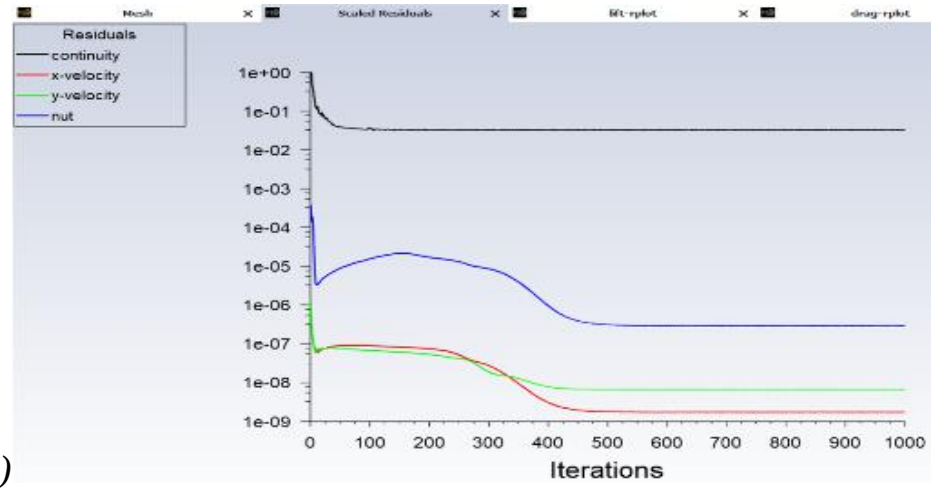

(a)

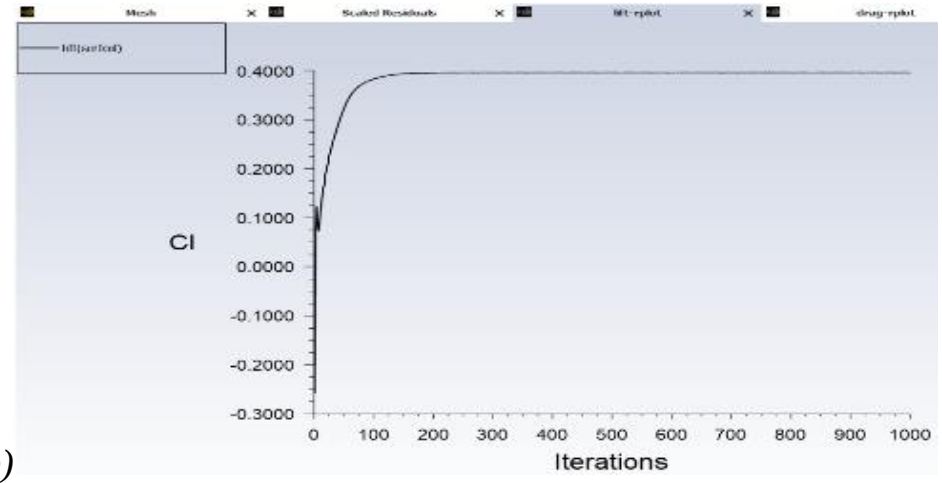

(b)

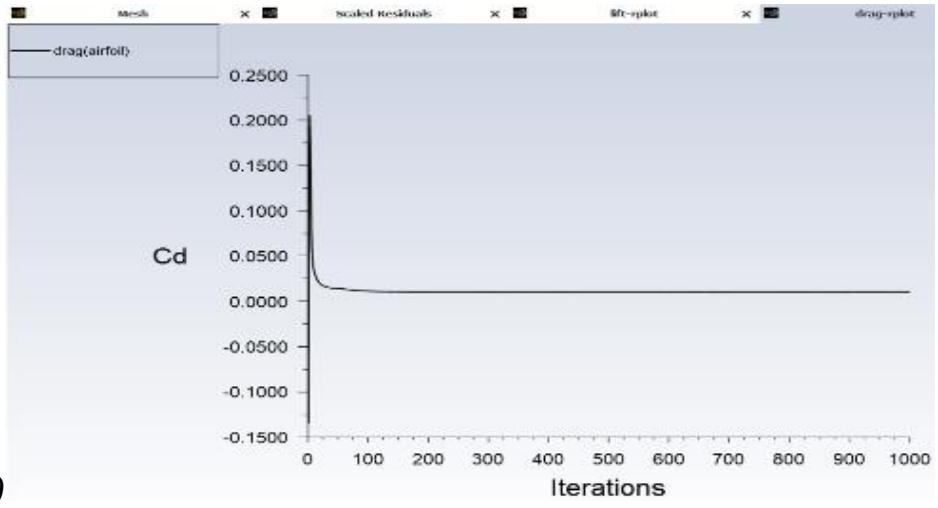

(c)

Figure 3.32. The scaled residuals (a), lift coefficient (b) and drag coefficient (c) during running progress

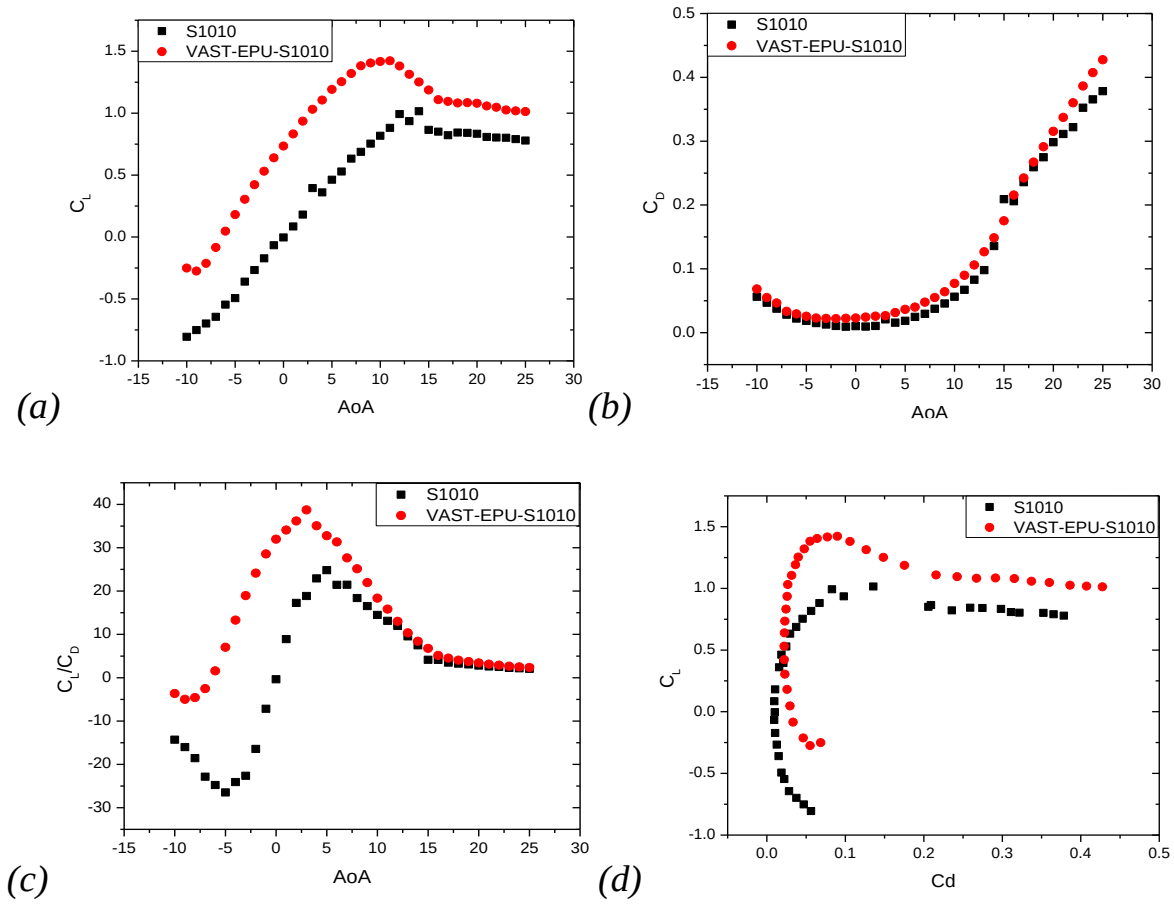

Figure 3.33. Obtained values of C_l (a), C_d (b), C_l/C_d (c), C_l compared to C_d (d) when operating at a wind speed of 4.0 m/s

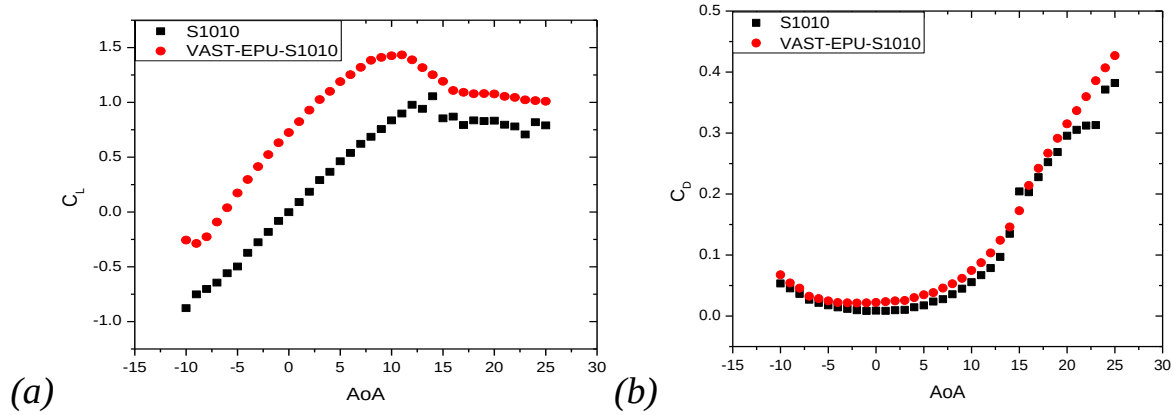

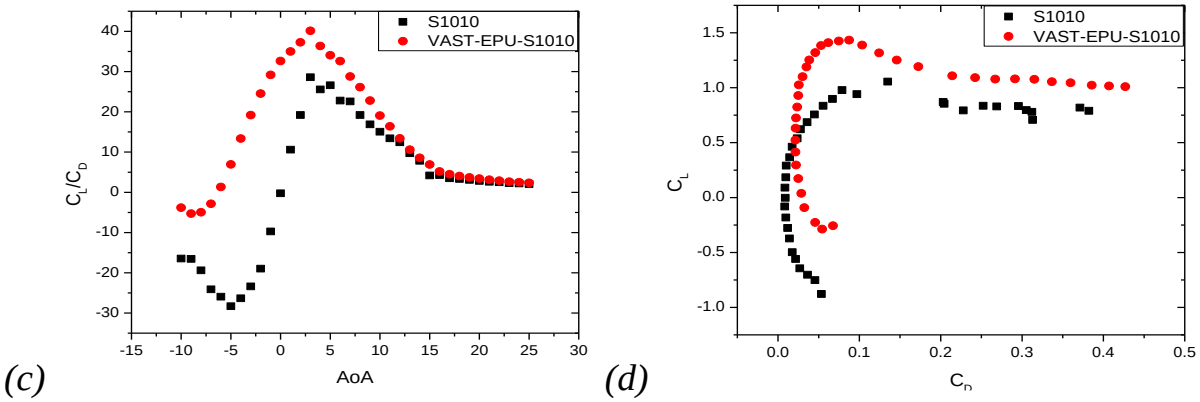

(c) (d)

Figure 3.34. Obtained values of C_l (a), C_d (b), C_l/C_d (c), C_l compared to C_d (d) when operating at a wind speed of 5.0 m/s

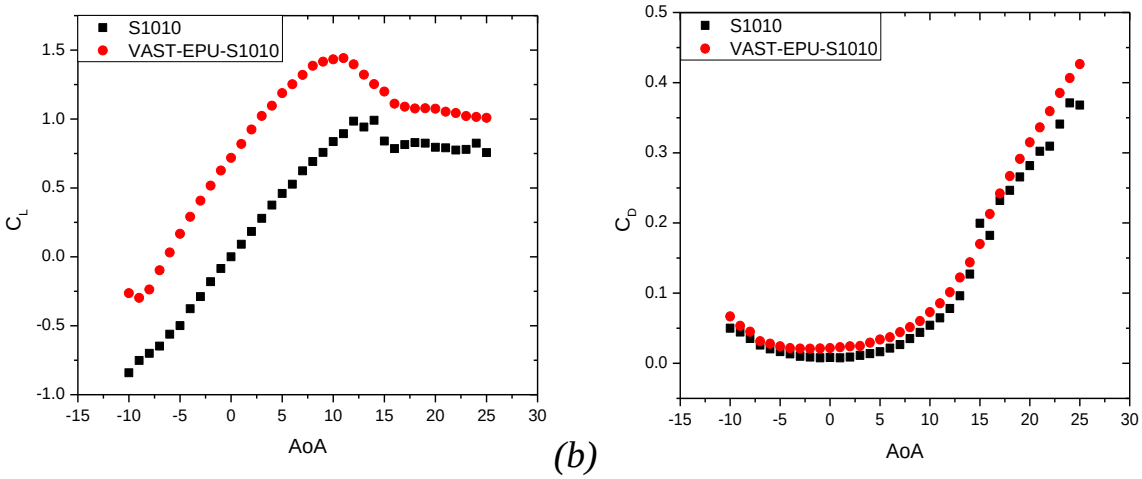

(a) (b)

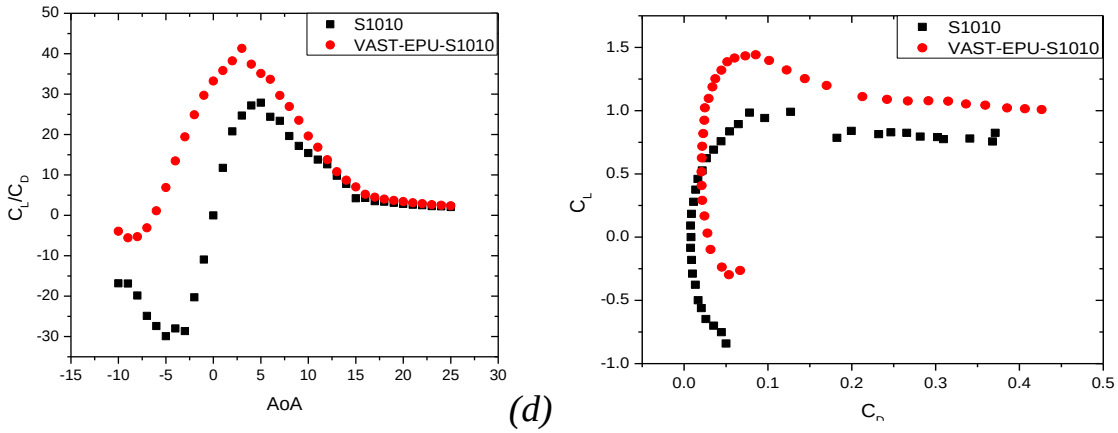

(c) (d)

Figure 3.35. Obtained values of C_l (a), C_d (b), C_l/C_d (c), C_l compared to C_d (d) when operating at a wind speed of 6.0 m/s

The results obtained by the CFD analysis models can also be presented in the form of visual images showing the flow passing through the VAST-EPU-S1010 airfoil surface, along with the flow separation locations and the magnitude

of the eddies according to the AoA angles. This is a great advantage of the CFD method in the problems of aerodynamic analysis. These results are shown in Figure 3.36, Figure 3.37 and Figure 3.38, respectively.

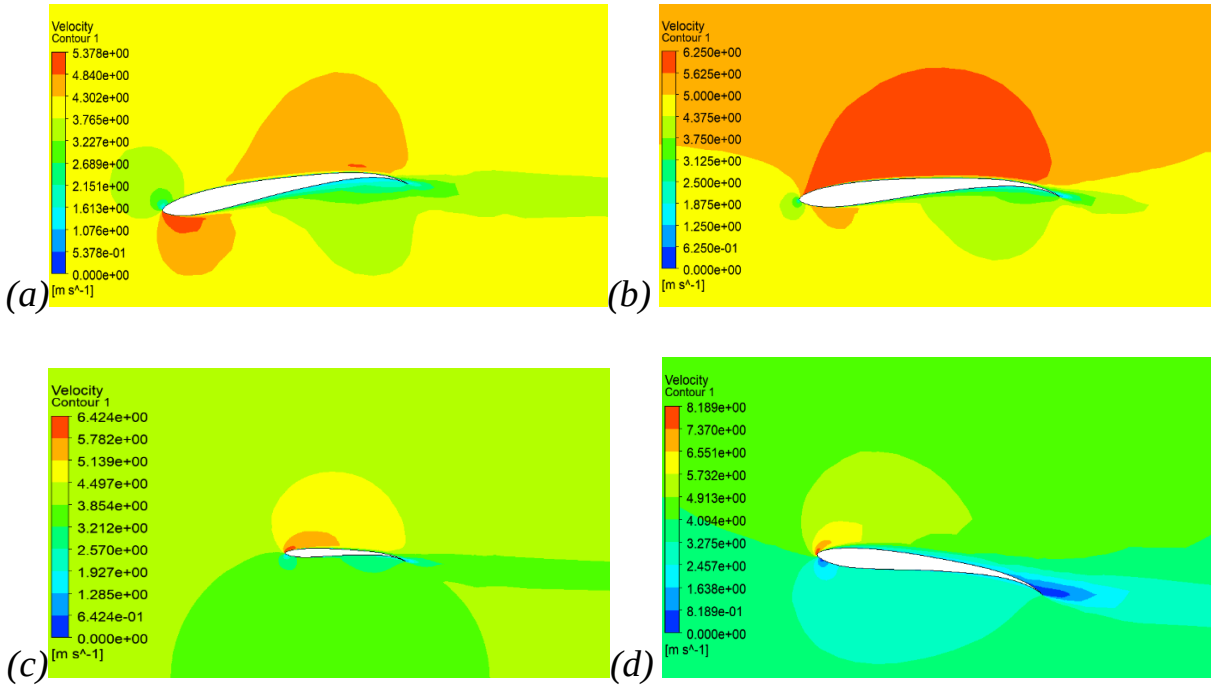

Figure 3.36. Airflow contours and eddies when interacting with the VAST-EPU-S1010 airfoil surface with angles: AoA=-5º (a), AoA=-0º (b), AoA=5º (c), AoA=10º(d) at a wind speed of 4.0 m/s

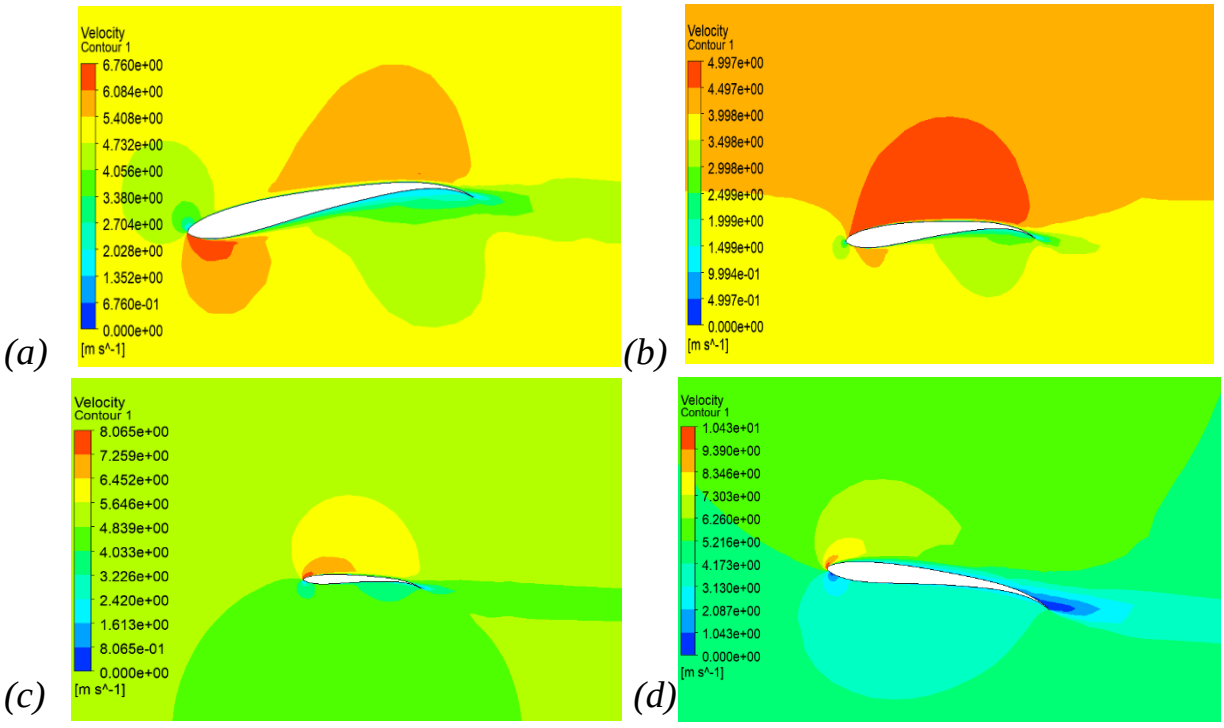

Figure 3.37. Airflow contours and eddies when interacting with the VAST-EPU-S1010 airfoil surface with angles: AoA=-5^o (a), AoA=-0^o (b), AoA=5^o (c), AoA=10^o(d) at a wind speed of 5.0 m/s

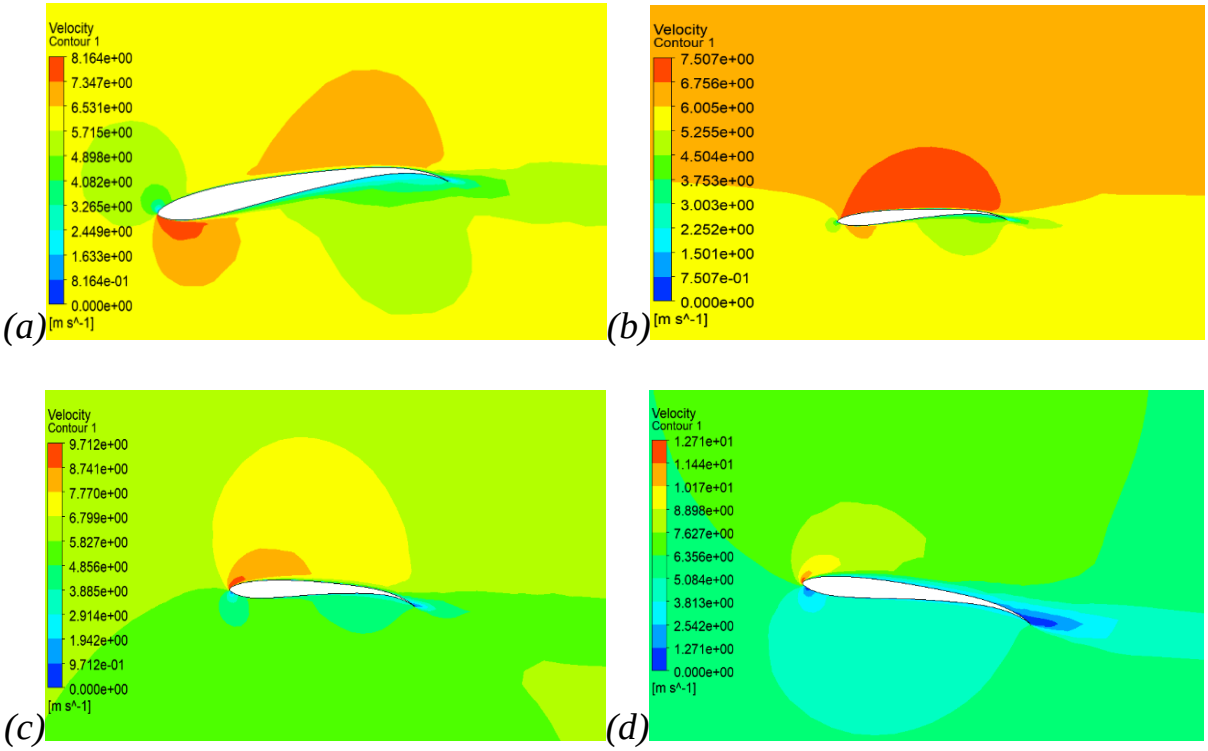

Figure 3.38. Airflow contours and eddies when interacting with the VAST-EPU-S1010 airfoil surface with angles: AoA=-5^o (a), AoA=-0^o (b), AoA=5^o (c), AoA=10^o(d) at a wind speed of 6.0 m/s

From the obtained results, the CFD method gives more reliable results than PM. Through the results obtained from CFD analysis, it is once again confirmed that the new airfoil models proposed in this thesis can achieve much higher lift-to-drag coefficient ratio values than their original models.

III.2.4. Optimized turbine blade profiles

According to the design model as shown in Figure 3.15, the first 7 steps help to design the airfoil models for the largest C_l/C_d. From steps 8 to 11, these airfoil models will be arranged according to different sizes and twist angles depending on the rotor radius. The final goal is to find the blade profiles for the largest power coefficients under the specific operating conditions of the turbines.

Among the new airfoil models, VAST-EPU-S1223 is continued to be used to design the complete turbine blades based on the BOM theory.

Firstly, to have a basis to verify the superiority of these new airfoil models. The SG6043 airfoil model is used to optimally design the turbine blade profile operating in the wind speed range from 3.0 m/s to 10.0 m/s according to BOM theory. The SG6043 airfoil model is known as the model with very high wind energy exploitation efficiency and has been researched by many scientists in the world. The blades using SG6043 airfoil will have different lengths ranging from 1.0 m to 10.0 m. According to BOM theory, the relationship between the length, the twist angle of the airfoil sections and the entire blade length is shown in Figure 3.39.

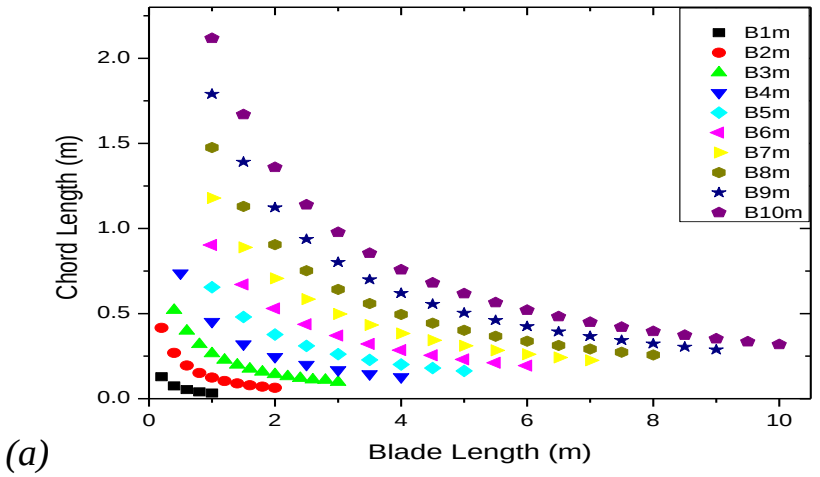

(a)

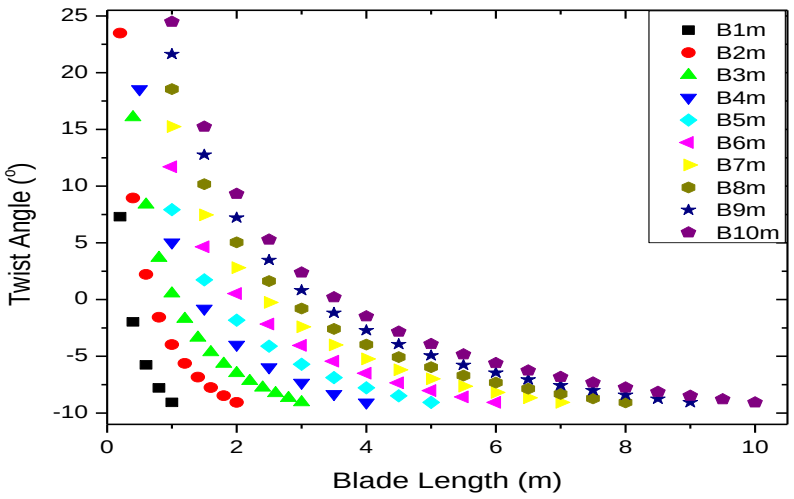

(b)

Figure 3.39. Relationships between the length (a), twist angle (b) of the airfoil sections and the entire blade lengths using SG6043 model

These blades are used to design 3-blade horizontal axis turbines respectively. The operating parameters of the turbine such as TSRs and rotor rotation speeds are adjusted in a wide range. The TSR value varies from 0 to 12, the rotor rotation speed varies from 30 rpm to 360 rpm. The operating parameters of the turbines are described by LLFVWM combined with BEM. Finally, the values of maximum power coefficients and maximum output electric powers of the turbines against wind speeds are shown in Figure 3.40.

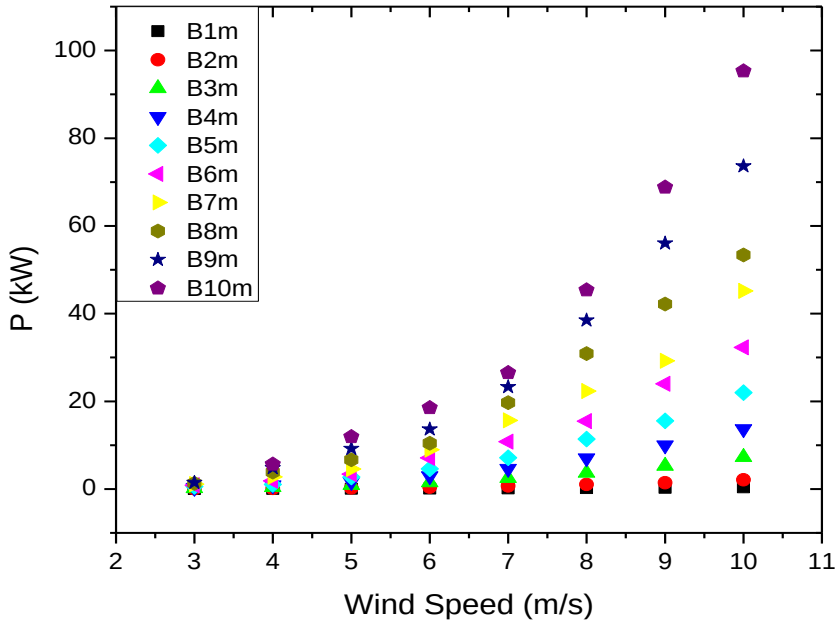

(a)

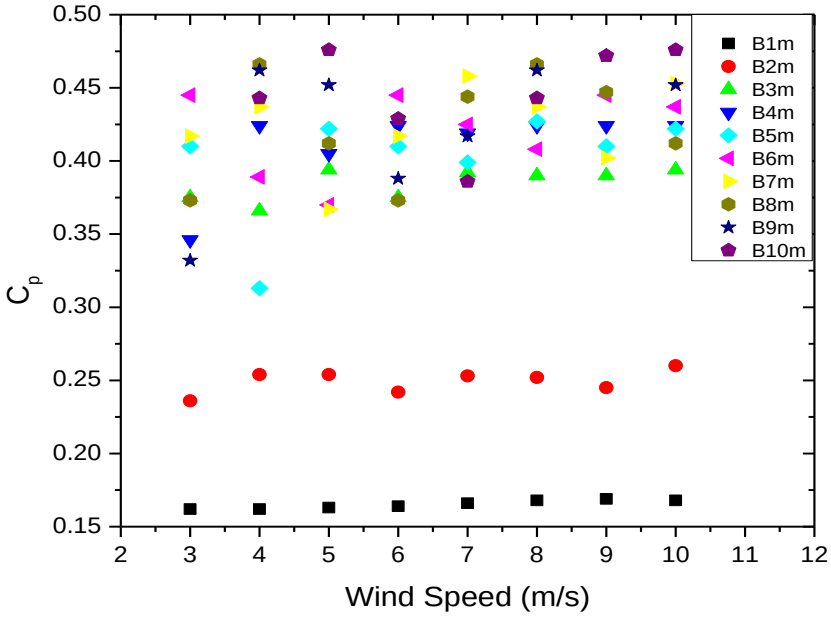

(b)

Figure 3.40. Maximum output electric powers (a) and maximum power coefficients (b) of the turbines using SG6043 according to wind speeds

From the data shown in Figure 3.40 (a), the longer the turbine blades, the greater the output electric powers. However, according to Figure 3.40 (b), it is clear that the turbines have increasing C_P values as the blade length increases from 0.0 m to 8.0 m when operating at wind speeds less than 8.0 m/s. The C_P value will decrease as the blade length continues to increase. This clearly shows that turbines operating in the common wind speeds in Vietnam should only be designed with a maximum blade length of 8.0 m to obtain the maximum C_P value. For turbine blades using SG6043 model, C_P can be achieved approximately 48% when operating at wind speeds between 4.0 m/s and 8.0 m/s.

When considering the wind speeds from 4.0 m/s to 6.0 m/s, the turbine with a blade length of 5.0 m gives the largest power coefficient, C_P=47.6%. The largest output electric power is 2.75 kW when operating at a wind speed of 5.0 m/s. The design of this turbine is classified as a small turbine, suitable for use by households in rural areas, forests, and islands. The design parameters of this 5m long blade profile are shown in Figure 3.41 (a).

From the results obtained in the study with the SG6043 blade profile, the VAST-EPU-S1223 airfoil model will be optimally designed with a blade length of 5.0 m. The design parameters and profile of this blade are shown in Figure 3.41 (b). Under similar conditions to the case of the SG6043 blade, the maximum output electric power of the turbine using the VAST-EPU-S1223 is 3.05 kW, with a maximum power coefficient of up to 50.5%. This power coefficient value is approximately 1.59 times larger than the original airfoil model and 1.11 times larger than the SG6043 model under the same operating conditions with a wind speed of 5.0 m/s. In fact, the best commercial turbines today can only achieve a power factor value of about 45% to 48%.

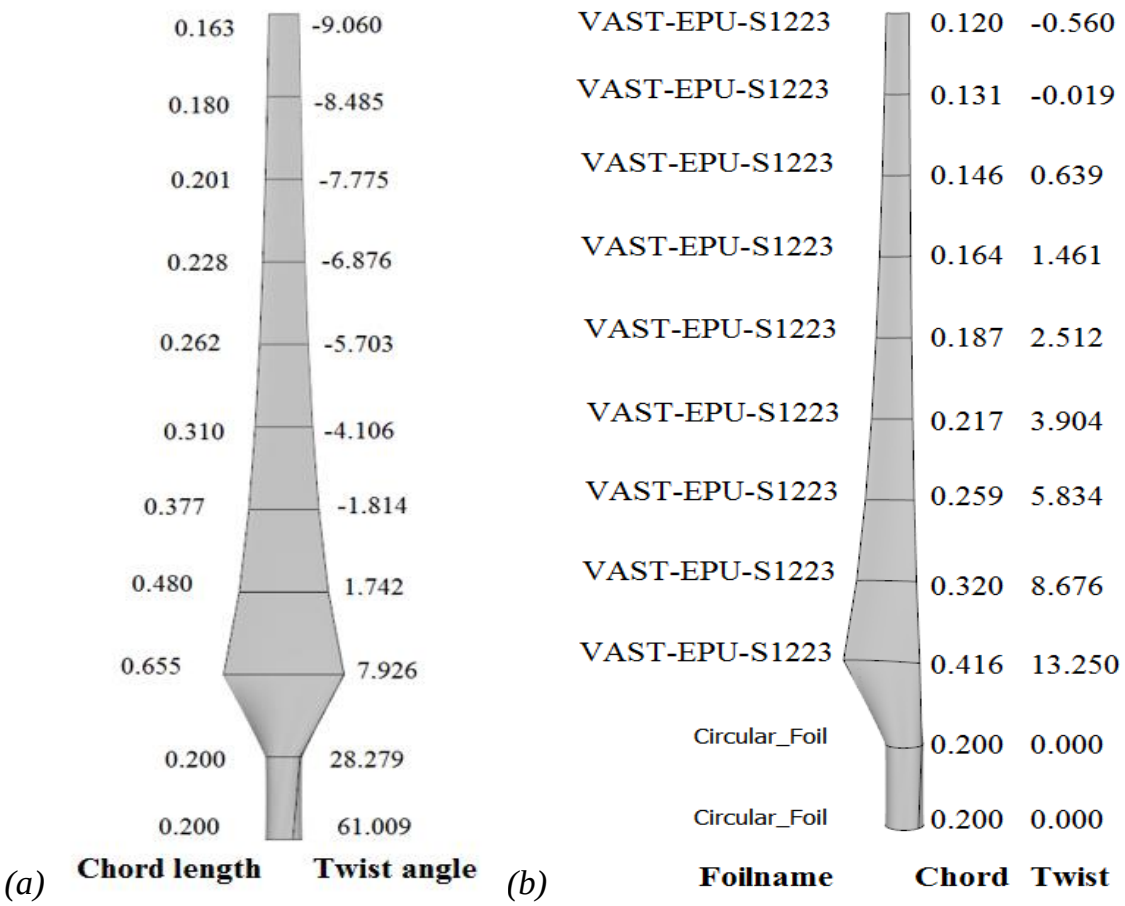

Figure 3.41. Design parameters of 5.0 m long turbine blades using the SG6043 model (a) and the VAST-EPU-S1223 model (b)

One of the main objectives of the thesis is to develop a turbine blade profile design model for good wind energy exploitation efficiency in the common wind speed range from 4.5 - 6.5 m/s. Through the results obtained, some small-sized VAST-EPU blade designs (blade length under 10m) have been identified.

To manufacture these blades, more researches are needed related to the technical-economic analysis problems, specifically manufacturing technology, materials, and costs. These studies are being planned for the next research phase of this thesis.

However, some studies have been published by other research groups with specific relevance as follows:

- According to Suresh A. [70], a 100W small turbine design was fabricated by 3D printing technology using Polylactic Acid (PLA) material. This turbine

uses the SD7080 airfoil model, similar to the VAST-EPU models. The blade made from 100% PLA material will have a density of 1.25 kg/m3, a Young's Modulus of 3.0 N/m2 and a Poisson Ratio of 0.552. When operating at a wind speed of 8.0 m/s, the PLA blade is subjected to a stress of 3.73 × 106 Pa and at a wind speed of 15.0 m/s, the blade is subjected to a stress of 1.31 × 107 Pa. This confirms the structural integrity and fatigue load of the blade under harsh operating conditions.

- According to [71], the cost to manufacture a turbine with a rotor radius of 0.117m using PLA material using 3D printing technology is 43.71 $. The cost calculated by rotor mass is 124.18 $/kg.

- According to Jakub Jurasz [72], small turbines have high economic potential in Poland under the condition of 20 years operating life. Among them, small turbines of 3.0 kW, rated wind speed of 5.0 m/s, are the most efficient. The average CapEx is 3,367.5 $/kW; the average OpEx is 84.1 $/kW/year; the discount rate is 6.0%. From that, the average LCOE of small turbines is 336.4 $/MWh. Clearly, the LCOE of small turbines is still about 4 times higher than that of large turbines.

Summary:

To design or select a turbine suitable for the onshore wind power project development area, it is necessary to carry out two main contents including: Determining the terrain characteristics and wind resources in the area according to different locations and heights; calculating the design or selecting a turbine design suitable for the terrain characteristics and wind resources to obtain the largest power coefficient value. This proposed design model combines the powerful features of both theoretical models and numerical simulations. The obtained results are highly reliable and visual.

For areas with high average wind speeds, turbine blades are often designed longer, the airfoil models used also have large MT and small MC. For the actual wind speeds in Vietnam, mainly from 4.0 m/s to 6.0 m/s, the turbine blade length should be designed in the range of 4.0 m to 8.0 m. The airfoil models used should

have small MT (MT<10%) and large MC (MC>10%) to obtain the largest power coefficient value. This ensures the most efficient wind energy exploitation of the turbines.

The turbine blade profile design model in this thesis is to find the blade designs that give the best efficiency for the common wind speeds in Vietnam. Therefore, the methods used for design and analysis are FIDM, PM and CFD. If this model is used to design the blade for the high wind speed regions, it will still meet the requirements. However, at this time, the PM method will no longer be able to participate in the initial survey. All aerodynamic analyses with the blade model must be performed by CFD method. The CFD is a method that requires a lot of time to perform. Each analysis model can take hours. Therefore, applying the model proposed in this thesis to the high wind speed regions is completely feasible, but the implementation time is longer.

Obviously, the turbine blade profile design model proposed in this thesis can help design blade profiles for the best wind energy exploitation efficiency according to the characteristics of the terrain and wind resources in the wind farm development areas. The output electric powers of these turbines will be important input parameters of the wind farm configuration design problem.

Once the turbines have been designed to best suit the characteristics of the terrain and wind resources, the next problem that needs to be solved is the configuration of the installation location of these turbines in the wind farm area. Because, when the turbines operate, they will cause losses in wind speeds and increase the intensity of turbulence. These effects will cause energy losses for neighboring turbines in the same farm. In addition, the terrain factors also cause energy losses and turbulence intensity of the incoming flow. The problem of designing the wind farm configuration to obtain the largest AEP value and reasonable LCOE value will be solved in Chapter IV.

CHAPTER IV. A PROPOSED MODEL FOR DESIGNING INSTALLED CONFIGURATIONS OF ONSHORE WIND FARMS

IV.1. A model for designing wind farm installation configurations

When an onshore area has been identified as having potential and planned for wind power project development, it is necessary to exploit the wind energy resources in this land area most effectively. The efficiency of wind energy exploitation depends mainly on factors such as wind resource characteristics, turbine design, and turbine arrangement configuration in the wind farm. Wind resource characteristics will change continuously depending on the terrain and turbine arrangement as analyzed in the previous sections. When the wind collides with obstacles, it will create eddies, causing turbulence and energy loss of the flow, which will ultimately reduce the output electric powers of the turbines. This thesis presents an optimal design model for the installation configuration of turbines in an onshore wind farm based on the combination of GIS, CFD numerical simulation models and BEM, Jensen theories. The objective of this optimization model is to determine the installation configuration of certain turbines in a farm area to obtain the largest AEP value and reasonable LCOE value. A reasonable LCOE value means it must be less than the regional wind farm electricity purchase price (EPP) currently applied in Vietnam. The flowchart of the model for designing this turbine installation configuration is shown in Figure 4.1.

The proposed model consists of five main processes:

- The 1st process: The terrain and wind resource characteristics in the wind farm development area are collected. The details of this work have been described in the first part of Chapter III.

- The 2nd process: Simulate the interaction process of wind resources with the terrain of the farm area under different conditions. Through the GIS - CFD combined analysis model, wind energy losses due to terrain factors will be determined. The results are wind speed distribution functions at different locations

and heights. From there, the types of turbines and the expected installation configurations in the farm area will be determined. The details of this work have been described in the first part of Chapter III.

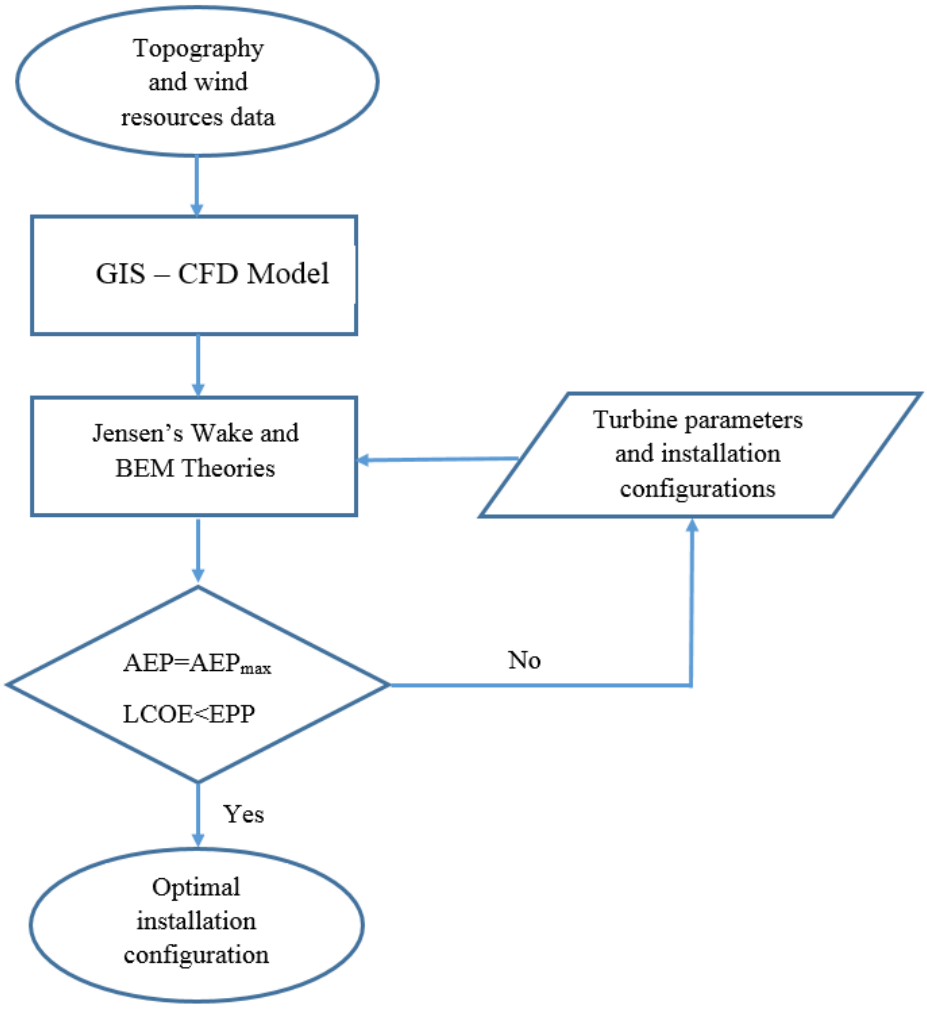

Figure 4.1. The flowchart of the model for designing turbine installation configurations

- The 3rd process: Wind energy losses due to turbines with different installation configurations will be determined using Jensen's wake theory. Different configurations will be based on different spaces of turbine rows. The distances will have increasing values from small to large. Then, the actual operating power of the turbines will be determined using the BEM theory. Detailed descriptions of Jensen and BEM theories as presented in Chapter II.

- The 4th process: The AEP and LCOE values of different turbine installation configurations will be determined in turn according to theoretical

functions based on wind resource data after correcting for energy losses caused by terrain and turbine factors. At each installation configuration, the corresponding AEP and LCOE values will be determined. If the AEP of the configuration is larger than that of the previous configuration, the turbine installation configuration will continue to be changed. If the configuration has a smaller AEP than the previous configuration or the distance between turbine rows has exceeded the width of the wind farm area, the configuration change process will stop. At this time, check which configuration gives the largest AEP value and consider the condition that LCOE is smaller than EPP. In the case that the configuration meets the largest AEP but LCOE is larger than EPP, the configuration with the largest AEP will still be given priority. Because the objective function aims at the maximum efficiency of wind energy exploitation.

- The 5th process: Determine the optimal installation configuration which is the configuration that simultaneously satisfies both constraints of the largest AEP and LCOE<EPP. If the analysis results show that LCOE is larger than EPP, this result can be used as a scientific basis to convince state managers such as EVN to adjust the EPP value more appropriately.

IV.2. Apply the designing model to an onshore wind farm area in Khanh Hoa province

This design model is applied to an area in the Khanh Hoa province (Ninh Thuan), around the coordinates (11°27'51.1"N; 109°00'17.6"E). There is a wind farm in operation here but the wind farm has been sold to a foreign energy group. This farm currently has 16 wind turbines and a series of other areas with solar panels. To avoid the effects of photovoltaic panels on the wind resources in the area, this thesis has removed the area containing photovoltaic panels, this removed area has 6 turbines. The remaining area contains 10 turbines of the ENERCON E103/2350. The main parameters of the turbine are shown in Table 4.1 [73], [74].

Table 4.1. Main parameters of ENERCON E103/2350 turbine

Parameters	Value	Parameters	Value
Manufacturer	Enercon	Minimum rotor speed	6 rd/min
Name	E103/2350	Maximum rotor speed	15 rd/min
Rotor diameter	103 m	Cut-in wind speed	2.5 m/s
Number of blades	3	Rating wind speed	12.0 m/s
HUB's height	98 m - 138 m	Cut-out wind speed	25.0 m/s
Power control	Pitch	Rating power	2,350 kW

The thesis use the design model as shown in Figure 4.1 to study and evaluate whether this farm has selected the appropriate turbine type and installation configuration, from which an optimal installation configuration for this area will be proposed. The first task is to build a topographic map and wind resources in the area around the coordinates (11°27'51.1"N; 109°00'17.6"E) as in the 1st step and 2nd step. The implementation of these two steps has been presented in detail in Section III.1. The modeled area has parameters shown in Figure 4.2.

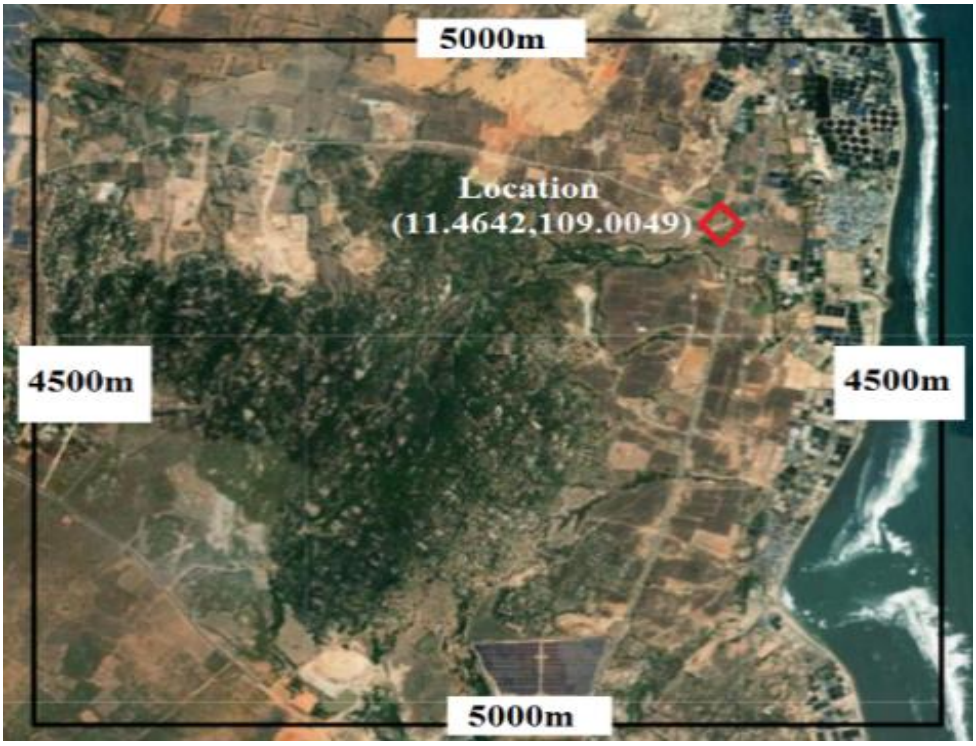

Figure 4.2. Farm area around the coordinates (11°27'51.1"N; 109°00'17.6"E)

The terrain elevation distribution of this area is also determined based on the digital terrain elevation data source DEM (SRTM 30m) integrated in QGIS as shown in Figure 4.3.

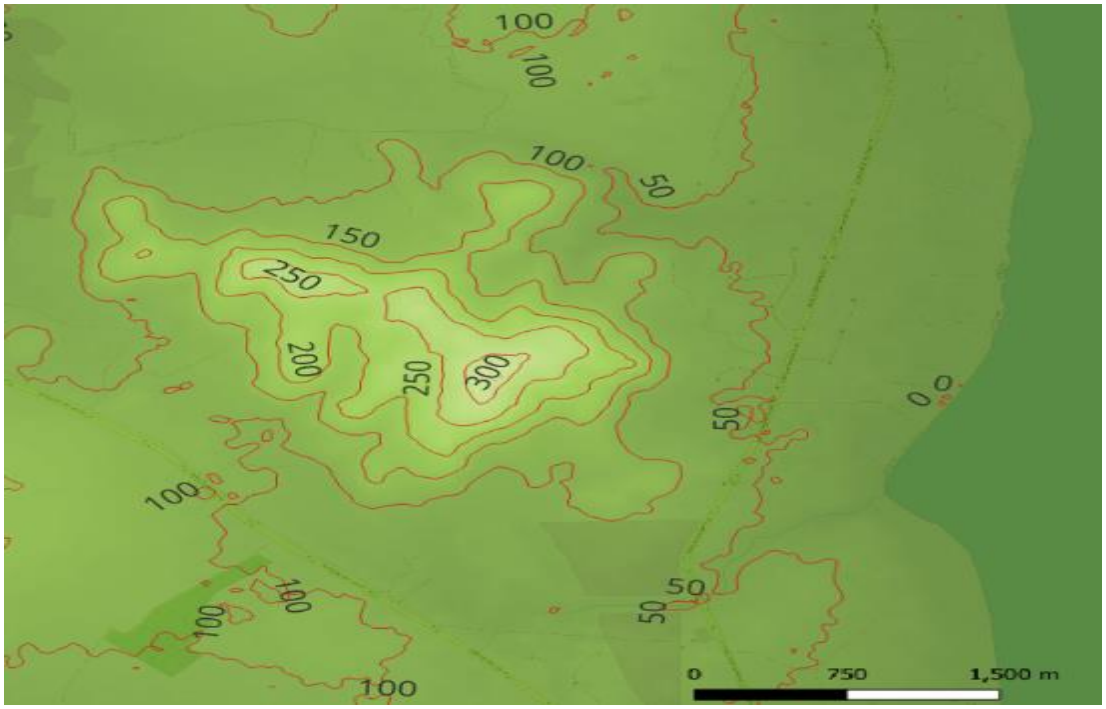

Figure 4.3. Terrain elevation distribution of the area around coordinates (11°27'51.1"N; 109°00'17.6"E)

The analytical model was built on Ansys CFX software (student version) with a length of 5,000 m, a width of 4,500 m, and an air layer height of 500 m above sea level. The mesh type used is a mixture of Quadrilateral and Hexagonal. The largest mesh size is 100 m, the total number of meshes is 166,495, and the total number of nodes is 38,618. Then, the model is set up with boundary conditions as shown in Figure 4.4. The detailed explanations of the model building process, meshing, setting up boundary conditions, and initial conditions are similar to those in Section III.1.

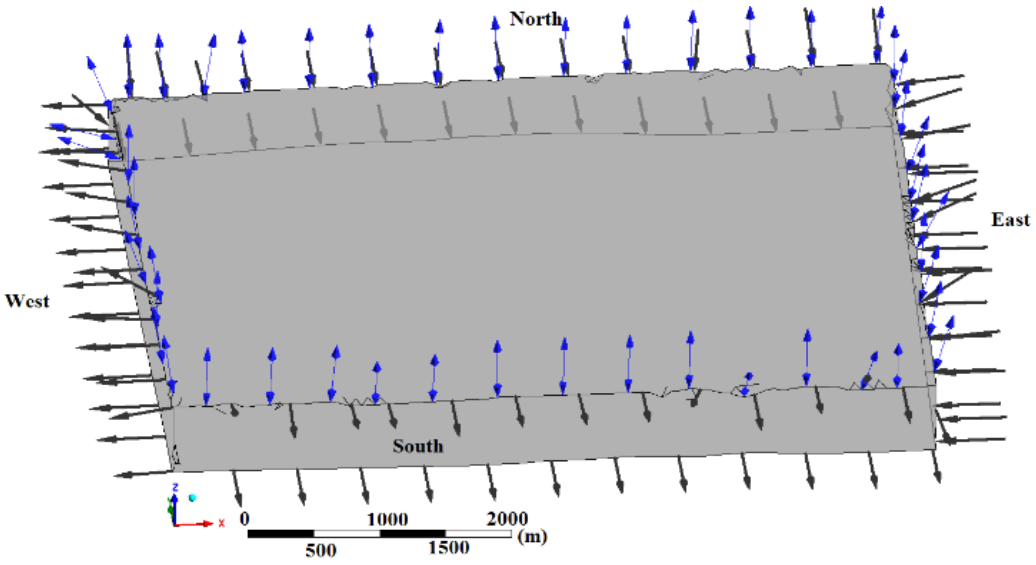

Figure 4.4. Setting up boundary and initial conditions for the model

The average wind speeds by heights in this area are determined based on wind resource data provided by the WorldBank [62]. The theoretical fitting function for the average wind speed distribution by height is shown in Figure 4.5 and equation (4.1). The wind direction and wind speed frequency distribution are shown in Figure 4.6.

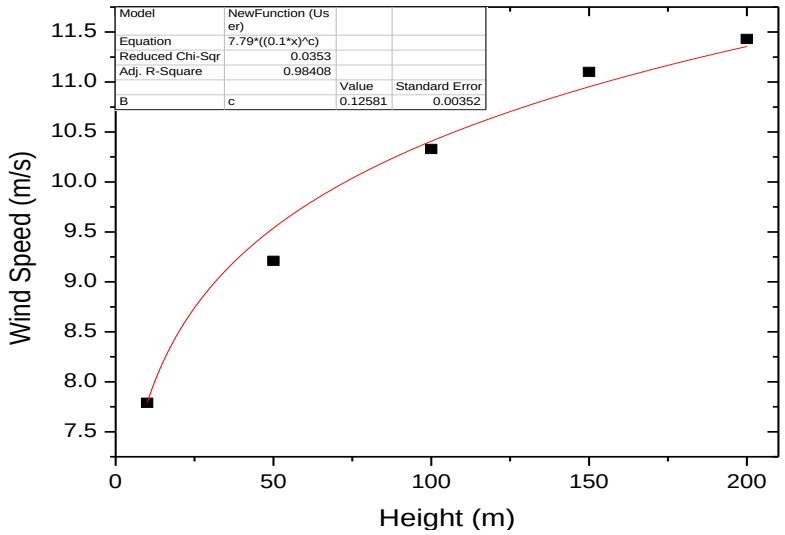

Figure 4.5. Wind speed distribution function with height

The average wind speed distribution function with height is determined as in equation (4.1):

$$WindSpeed = 7.79 \times \left(\frac{h}{10}\right)^{0.13} \quad (4.1)$$

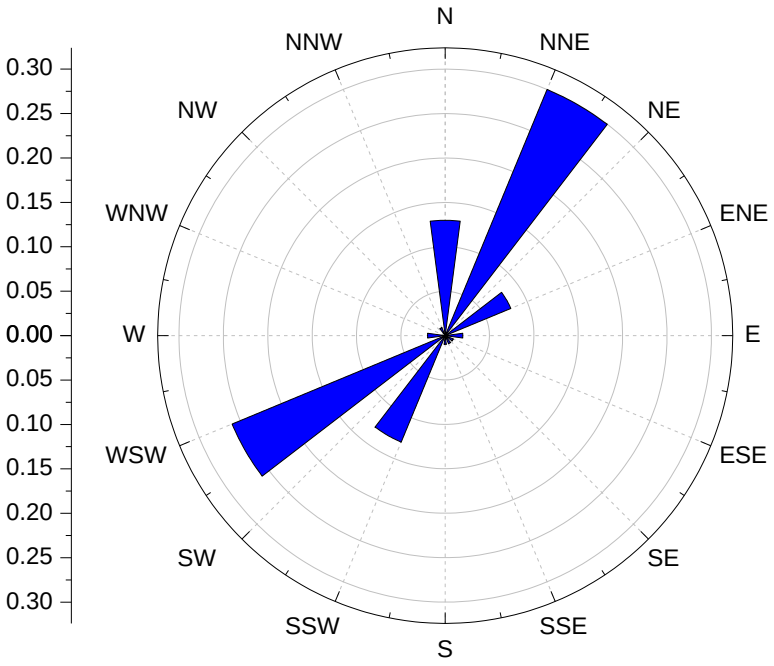

Figure 4.6. Windrose diagram at this farm area

The wind speed distribution with height at the entrance surface and the incoming wind direction are set into the analysis model in Figure 4.4 to establish the initial conditions. The main incoming wind direction is determined to be from the Northeast to the Southwest. The main wind direction is 60^{o} with the OX axis. The boundary conditions of this analysis model are that the ground surface is set as a solid, fixed medium and the surrounding air is open. The turbulence model used in this analysis is $k-\varepsilon$. Then, this model will be solved by the RANS method with a total of 500 iterations. The variation processes of the quantities participating in the simulation model are shown in Figure 4.7.

(a)

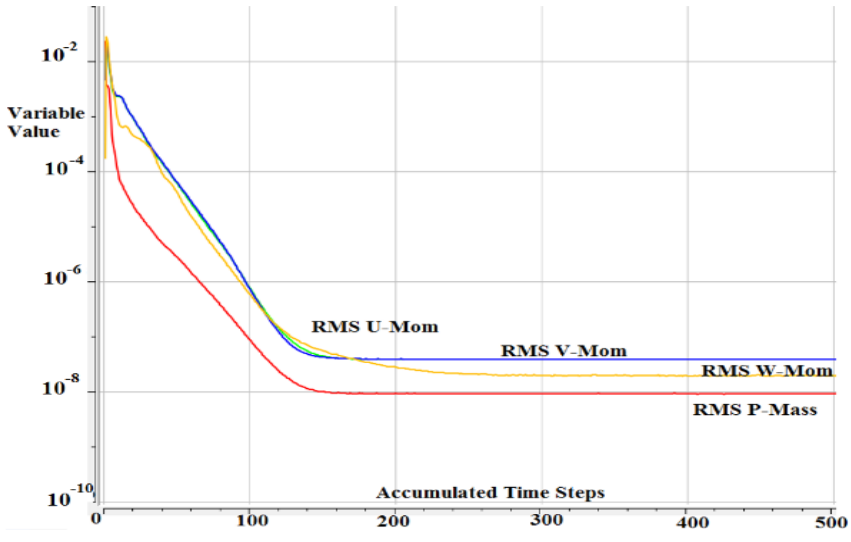

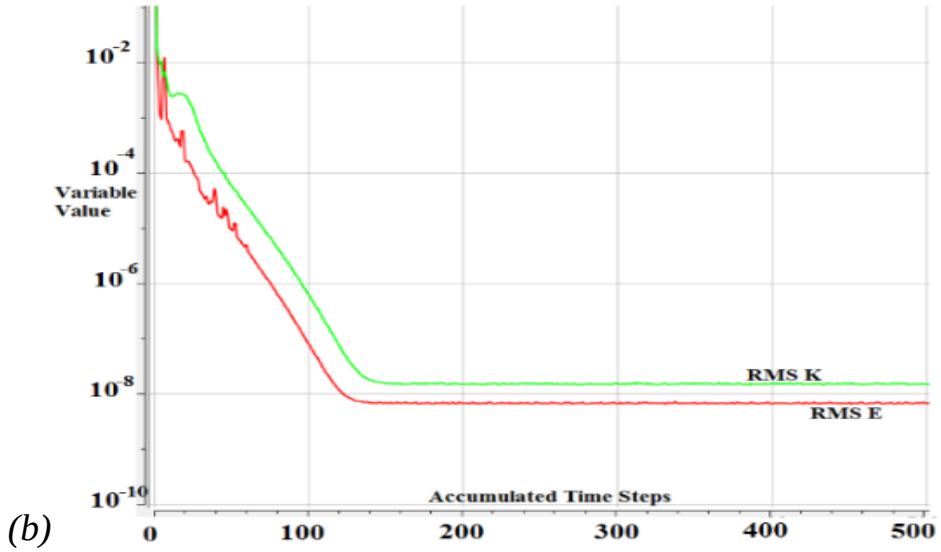

(b)

Figure 4.7. Error fluctuations of the quantities: speed and momentum (a); k and ε (b)

The error variation of the quantities such as flow velocity along the axes OX, OY, OZ, momentum, and all converge after about 250 iterations. Therefore, the results obtained from this analysis model ensure reliability in terms of calculation method. This analysis model will be stopped to record the results after 500 iterations.

The obtained results show detailed parameters of wind speeds and main direction at all spatial points contained in the model. However, to reduce the data, only a few potential areas will be processed, analyzed, and evaluated further. From the satellite data as shown in Figure 4.2, Figure 4.3, the mountain top and western areas have steep terrain, about 200 m above sea level. Therefore, it is difficult to install wind turbines here. The eastern area has flat terrain, with convenient roads for transporting and installing wind turbines. Therefore, this area will be surveyed in detail. Vertical sections perpendicular to the East direction are constructed, each section is 1,000 m apart. Along the section are vertical positions, each line is 500 m apart as shown in Figure 4.8.

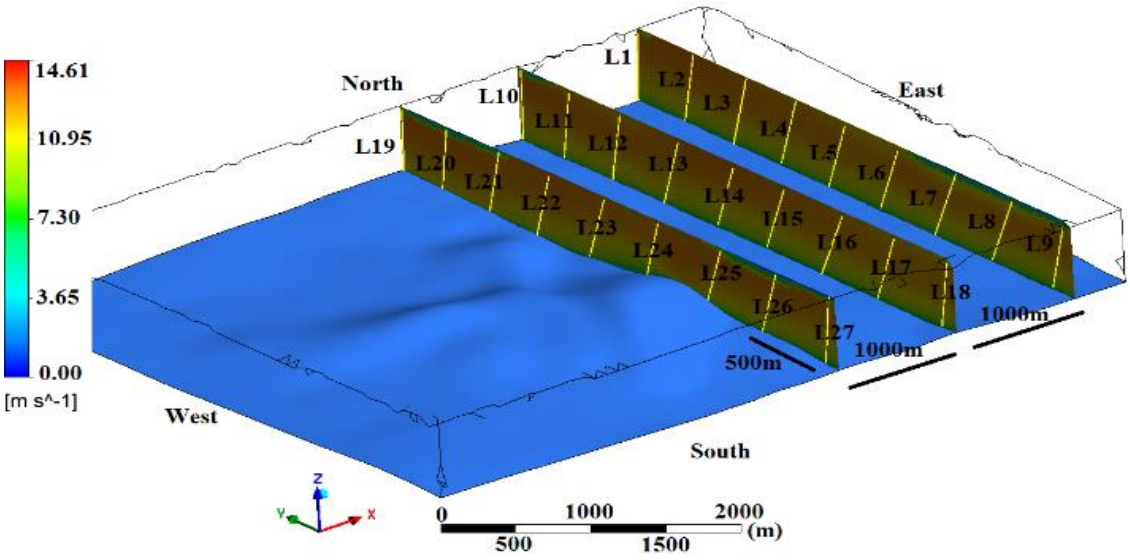

Figure 4.8. Locations surveyed in detail in the model

The wind speed distributions according to the height of about 200 m above the ground of the locations are shown in Figure 4.9. The results show that the terrain height increases gradually from the East to the West. The height difference between the cross-sections is about 30 m. The wind speed at the height of about 150 m above the ground also increases gradually from the East to the West. Figure 4.9 (a) shows that this wind speed is about 10.5 m/s, Figure 4.9 (b) shows that this wind speed is about 11.0 m/s, Figure 4.9 (c) shows that this wind speed is about 11.5 m/s. The wind speed increases due to the increase in terrain height, the volume of space is reduced according to Bernoulli's law.

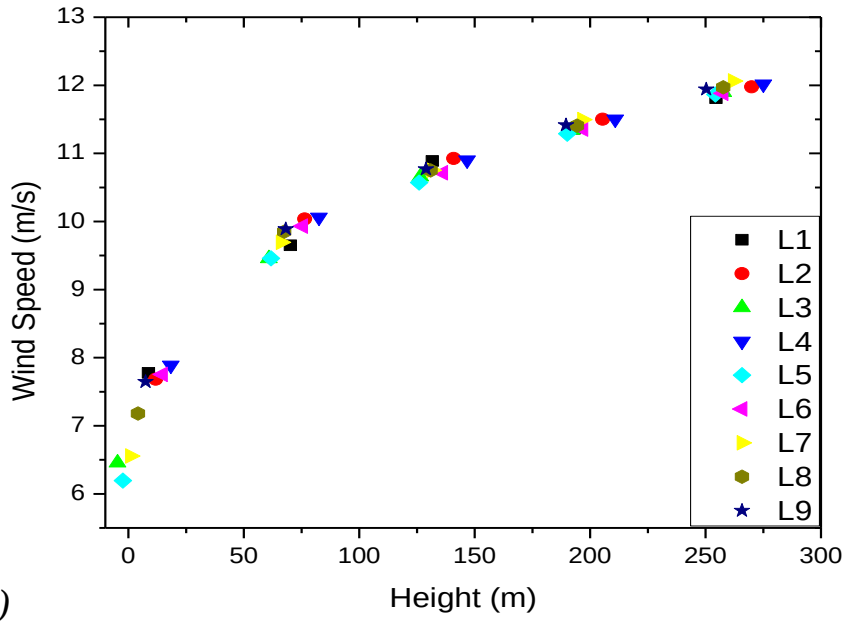

(a)

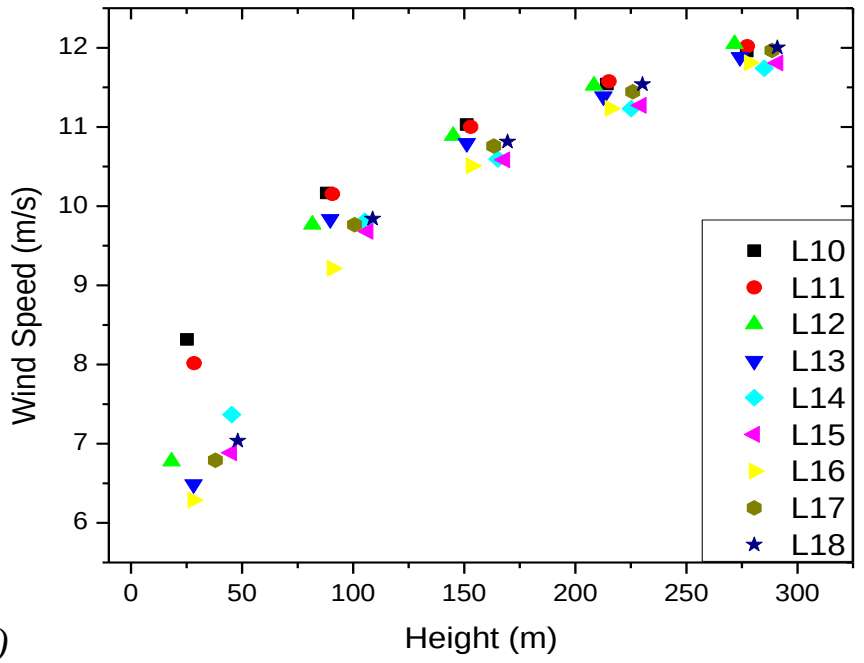

(b)

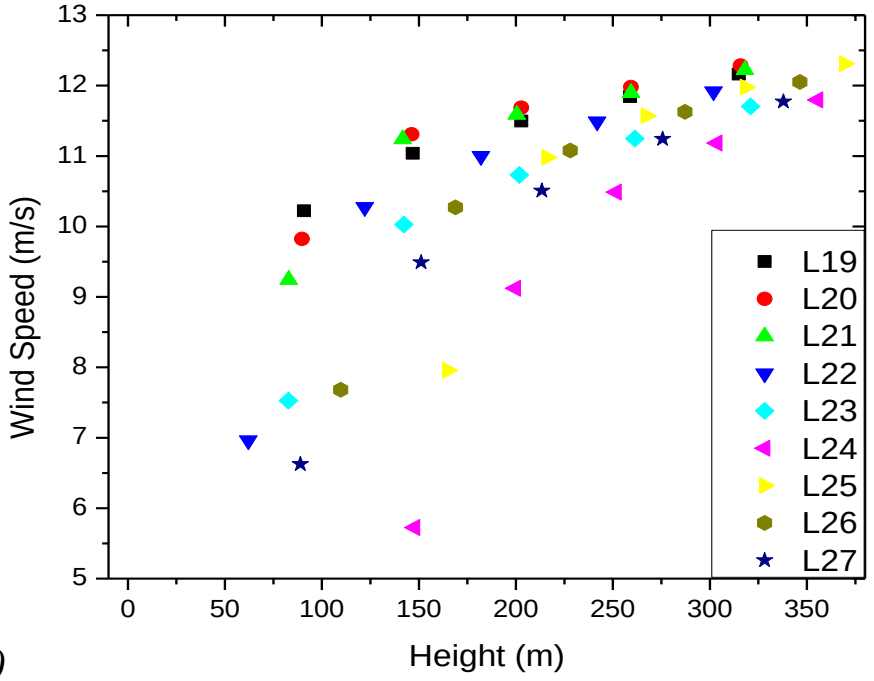

(c)

Figure 4.9. Wind speed distributions according to height at different locations

For comparison and verification of the WorldBank wind resource data, experimental data from 2008 to 2010 in this area were also used [75], [76]. The values of wind speed and main wind direction are similar to the results obtained from the analytical model with the WorldBank wind resource data. The Weibull wind speed distribution function in this area according to the main wind direction

NNE has parameters W=2.8 and S=8.9. The wind speed distribution values according to the Weibull function are shown in Figure 4.10 [77].

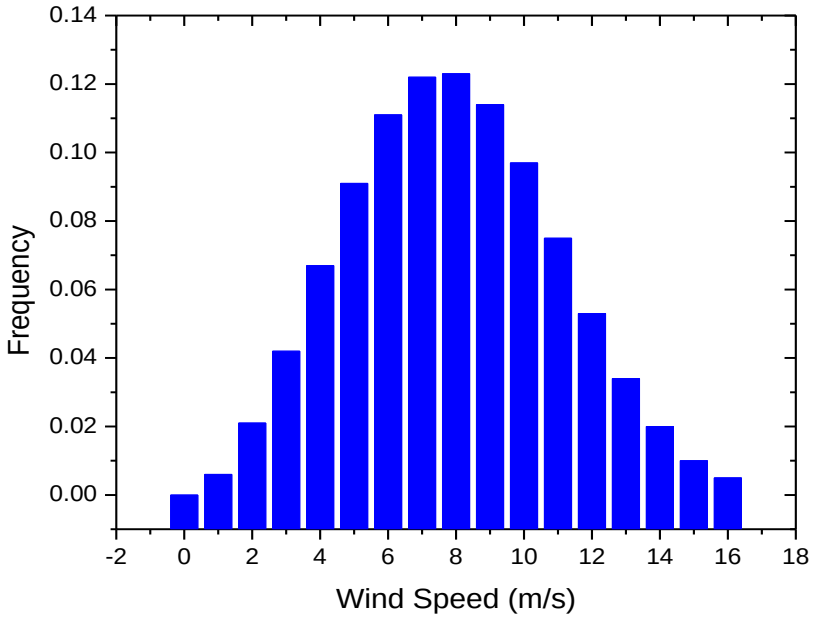

Figure 4.10. Weibull wind speed distribution function in the farm area

From the results obtained as in Figure 4.9, the rate of change of wind speeds at 100 m height according to the terrain (r_{cw}) of this area from East to West is determined as in Figure 4.11. This change is due to the impact of terrain factors on the wind resource.

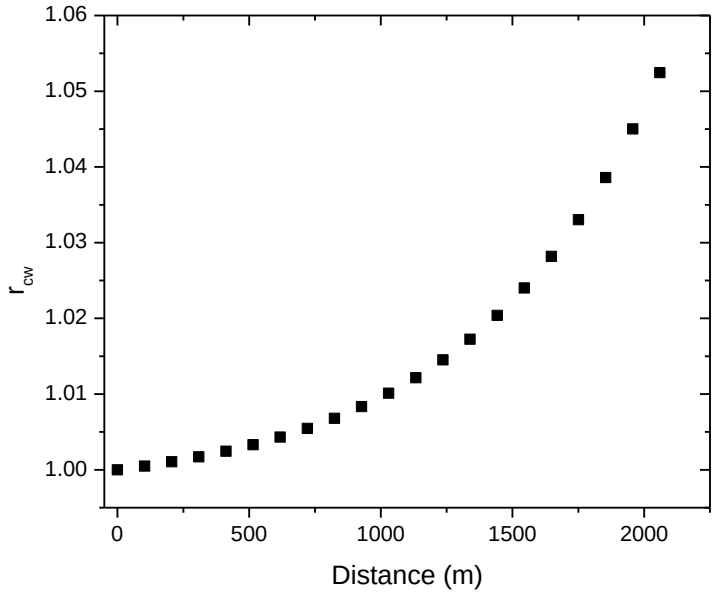

Figure 4.11. Rate of change in wind speed at 100 m height according to regional terrain

The values of r_{cw} are used to recalibrate the values of wind speed and frequency at different locations in the analysis area. From there, the Weibull wind speed frequency distribution function of this area is calibrated and represented as in Figure 4.12.

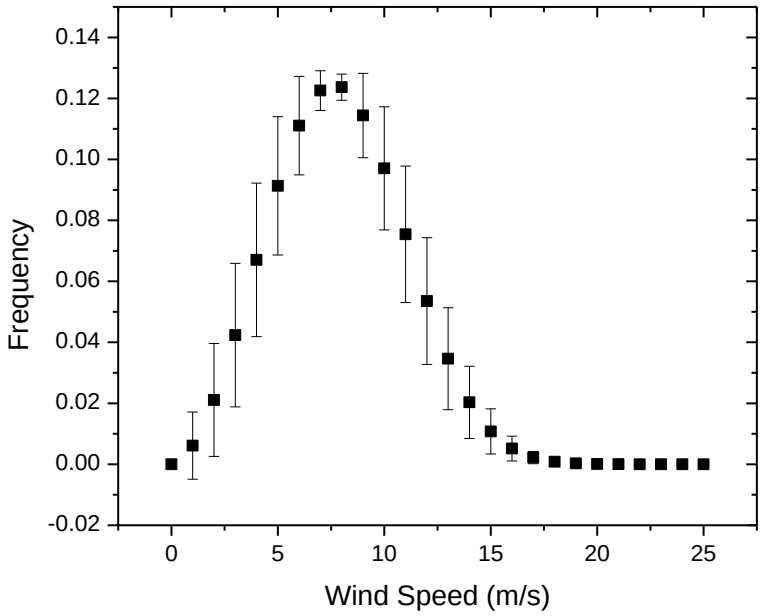

Figure 4.12. Corrected Weibull wind speed frequency distribution function

The wind speed and wind speed frequency values after correction will contain certain errors. The contributions of these errors to the AEP calculation results are described in equations (2.34) – (2.36).

The wind speed at the points in this farm is shown in Figure 4.9, the wind speed value is in the range of 10.5 m/s to 11.5 m/s at a height of 100 m above the ground. Therefore, the turbines designed with rating wind speeds in this range are suitable.

As mentioned above, this area is currently being installed with 10 Enercon E103 turbines. These turbines are designed with a rating wind speed of 12.0 m/s. Therefore, this turbine is also relatively suitable for operation in this farm area. The locations of these turbines are marked with red stars as shown in Figure 4.13.

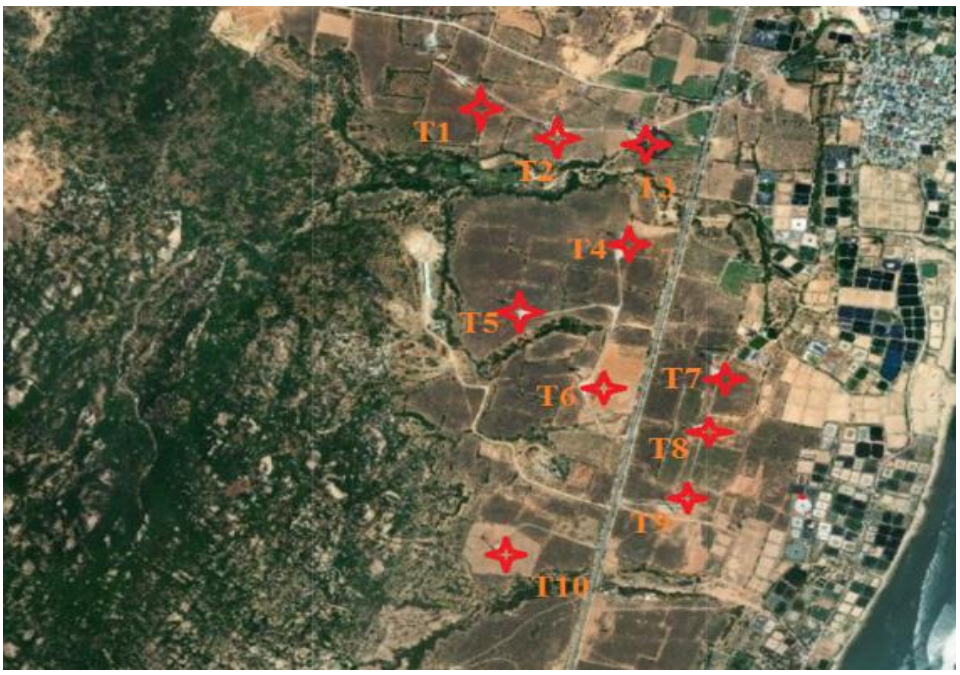

Figure 4.13. Locations of 10 E103 wind turbines in the area

The E103 is a 3-blade horizontal axis turbine with a rotor diameter of 103 m and a tower height of up to 138 m. The designed capacity is up to 2,350 kW when operating at a wind speed of 12.0 m/s. The dependences of the capacity and power coefficient of the E103 turbine on wind speed are shown in Figure 4.14.

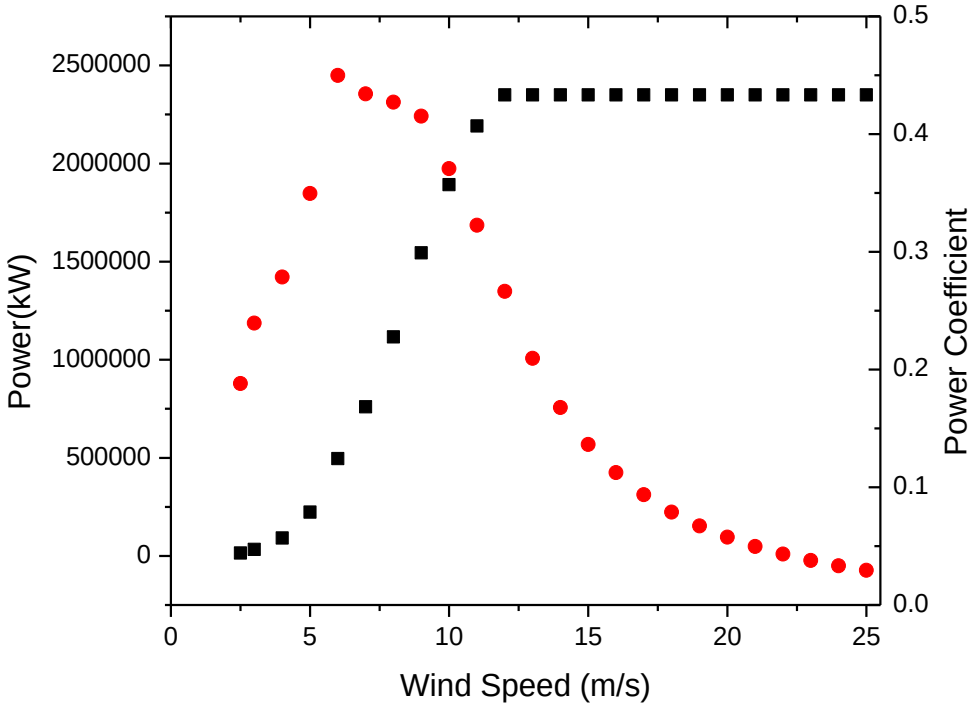

Figure 4.14. Capacity and power coefficient of the E103 turbine according to the wind speeds

From Figure 4.13, 10 turbines have been installed scattered in the Eastern area. The distance between the turbines is about 3Drotor, d=309 m. The AEP, WL values of the total of these 10 turbines are determined by formula (2.29) - (2.37), Figure 4.11 and Figure 4.12 are $(99,907,006.4 \pm 25,023,328.2)$ kWh and WL=0%. According to the guidelines in IEC-61400-12-1 [78] and IEC-61400-12-5 standards [79], the horizontal distance between the 2 nearest turbines is between 2Drotor and 4Drotor. The vertical distance between the two nearest turbines is between 2Drotor and 20Drotor depending on the complexity of the terrain. Therefore, the E103 turbines installed in this farm meet this requirement. According to the data in Figure 4.3 and Figure 4.9, the turbines T3, T7, T8, T9 are installed at lower positions than the remaining turbines. The maximum height difference is about 50 m. This shows that the installed configuration of these 10 turbines has not achieved the maximum AEP value. According to equation (4.1), the higher the positions, the higher the average wind speeds. Therefore, all 10 turbines should be installed in areas between the contour lines from 50 m to 100 m as shown in Figure 4.15.

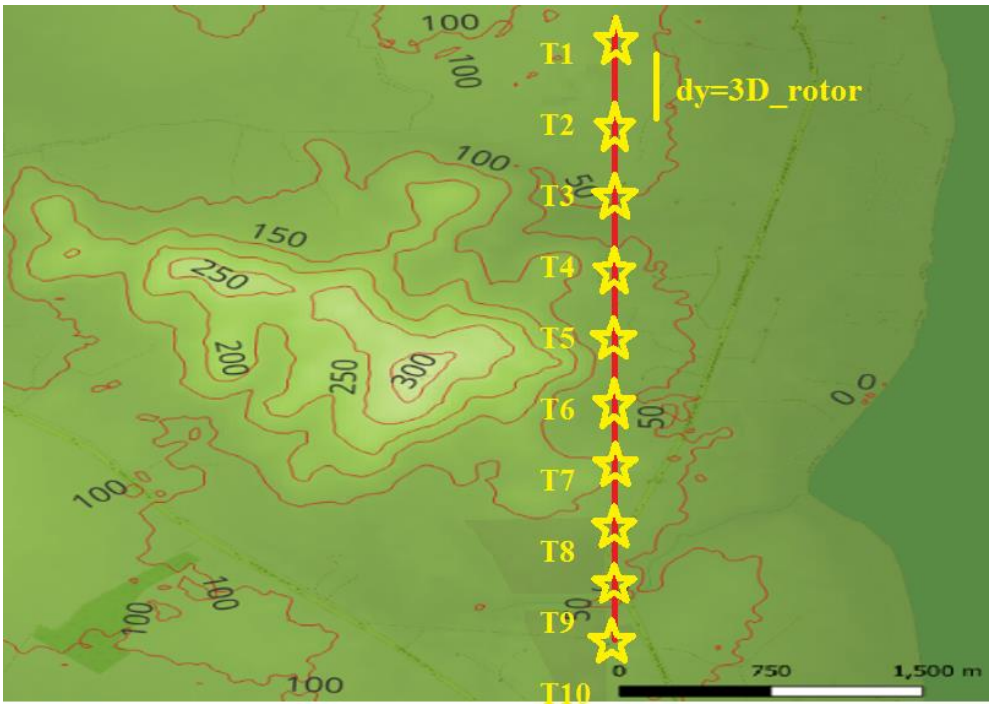

Figure 4.15. Proposed installation configuration of 10 turbines

If the 10 turbines are installed according to this newly proposed configuration, the wind resource to the turbines will be more uniform and have a larger average value (r_{cw}=1.05). The annual electricity production value is ($104,054,042 \pm 26,518,798$) kWh. Obviously, when using this new installation configuration, the AEP value of 10 turbines will increase by 4,147,035.8 kWh (4.2%). This brings higher economic benefits with the amount of electricity sold increasing by about 7.6 billion VND/year based on the wind electricity purchase price for the South regions in 2025.

In fact, the positions of the turbines are not arranged in straight rows, not in any relative shape. This leads to the turbines operating at uneven wind speeds, causing instability in the control of the output power parameters. Obviously, the turbines should be installed in horizontal rows perpendicular to the East direction so that all turbines in a row will operate at the same wind speed as illustrated in Figure 4.16. From here, the next steps of the design model as shown in Figure 4.1 will be implemented in turn to evaluate and select the optimal installation configuration with the characteristics of this farm area. The horizontal turbine space is about 3Drotor as in practice today. The vertical turbine space from East to West will be changed from 3Drotor to 20Drotor. The axial induction factor values of E103 turbine with wind speed are shown in Figure 4.17. When this turbine operates at wind speeds of about 11.0 m/s or more, the value of a is 0.1.

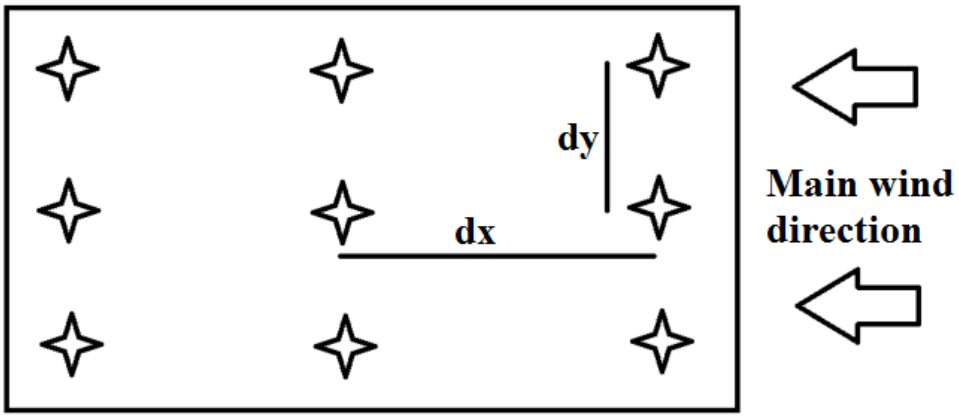

Figure 4.16. Illustration of the installation configuration of turbines

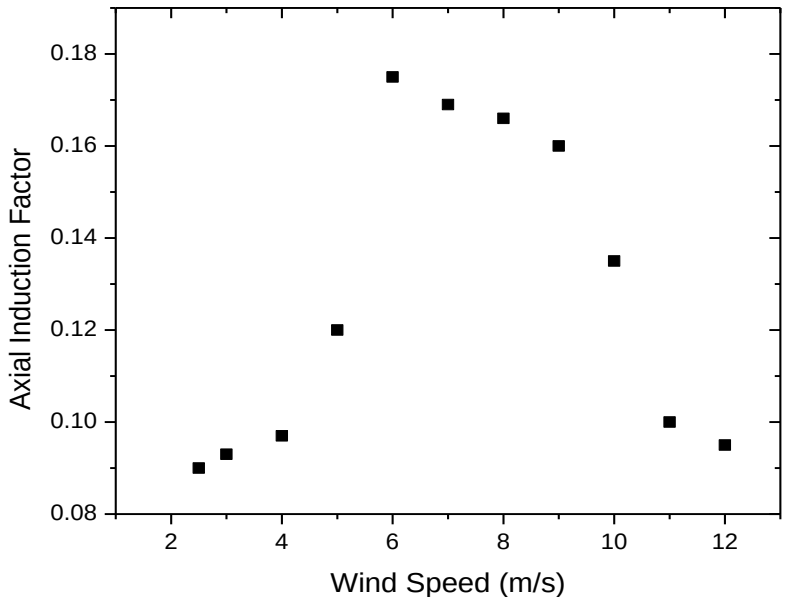

Figure 4.17. Axial induction factor of E103 with wind speed

The wind velocity deficit with distance of the rear turbine is determined based on Jensen's wake theory for the E103 turbine as shown in Figure 4.18. The data shows that the wind velocity deficit decreases sharply with distance from 2Drotor to 10Drotor. From distances greater than 10Drotor, the wind velocity deficit decreases insignificantly. From here, the optimal distance for installing the rear turbines is 1030 m. At this distance, the wind velocity deficit is 11.8%. This value is generally accepted in the actual operation of onshore wind farms.

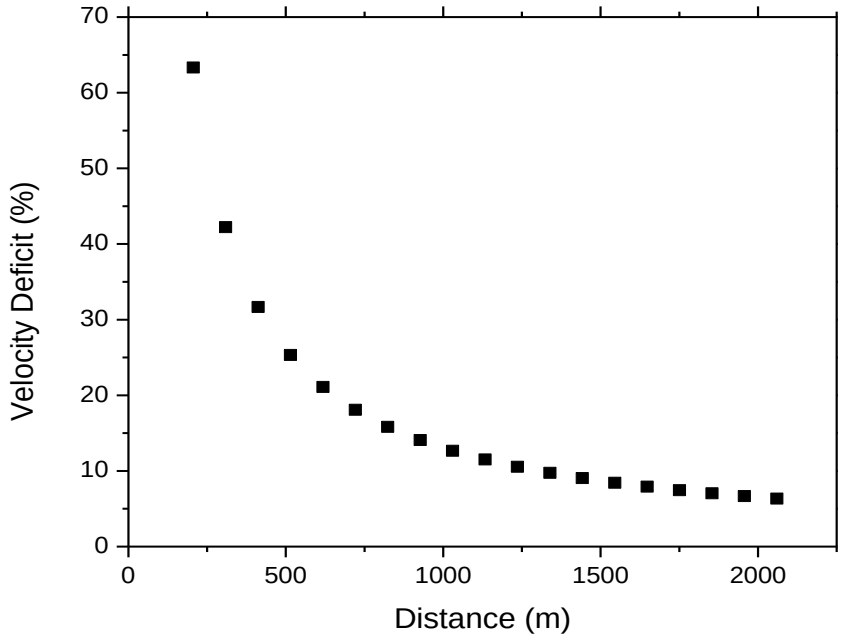

Figure 4.18. Wind velocity deficit with distance of E103 turbine

According to Figure 4.2, Figure 4.3, the flat area from the coast to the foot of the mountain is about 2,500 m. When excluding residential areas, the area where wind turbines can be installed is about 2,000 m wide and 4,000 m long. The configurations that can be installed are as follows: If the distance between turbine rows is 3Drotor, 6 rows can be installed; if the distance is 4Drotor, 4 rows can be installed; if the distance is 5Drotor to 6Drotor, 3 rows can be installed; if the distance is 7Drotor - 10Drotor, 2.5 rows can be installed; if the distance is from 11Drotor to 19Drotor, 2 rows can be installed; if the distance is over 20Drotor, 1 row can be installed. These configurations are calculated specifically as follows:

- The 1st configuration: Installed configuration with a row spacing of 3Drotor, the distance between the two closest turbines in each row is 309 m, the total number of turbines is 72. Then the wind speed at each row of turbines behind will be reduced by 42.2% respectively as shown in Figure 4.18. This causes the turbines in the 4th row to have wind speeds below the operating level, only the first 3 rows can operate. The total AEP is $(152,778,722.7 \pm 41,745,155.8)$ kWh and WL is 78.8%.

- The 2nd configuration: Installed configuration with a row spacing of 4Drotor, the distance between the two closest turbines in each row is 412 m, the total number of turbines is 48. Then the wind speed at each row of turbines behind will be reduced by 31.7% respectively as shown in Figure 4.18. The total AEP is $(184,596,510.4 \pm 51,939,780.0)$ kWh and WL is 61.5%.

- The 3rd configuration: Installed configuration with a row spacing of 6Drotor, the distance between the two closest turbines in each row is 618 m, the total number of turbines is 36. Then the wind speed at each row of turbines behind will be reduced by 21.1% respectively as shown in Figure 4.18. The total AEP is $(230,843,859.7 \pm 64,878,160.2)$ kWh and WL is 35.8%.

- The 4th configuration: Installed configuration with a row spacing of 10Drotor, the distance between the two closest turbines in each row is 1,030 m, the total number of turbines is 30. Then the wind speed at each row of turbines behind will be reduced by 12.7% respectively as shown in Figure 4.18. The total AEP is $(230,843,859.7 \pm 64,878,160.2)$ kWh and WL is 15.8%.

- The 5th configuration: Installed configuration with a row spacing of 19Drotor, the distance between the two nearest turbines in each row is 1,957 m, the total number of turbines is 24. Then the wind speed at each row of turbines behind will be reduced by 6.7% respectively as shown in Figure 4.18. The total AEP is $(236,118,269.7 \pm 59,766,995.9)$ kWh and WL is 1.5%.

- The 6th configuration: Installed configuration with a row spacing of 20Drotor, the distance between the two nearest turbines in each row is 2,060 m, the total number of turbines is 12. Then the wind speed at each row of turbines behind will be reduced by 6.3% respectively as shown in Figure 4.18. The total AEP is $(119,888,407.7 \pm 30,027,993.8)$ kWh and there is no wake loss due to the front turbine in this case.

These results are shown in Figure 4.19.

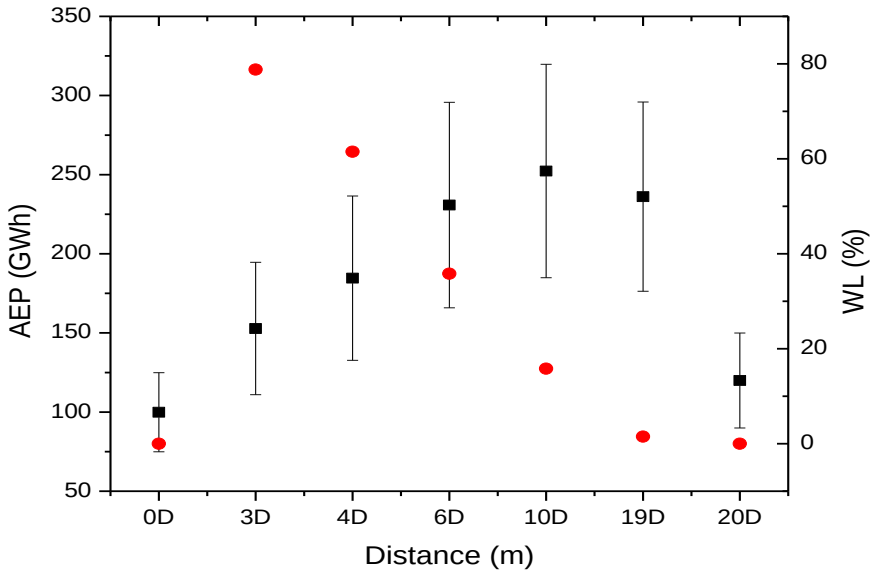

Figure 4.19. Changes of AEP and WL according to different installation configurations

Comparing the results obtained from 6 different installation configurations as shown in Figure 4.19, the 4th configuration with a turbine row spacing of 10Drotor gives the largest AEP and a wake loss of only 15.8%. This is the most optimal configuration for the E103 turbines installed at this wind farm. The third row of this configuration has half of it passing through the foothills, so it is not possible to install the turbines here. Figure 4.20 illustrates the installation configuration of the E103 turbines in the survey area according to the 10Drotor spacing. The installation locations of the turbines are shown as yellow stars.

Figure 4.20. Optimum configuration for installing the E103 turbines at the farm area

If the E103 turbines are installed at the locations marked with yellow stars in Figure 4.20, the power of the turbines will be more uniform. This helps with the control and output power quality issues. In addition, the total number of turbines that can be installed in this area is 30, which is 3 times larger than the actual number. The annual electricity production of the optimal configuration can be about 2.5 times larger than the current configuration.

Wind farms impact the national grid by causing voltage and frequency fluctuations due to the variable and intermittent nature of wind. This can affect the quality and stability of electricity, especially at high penetration levels. Optimum configuration of wind farms will help to achieve more uniform power output from turbines. However, the nature of wind resources is intermittent. Therefore, wind farms still cause some specific problems as follows:

- Intermittency and fluctuation: Wind power output fluctuates based on wind speeds, which can cause sudden changes in power generation. This makes it difficult to balance supply and load in real time.

- Power quality issues: Changing wind speeds can cause voltage fluctuations and harmonics, which can affect power quality.

- Reduced grid inertia: Modern wind turbines are connected via inverters, without the physical inertia of traditional synchronous generators. This reduces the overall inertia of the grid, making it less resilient to sudden disturbances and increasing the risk of frequency sags.

- Grid stability challenges: High penetration can lead to stability issues, such as power fluctuations, which may require additional control systems to manage.

- Infrastructure needs: Many areas with high wind speeds are remote, requiring the construction of new transmission lines to transport electricity to population centers.

However, optimally designed wind farms can also have positive impacts, such as:

- Voltage support: Wind farms, especially those with reactive power control systems such as STATCOMs, can support and stabilize voltage, especially in areas with poor voltage quality at the end of long and weak lines.

- Improved grid management: Geographical diversification of wind farms can help smooth out power output fluctuations.

- Modern turbine technology: New turbines are designed with advanced control systems to help maintain stability and overcome disturbances without disconnecting from the grid.

- Control technology: New control technologies and integration of energy storage systems are being developed to help modern wind turbines provide grid services such as frequency response and aggregate inertia.

To increase the feasibility of this optimal installation configuration, the thesis continues to calculate the LCOE value of the proposed installation configurations according to equation (2.38). LCOE is determined based on four main quantities: CapEx, OpEx, rd and AEP. CapEx includes all initial investment costs such as turbine purchase costs, transportation, installation, land rental, project management costs, etc.; OpEx includes costs related to operation and maintenance, and repair of the turbine throughout its operating life. The discount rate, rd, is the interest rate used to discount the cash flows in and out of the project; AEP is the annual electricity production of the wind farm.

According to IRENA [80], the global average total installation cost decreased by about 12% per year in the period 2010-2024. The global average CapEx is 1,041 $/kW in 2024. The CapEx of the Vietnamese market is about 1,500 $/kW in 2024. This is because the turbines have to be completely imported, mainly from European suppliers. This leads to higher project management and transportation costs. In general, the world average CapEx is relatively stable. This also helps the CapEx value for the Vietnamese market to maintain a steady downward trend. The decrease in CapEx value is mainly due to the expansion of production scale and improved capacity factor of turbines.

Operation and maintenance costs play an important role in maintaining the performance, reliability and long-term efficiency of wind energy projects. As

wind power deployment expands globally and operations and maintenance techniques become more sophisticated, data-driven, and cost-optimized, this has led to a significant decline in OpEx values over the 2010-2024 period. In addition, OpEx is also subject to a number of changing factors such as insurance, land rental prices, and tax incentives from countries. For Vietnam, the government has always affirmed tax exemptions and land rental costs for renewable energy projects, especially wind power. Obviously, OpEx will maintain a stable value for the next several decades.

Currently, wind power projects in Vietnam mainly involve large foreign corporations. Investment cash flow is relatively stable. In addition, the Vietnamese market is also a stable market. Therefore, changes in the discount rate of wind power projects are insignificant, with very little impact on LCOE. Also according to IRENA, the global average LCOE value for onshore wind power projects decreased by 3% per year during the period 2010 – 2024. LCOE values ranged from 24.0 $/MWh to 75.0 $/MWh in 2024.

Detailed calculations of LCOE are not the research objective of this thesis. LCOE is only used as a value showing the conformity with the actual electricity purchase price currently applied in Vietnam. Therefore, based on published figures for an equivalent turbine (2.6 MW) as in references [60] and [61]. CapEx is determined based on three main quantities: turbine capital cost (991 $/kW), balance of system (326 $/kW), financial costs (120 $/kW). From there, CapEx is determined to be 1,436 $/kW. The OpEx of this onshore turbine depends on the policies of each country, the OpEx value is usually between 32 $/kW/year and 54 $/kW/year. In this thesis, the OpEx value is determined to be 43 $/kW/year. The discount rate depends on the markets, policies and capital of the investor. In this calculation, rd is chosen to be 14.6% and the operating time is 20 years [80]. The calculation results are shown in Table 4.2 and Figure 4.21.

Table 4.2. WL, AEP and LCOE values according to different turbine installation configurations in the farm

Configurations	WL (%)	AEP (GWh/year)	LCOE ($/MWh)
Reality	0	99.9 ± 25.0	67.1 ± 16.8
3D	78.8	152.8 ± 41.8	315.7 ± 86.3
4D	61.5	184.6 ± 51.9	174.3 ± 49.0
6D	35.8	230.8 ± 64.9	104.5 ± 29.4
10D	15.8	252.3 ± 67.4	79.7 ± 21.3
19D	1.5	236.1 ± 59.8	68.1 ± 17.2
20D	0.0	119.9 ± 30.0	67.1 ± 16.8

From the data shown in Figure 4.21, the LCOE value of the optimal installation configuration is 79.7 $/MWh, the actual installation configuration is 67.1 $/MWh. These two values are approximately equal and are completely acceptable according to the electricity purchase price from wind power projects in Vietnam, EPP=79.5 $/MWh in 2025 [7]. This once again confirms that the 4th configuration is the optimal installation configuration for this wind farm area.

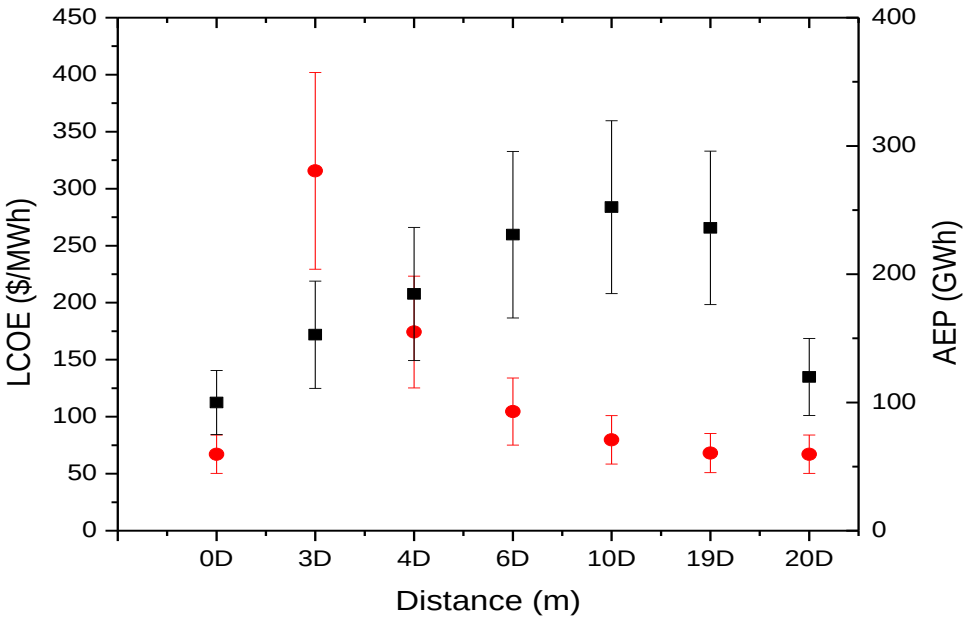

Figure 4.21. Changes of LCOE and AEP according to different installation configurations

If the E103 turbines are installed at the locations marked with yellow stars in Figure 4.20, the output electric powers of the turbines will be more uniform. This helps to control and improve the quality of the output electric power. In addition, the total number of turbines that can be installed in this area is 30, which is 3 times the actual number. The annual electricity production of the optimal installation configuration can be about 2.5 times larger than the current configuration.

When considering the problem, assume the installation of a small wind turbine using the VAST-EPU-S1223 model as designed in Chapter III. The rotor diameter of the VAST-EPU-S1223 turbine is 10.0 m. The rated power of this turbine is 6.57 kW when operating at a rated wind speed of 8.0 m/s. This rated wind speed is consistent with the average wind speed in the farm. These turbines will also be installed in the optimal configuration as for the E103 turbines. From the area of the farm and the rotor diameter, this farm will be able to install 25 rows of turbines, each row will have 130 turbines. The changes in power and power coefficient of the VAST-EPU-S1223 turbine with wind speeds are shown in Figure 4.22.

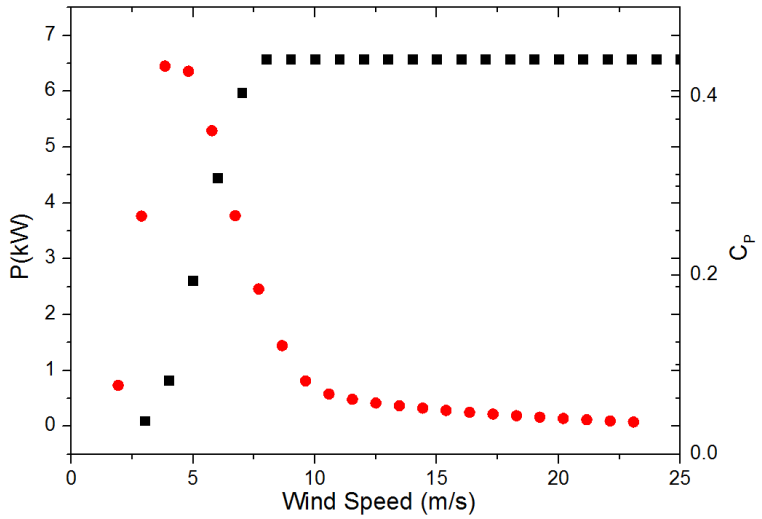

Figure 4.22. Capacity and power coefficient of the VAST-EPU-S1223 turbine according to the wind speeds

Performing the same calculation steps as for the E103 turbines, the AEP values obtained from the VAST-EPU-S1223 turbine rows are given in Table 4.3.

Table 4.3. AEP values obtained from the VAST-EPU-S1223 turbines

Row	AEP (kWh)	Row	AEP (kWh)
1	5763044.0 ± 1154155.4	9	266537.3 ± 103308.2
2	4621008.9 ± 1036440.1	10	155582.9 ± 67246.6
3	3582920.6 ± 902152.7	11	85362.7 ± 41528.2
4	2654905.2 ± 739043.1	12	30188.7 ± 18757.5
5	1754776.5 ± 515870.3	13	13053.4 ± 9144.9
6	1191269.9 ± 354379.8	14	2686.6 ± 2363.9
7	752238.9 ± 231674.5	15	362.6 ± 393.2
8	455214.8 ± 154076.1	16	≈ 0

When the turbines are installed with 3Drotor apart in the perpendicular direction and 10Drotor in the main wind direction, only the first 15 turbine rows receive enough wind energy to operate. The wind speeds up to the 16^{th} turbine row onwards has a value less than 3.0 m/s, so these turbines cannot operate. The average AEP value of this configuration is 21,329,153.2 kWh. This value is only 21.3% compared to the actual configuration and only 9.2% compared to the newly proposed configuration. This shows that turbines optimally designed for wind speeds between 4.0 m/s and 6.0 m/s will not operate efficiently when working at an average wind speed of 8.0 m/s.

Summary:

The wind farm installation configuration design model proposed in this thesis can determine the influence of terrain factors, wind resources, turbine types and turbine installation configurations in a wind farm development area on the AEP value. The goal of this design model is to determine the installation configuration of turbines in the farm to obtain the largest AEP value. This model uses GIS-based terrain data sources. Therefore, the farm's terrain surface data such as roughness and elevation are presented visually and clearly. Then, only wind

resource data at a point in the farm area is needed. The CFD method simulates the entire interaction processes of this wind resource with the specific terrain. From there, the wind resource characteristics at each location in the wind farm area are determined. This is a great advantage of CFD compared to all other methods. Obviously, the GIS – CFD combined model has many outstanding features in solving the aerodynamic problems of wind farms.

Jensen and BEM theories perform calculations to determine AEP based on the results obtained from the GIS – CFD model. Combining theories and simulation models simultaneously makes this design model perfect, simultaneously evaluating many different factors affecting the AEP of an onshore wind farm.

CONCLUSIONS

The thesis has conducted research and proposed the models for designing turbine blade profiles and turbine installation configurations of onshore wind farms. These models include three main parts: determining locations with high wind energy potential, turbine blade profiles for the largest power coefficients and installation configurations for the largest annual electricity productions.

These design models include both analytical theories and numerical simulation methods. The theories help determine the relationships between the quantities describing the operation of wind turbines. Simulation models help to correct the values of wind speed, turbulence intensity, wind speed frequency, and wind direction at locations in the wind farm development area. These models are highly suitable and general for actual conditions in Vietnam.

In addition, the boundary conditions of the models are terrain conditions, and the initial conditions are wind resource characteristics. Therefore, these design models only need wind resource data measured at a location in the farm area. Then, the entire processes of movement, interaction and transformation of wind resource characteristics according to the terrain will be accurately described by the GIS - CFD model. From there, some hypothetical risk analysis cases under extreme weather conditions can also be easily identified, helping to minimize problems related to incidents and accidents throughout the life cycle of the turbines. This is also a great advantage of the model compared to other design models.

The design models proposed in this thesis are highly effective and intuitive. However, the participating models such as GIS and CFD are modern, big data models. To use these tools, a computer system with a large enough configuration is required and the person performing these analyses must have sufficient knowledge and experience. Especially experiences in selecting mesh type, meshing, selecting solver, turbulence model in CFD models.

Some new scientific and practical contributions:

- In terms of science: This thesis studies and proposes the design models base on the combination of BEM, Jensen theories and modern numerical simulation models such as GIS, CFD. GIS models use large, high-resolution spatial data sources to accurately determine the terrain characteristics of the wind farm area. CFD models are modern analysis and simulation tools. Systems of conservation equations are used to accurately and visually describe all possible interactions of wind resources in the farm area. Determining meshing methods, choosing turbulent flow models, boundary conditions and initial conditions play a decisive role in the accuracy of the CFD simulation models. The specific parameters of the CFD simulation models used in this thesis are new scientific contributions.

- In terms of practice: Vietnam is strongly developing renewable energy. In which, wind power will contribute a large proportion to the power source structure in the future. Currently, Vietnam is in the process of implementing many onshore and offshore wind power projects. This thesis provides the models for designing blade profiles and installation configurations of onshore wind farms. These models can contribute to the management and investment efficiency of onshore wind power projects in Vietnam. The thesis has contributed 02 new design models, specifically including:

+ Proposing the design model of turbine blade profiles according to actual wind resource conditions in Vietnam, in order to obtain the largest power coefficients.

+ Proposing the design model of turbine installation configurations of onshore wind farms according to actual terrain and wind resource conditions in Vietnam, in order to obtain the largest AEP values.

Related contents that have not been implemented:

- The turbine blade design model only stops at the goal of designing the blade profiles for the highest wind energy exploitation efficiency. It has not

considered different issues of materials, structures, manufacturing capabilities, costs, etc.

- The turbine installation configuration design model in the farms only provides specific location configurations and then calculates the value of annual electricity production. This thesis has not comprehensively considered different types of turbines, and has not surveyed in detail the wake effects in different directions. Therefore, the initial application results of the model are still limited. These limitations are largely due to the lack of actual data from wind farms in Vietnam.

Future Work:

The results presented in this thesis are only the first step. In the next steps, research directions related to the selection of materials for manufacturing turbine blades and turbine blade manufacturing technology based on modern technologies such as 3D printing will be prioritized. In addition, studies using artificial intelligence models will also be conducted to compare and verify with the results obtained from the models proposed in this thesis.

LIST OF SCIENTIFIC PUBLICATIONS

Research results published during 2022 - 2025 related to the thesis: 02 articles published in international scientific journals in the SCIE Q1 category; 01 article published in an international scientific journal in the ESCI Q2 category; 02 articles published in international scientific journals in the Scopus Q3 category; 04 international scientific conference reports in the Scopus category; 04 articles published in domestic scientific journals in the scoring category of the State Council For Professorship.

Table 6.1. List of published scientific articles

No.	Articles	Year	Journals
1	Technology trends in onshore wind turbine design – Performance assessment in Vietnam	2025	2nd Asia Meeting on Environment and Electrical Engineering (EEE-AM), Hanoi, Vietnam, 2025, pp. 1-5. IEEE Xplore. **(Scopus)**
2	Study on design of NREL 5MW equivalent turbine blade using VAST-EPU-N6409 airfoil model	2025	2nd Asia Meeting on Environment and Electrical Engineering (EEE-AM), Hanoi, Vietnam, 2025, pp. 1-4. IEEE Xplore. **(Scopus)**
3	A proposed airfoil configuration to improve aerodynamic efficiency applied in the design of small wind turbines.	2025	Journal of Advanced Research in Fluid Mechanics and Thermal Sciences, Vol. 133, No. 2, pp. 140 - 154. https://doi.org/10.37934/arfmts.133.2.140154. ISSN: 2289 – 7879. **(Scopus Q3)**
4	Optimization method of	2025	IEEE Access, Vol. 13, pp.

No.	Articles	Year	Journals
	wind turbine locations in complex terrain areas using a combination of simulation and analytical models.		114384 - 114400. https://doi.org/10.1109/ACCESS.2025.3584560. ISSN: 2169 - 3536. **(SCIE Q1)**
5	A method to design an efficient airfoil for small wind turbines in low wind speed conditions using XFLR5 and CFD simulations.	2024	Energies, Vol. 17, No. 16, pp. 1 - 19. https://doi.org/10.3390/en17164113. eISSN: 1996 - 1073. **(SCIE Q1)**
6	Analysis and comparison of aerodynamics of NACA airfoils under low wind speed conditions.	2024	Hanoi University of Industry Journal of Science and Technology, Vol. 60, No. 7, pp. 150 - 156. P-ISSN: 1859-3585; E-ISSN: 2615-9619
7	Consideration of various configurations of SG6043-based rotor applied in small capacity horizontal axis wind turbine.	2024	Int. J. Renew. Energy Dev., Vol. 13, No. 3, pp. 396 - 404. https://doi.org/10.61435/ijred.2024.60036. ISSN: 2252 - 4940. (**ESCI Q2)**
8	Aerodynamic analysis of NACA64A010 airfoil using XFLR5 and ANSYS Fluent.	2024	GMSARN International Journal, Vol. 18, No. 2, pp. 258 - 266. ISSN: 1905 - 9094. **(Scopus Q3)**
9	Modifying NACA6409 airfoil configuration to improve aerodynamic performance in low wind speeds.	2023	1st Asia Meeting on Environment and Electrical Engineering (EEE-AM), Hanoi, Vietnam, pp. 1-5. IEEE Xplore. https://doi.org/10.1109/EEE-

No.	Articles	Year	Journals
			AM58328.2023.10395332. **(Scopus)**
10	Study to evaluate the effect of terrain surface on performance of a wind farm in Ninh Thuan province, Vietnam.	2023	E3S Web of Conferences Vol. 470, ID. 01038, pp. 1 – 11. https://doi.org/10.1051/e3sconf/202347001038. eISSN: 2267-1242. **(Scopus)**
11	Evaluating the wind resources in an area that is equivalent to the size of a wind power plant: a methodology.	2023	TNU Journal of Science and Technology, Vol. 228, No. 02, pp. 343 – 351. ISSN: 1859 - 2171, 2374 - 9098; e-ISSN: 2615 - 9562.
12	Analysis of aerodynamic parameters of the S1210 wind turbine airfoil under the condition of low Reynolds number.	2022	UD-JST, Vol. 20, No. 10.1, pp. 77 – 81. ISSN: 1859 -1531.
13	Aerodynamic analysis of NACA6409 airfoil in wind turbine by using Panel method.	2022	TNU Journal of Science and Technology, Vol. 227, No. 8, pp. 227 – 235; ISSN: 1859-2171, 2374-9098; e-ISSN 2615-9562.

REFERENCES

[1] World Meteorological Organization (2025), *State of the Global Climate 2024*, *WMO-No. 1368*, ISBN 978-92-63-11368-5, CH-1211 Geneva 2, Switzerland.

[2] Decision No. 2157/QD-TTg dated December 21, 2021 of the Prime Minister on the establishment of the National Steering Committee to implement Vietnam's commitments at the COP26 Conference.

[3] Decision No. 1009/QD-TTg dated August 31, 2023 of the Prime Minister on the approval of the Project for the implementation of the Political Declaration on the establishment of the Just Energy Transition Partnership (JETP).

[4] Decision No. 768/QD-TTg dated April 15, 2025 of the Prime Minister on the approval of the adjusted Power Plan VIII.

[5] EVN, Updated to April 30, 2025: 30 transitional renewable energy projects have generated more than 6.082 billion kWh to the grid, https://www.evn.com.vn/d/vi-VN/news/Cap-nhat-den-ngay-3042025-30-du-an-NLTT-chuyen-tiep-da-phat-hon-6082-ty-kWh-len-luoi--60-2014-502708

[6] Global Wind Energy Council (2025), *Global Wind Report*, The Unicorn Factory, Av. Infante D. Henrique 143 S09, Lisbon. Portugal.

[7] Decision approving the electricity generation price framework for wind power plants in 2025, 1508/QD-BCT dated May 30, 2025 of the Minister of Industry and Trade.

[8] Decision approving the electricity generation price framework for offshore wind power plants in 2025, 1824/QD-BCT dated June 26, 2025 of the Minister of Industry and Trade.

[9] Hiep Van Nguyen, Pham Xuan Thanh, Nguyen Duc Nam, Nguyen Xuan Anh, Pham Le Khuong, Hoang Hai Son, Nguyen Tien Manh, and Pham Chi Cong (2021), "Observation and Simulation of Wind Speed and Wind Power Density over Bac Lieu Region", *Advances in Meteorology*, Volume 2021, Article ID 8823940, 17 pages. https://doi.org/10.1155/2021/8823940

[10] Quang Vu Dinh, Quang-Van Doan, Thanh Ngo-Duc, Van Nguyen Dinh, Nguyen Dinh Duc (2022), "Offshore wind resource in the context of global climate change over a tropical area", *Applied Energy* 308. https://doi.org/10.1016/j.apenergy.2021.118369.

[11] Nguyen Thi Thanh Nguyet, Du Van Toan (2023), "Marine spatial planning for offshore wind power using GIS", *Journal of Environment*, No. 1, pp. 41-47.

[12] Nguyen Van Doai (2017), "Study the overview of wind turbines and the factors that affect the power output of the turbine", *Journal of Science of Lac Hong University*, Special issue, pp. 21-25.

[13] Nguyen The Mich, Do Huy Cuong, Doan Kim Binh (2017), "Research and calculation design for counter – rotating wind turbine use with low wind speed range", *The Vietnam Journal of Mechanical Engineering*, No.9.

[14] Minh Bach Duc, Hung Tran The, Nguyen Dinh Duc, Trinh Chu Duc, Anh Dinh Le (2023), "Performance enhancement of savonius wind turbine by multicurve blade shape", *Energy Sources, Part A: Recovery, Utilization, and Environmental Effects*, Volume 45, Issue 1.

[15] Nguyen Xuan Truong, Nguyen Trung Hieu, Nguyen Van Vuong (2017), "Aerodynamics of 2 kW vertical wind turbine", *National Conference on Solid State Physics and Materials Science – SPMS 2017*, pp. 629 – 633.

[16] Xiao Yu Tang, Shumian Zhao, Bo Fan, Joachim Peinke, Bernhard Stoevesandt (2019), "Micro-scale wind resource assessment in complex terrain based on CFD coupled measurement from multiple masts", *Applied Energy* 238.

[17] Nicolo Pollini (2022), "Topology optimization of wind farm layouts", *Renewable Energy* 195.

[18] A. Z. Dhunny, M. R. Lollchund, S. D. D. V. Rughooputh (2017), "Wind energy evaluation for a highly complex terrain using Computational Fluid Dynamics (CFD)", *Renewable Energy* 101.

[19] Madsen, M. H. A., Zahle, F., Horcas, S. G., Barlas, T. K., & Sørensen, N. N. (2022), "CFD-based curved tip shape design for wind turbine blades", *Wind Energy Science*, Vol. 7, No. 4.

[20] Devashish Jha, Saket Saurabh (2023), "NACA2412 airfoil based method for design and aerodynamic analysis of small HAWT using modified BEM approach", *Science and Technology for Energy Transition* 78, 2.

[21] Hamed Sedighi, Pooria Akbarzadeh, Ali Salavatipour (2020), "Aerodynamic performance enhancement of horizontal axis wind turbines by dimples on blades: Numerical investigation", *Energy* 195.

[22] M. E. Nakhchi, S. Win Naung, M. Rahmati (2021), "High-resolution direct numerical simulations of flow structure and aerodynamic performance of wind turbine airfoil at wide range of Reynolds numbers", *Energy* 225.

[23] Widad Yossri, Samah Ben Ayed, Abdessattar Abdelkefi (2021), "Airfoil type and blade size effects on the aerodynamic performance of small-scale wind turbines: Computational fluid dynamics investigation", *Energy* 229.

[24] Joseph B. Olson, et al. (2019), “Improving Wind Energy Forecasting through Numerical Weather Prediction Model Development”, *Bulletin of the American Meteorological Society*, Vol. 100, No. 11, pp: 2201–2220. https://doi.org/10.1175/BAMS-D-18-0040.1

[25] Jin, C., Yang, Y., Han, C., Lei, T., Li, C., & Lu, B. (2024), “Evaluation of forecasted wind speed at turbine hub height and wind ramps by five NWP models with observations from 262 wind farms over China”, *Meteorological Applications*, 31 (6). https://doi.org/10.1002/met.70007

[26] Mao Yang, Yunfeng Guo, Tao Huang, Wei Zhang (2025), “Power prediction considering NWP wind speed error tolerability: A strategy to improve the accuracy of short-term wind power prediction under wind speed offset scenarios”, *Applied Energy*, Vol. 377, Part D, 124720. https://doi.org/10.1016/j.apenergy.2024.124720

[27] C. L. Huang, Y. K. Wu, Q. T. Phan, C. C. Tsai and J. S. Hong (2025), "Enhancing Wind Power Forecasts via Bias Correction Technologies for Numerical Weather Prediction Model", *IEEE Transactions on Industry Applications*, vol. 61, no. 4, pp. 5406-5419, July-Aug. 2025, doi: 10.1109/TIA.2025.3546589

[28] J. Perr-Sauer, C. Tripp, M. Optis and J. King (2020), “Short-term wind forecasting using statistical models with a fully observable wind flow”, *Journal of Physics: Conference Series* 1452, 012083. doi:10.1088/1742-6596/1452/1/012083

[29] Hao Liu, Huimin Ma, Tianyu Hu (2023), “Enhancing Short-Term Wind Speed Forecasting using Graph Attention and Frequency-Enhanced Mechanisms”, *arXiv:2305.11526v2 [cs.LG]*. https://doi.org/10.48550/arXiv.2305.11526

[30] Zhu, J.; Zhao, Z.; Zheng, X.; An, Z.; Guo, Q.; Li, Z.; Sun, J.; Guo, Y. (2023), “Time-Series Power Forecasting for Wind and Solar Energy Based on the SL-Transformer”, *Energies*, 16, 7610. https://doi.org/10.3390/en16227610

[31] Wu, Z., et al. (2022), “A comprehensive review on deep learning approaches in wind forecasting applications”, *CAAI Trans. Intell. Technol.* 7 (2), 129–143. https://doi.org/10.1049/cit2.12076

[32] Yang Zhang, Lingbo Liu, Xinyu Xiong, Guanbin Li, Guoli Wang, Liang Lin (2023), “Long-term Wind Power Forecasting with Hierarchical Spatial-Temporal Transformer”, *arXiv:2305.18724v1 [cs.LG]*. https://doi.org/10.48550/arXiv.2305.18724

[33] T. Kouser et al. (2025), "Machine Learning Approach to Aerodynamic Analysis of NACA0005 Airfoil: ANN and CFD Integration", *IEEE Access*, vol. 13, pp. 131088-131101, doi: 10.1109/ACCESS.2025.3592338

[34] Pilar Díaz-Cuevas (2018), "GIS-Based Methodology for Evaluating the Wind-Energy Potential of Territories: A Case Study from Andalusia (Spain)", *Energies*, 11, 2789; doi:10.3390/en11102789

[35] Flora, F.M.I., Donatien, N., Tchinda, R. and Hamandjoda, O. (2021), "Selection Wind Farm Sites Based on GIS Using a Boolean Method: Evaluation of the Case of Cameroon", *Journal of Power and Energy Engineering*, 9, 1-24. https://doi.org/10.4236/jpee.2021.91001

[36] Abdullah Demir, Ali Ersin Dinçer, Cihan Çiftçi, Sedat Gülçimen, Nigmet Uzal, Kutay Yılmaz (2024), "Wind farm site selection using GIS-based multicriteria analysis with Life cycle assessment integration", *Earth Science Informatics* 17:1591–1608. https://doi.org/10.1007/s12145-024-01227-4.

[37] GitHub, Inc. BlenderGIS. Available at: https://github.com/domlysz/BlenderGIS (accessed July 26, 2025).

[38] T Koblitz, A Bechmann, J Berg, A Sogachev, N Sørensen and P-E Rethore (2014), "Atmospheric stability and complex terrain: comparing measurements and CFD", *Journal of Physics: Conference Series* 555 012060. doi:10.1088/1742-6596/555/1/012060

[39] Ansys Inc., what is computational fluid dynamics, https://www.ansys.com/simulation-topics/what-is-computational-fluid-dynamics (accessed July 26, 2025).

[40] Naveen N. Kethavath, Niranjan S. Ghaisas (2024), "Effect of an abrupt rough-to-smooth surface roughness transition on wind farm wakes: An LES and analytical modeling study", *J. Renewable Sustainable Energy* 16, 033302. https://doi.org/10.1063/5.0202733.

[41] Ansys innovation courses, Calculating Turbulent Intensity, https://innovationspace.ansys.com/courses/courses/topics-in-turbulence-modeling-using-ansys-fluent/lessons/calculating-turbulent-intensity/. (accessed July 26, 2025).

[42] Sogachev A. (2009), "Boundary-Layer", *Meteorol.* Vol.130, pp. 423–435

[43] F. González-Longatt, P. Wall, V. Terzija (2012), "Wake effect in wind farm performance: Steady-state and dynamic behavior", *Renewable Energy* 39 329-338. Doi:10.1016/j.renene.2011.08.053.

[44] Peña, A., Réthoré, P. E., & Rathmann, O. (2014), "Modeling large offshore wind farms under different atmospheric stability regimes with the Park wake model", *Renewable Energy*, 70, 164–171. doi:10.1016/j.renene.2014.02.019

[45] James Manwell, Jon McGowan, and Anthony Rogers (2009), *Wind Energy Explained: Theory, Design and Application, Second Edition*, John Wiley & Sons, Ltd.

[46] Magdi R. and Adam M. R. (2011), *Wind Turbines Theory - The Betz Equation and Optimal Rotor Tip Speed Ratio, Fundamental and Advanced Topics in Wind Power*. ISBN: 978-953-307-508-2. InTech.

[47] Ding, J. J., Wang, H., Sun, L. P. and Ma, B. (2013), "Optimal Design of Wind Turbine Blades with Wilson and BEM Method Integrated", *Applied Mechanics and Materials*, vol. 404, pp. 286–291. Trans Tech Publications, Ltd. https://doi.org/10.4028/www.scientific.net/amm.404.286.

[48] Raghavendra S., Ravikumar T., Gnaendra R., Manjunatha K. and Madhusudhana S. (2020), "Design of wind blades for the development of low-power wind turbines using Betz and Schmitz methods", *Advances in Materials and Processing Technologies*, volume 8 (1), 808-827. DOI: 10.1080/2374068X.2020.1833605.

[49] S. Xueyi, W. Lin, L. Xianwu (2021), "Airfoil optimization using a machine learning-based optimization algorithm," Journal of Physics: Conference Series, vol. 2217. DOI:10.1088/1742-6596/2217/1/012009.

[50] M. Drela (1989), "XFOIL: An Analysis and Design System For Low Reynolds Number Airfoils," MIT Dept. of Aeronautics and Astronautics, Cambridge, Massachusetts.

[51] A. Septiyana, K. Hidayat, A. Rizaldi, Y. Wijaya (2020), "Comparative study of wing lift distribution analysis using numerical method", *Jurnal Teknologi Dirgantara*, vol. 18, no. 2, pp. 129-139.

[52] M. Selig, M. Maughmert (1992), "Multipoint inverse airfoil design method based on conformal mapping", *AIAA Journal*, vol. 30, no. 5.

[53] Qblade Homepage (2025) Qblade Documentation. https://docs.qblade.org/. (accessed July 26, 2025).

[54] Bangga, G., Parkinson, S., Collier, W. (2023), "Development and validation of the iag dynamic stall model in state-space representation for wind turbine airfoils", *Energies*, volume 16 (10), 1-25. https://doi.org/10.3390/en16103994.

[55] F. González-Longatt, P. Wall, V. Terzija (2012), "Wake effect in wind farm performance: Steady-state and dynamic behavior", Renewable Energy 39 329-338. Doi:10.1016/j.renene.2011.08.053.

[56] Barthelmie, R. J., Folkerts, L., Larsen, G. C., Rados, K., Pryor, S. C., Frandsen, S. T., Lange, B., & Schepers, G. (2006), "Comparison of wake model simulations with offshore wind turbine wake profiles measured by sodar", *Journal of Atmospheric and Oceanic Technology*, 23, 888-901. https://doi.org/10.1175/JTECH1886.1

[57] Gögmen, T., van der Laan, P., Réthoré, P. E., Pena Diaz, A., Larsen, G. C., & Ott, S. (2016), "Wind turbine wake models developed at the Technical University of Denmark: A review", *Renewable & Sustainable Energy Reviews*, 60, 752–769. https://doi.org/10.1016/j.rser.2016.01.113.

[58] Lattawan Niyomtham, Charoenporn Lertsathittanakorn, Jompob Waewsak and Yves Gagnon (2022), "Mesoscale/Microscale and CFD Modeling for Wind Resource Assessment: Application to the Andaman Coast of Southern Thailand", *Energies*, 15, 3025. https://doi.org/10.3390/en15093025.

[59] Z. R. Shu and Mike Jesson (2021), "Estimation of Weibull parameters for wind energy analysis across the UK", *J. Renewable Sustainable Energy* 13, 023303; doi: 10.1063/5.0038001.

[60] Stehly, Tyler, P. Beiter and P. Duffy. (2020), "Cost of Wind Energy Review", *National Renewable Energy Laboratory*. NREL/TP-5000-78471. https://www.nrel.gov/docs/fy21osti/78471.pdf.

[61] B. Thomas, X. Costoya, M. deCastro, D. Carvalho, M. Gomez-Gesteira (2024), "Wake effect impact on the levelized cost of energy in large floating offshore wind farms: A case of study in the northwest of the Iberian Peninsula," *Energy* Vol. 304, 132159. https://doi.org/10.1016/j.energy.2024.132159.

[62] World Bank Group (2025), "Global Wind Atlas", [Online]. Available: https://globalwindatlas.info/en/area/Vietnam/Ninh%20Thu%E1%BA%ADn. (accessed July 26, 2025)..

[63] L. K. Berg, M. Pekour, D. Nelson (2012), "Description of the Columbia Basin Wind Energy Study (CBWES)", *The U.S. Department of Energy*, PNNL-22036.

[64] N. K. Naveen, S. G. Niranjan (2024), "Effect of an abrupt rough-to-smooth surface roughness transition on wind farm wakes: An LES and analytical modeling study", *J. Renewable Sustainable Energy* 16, 033302. https://doi.org/10.1063/5.0202733.

[65] H. G. Kim, Y. H. Kang and J. Y. Kim (2017), "Evaluation of wind resource potential in mountainous region considering morphometric terrain characteristics," *Wind Engineering*, Vol. 41(2) 114–123. https://doi.org/10.1177/0309524X16689445

[66] B. Yang, Y. Qian, L. K. Berg, P. L. Ma, S. Wharton, V. Bulaevskaya, H. Yan, Z. Hou, W. J. Shaw (2016), "Sensitivity of Turbine-Height Wind Speeds to Parameters in Planetary Boundary-Layer and Surface-Layer Schemes in the Weather Research and Forecasting Model", *Boundary-Layer Meteorol* 162 (1), 117–142. DOI: 10.1007/s10546-016-0185-2

[67] National Weather Service – USA (2025), "Beaufort Wind Scale", [Online]. Available: https://www.weather.gov/mfl/beaufort (accessed July 26, 2025).

[68] IEC 61400-1 (2019), *"Wind energy generation systems - Part 1: Design requirements"*, IEC, Geneva, Switzerland.

[69] Michael S. Selig, James J. Guglielmo, Andy P. Broeren and Philippe Giguere (1996), "Summary of Low-Speed Airfoil Data, Volume 1", SoarTech Publications, Virginia Beach, Virginia.

[70] Suresh A., Raja kumar S., Belqasem A., Sudhakar Babu T. (2024), "Investigations of the performance of 3D printed micro wind turbine composed of PLA material", *Heliyon 10 e25356*, 1-15. https://doi.org/10.1016/j.heliyon.2024.e25356

[71] Mohammad S. , Ahmad A., Ghayda' A., Abdullah M., Mohamed R. (2023), "An investigation of a 3D printed micro-wind turbine for residential power production", *Int. J. Renew. Energy Dev.*, 12 (3), 550-559. https://doi.org/10.14710/ijred.2023.52615

[72] Jakub J., Bogdan B., Joanna W., Adam J., Alexander K., Mariusz F, (2025), "Energy potential and economic viability of small-scale wind turbines", *Energy 322 135608*, 1-20. https://doi.org/10.1016/j.energy.2025.135608

[73] The Wind Power (2025), "Enercon E103/2350", *The Wind Power*, [Online]. Available: https://www.thewindpower.net/turbine_en_1107_enercon_e103-2350.php. (accessed July 26, 2025).

[74] Viuredelaire, "Aerogenerator Enercon E-103 EP2", *Viuredelaire*, [Online]. Available: https://www.viuredelaire.cat/index.php?md=articles&id=13543&lg=eng. (accessed July 26, 2025).

[75] Huynh Kim An (2010), "Assessment of wind energy potential based on data in Phan Rang - Ninh Thuan published by the WorldBank", *Power Engineering Consulting Joint Stock Company 4*.

[76] AWS Truepower llc. (2011), [Online]. Available: https://www.esmap.org/sites/esmap.org/files/MOIT_Vietnam_Wind_Atlas_Report_18Mar2011.pdf. (accessed July 26, 2025).

[77] MedCalc (2024), Weibull distribution functions, MedCalc Software Ltd., [Online]. Available: https://www.medcalc.org/manual/weibull-distribution-functions.php. (accessed July 26, 2025).

[78] IEC 61400-12-1 (2022), *"Wind energy generation systems –Part 12-1: Power performance measurements of electricity producing wind turbines"*, IEC, Geneva, Switzerland.

[79] IEC 61400-12-5 (2022), *"Wind energy generation systems – Part 12-5: Power performance – Assessment of obstacles and terrain"*, IEC, Geneva, Switzerland.

[80] IRENA (2025), "Renewable power generation costs in 2024", *International Renewable Energy Agency*, Abu Dhabi. ISBN: 978-92-9260-669-5